Reviews in Mineralogy & Geochemistry
Vol. 88 pp. 191-256, 2022

Non-cratonic Diamonds from UHP Metamorphic Terranes, Ophiolites and Volcanic Sources

Larissa F. Dobrzhinetskaya

Department of Earth and Planetary Sciences,
University of California at Riverside,
900 University Ave, Riverside, CA 92521, USA

larissa@ucr.edu

Earl F. O'Bannon III

Physical and Life Sciences, Physics Division,
Lawrence Livermore National Laboratory,
Livermore, CA 94550, USA

obannon2@llnl.gov

Hirochika Sumino

Department of General Systems Studies,
Graduate School of Arts and Science,
University of Tokyo, 3-8-1 Komaba, Tokyo, Japan

sumino@igcl.c.u-tokyo.ac.jp

INTRODUCTION

The discovery of diamonds in metamorphic rocks of continental affinities occurred shortly after the discovery of coesite in similar rocks. These important discoveries led to a revolution in our understanding of the subduction and exhumation of continental materials and the establishment of a new discipline, ultra-high-pressure metamorphism (UHPM). After these discoveries more ultra-high pressure (UHP) minerals were found and dozens of UHPM terranes were established. Diamond is a remarkable material which is chemically inert and stable over geological timescales making it the perfect "geological container" where gas, fluid, and solid inclusions can be preserved. Moreover, its presence is indicative of specific pressure and temperature conditions which implie subduction to a minimum depth of ~120 km. The inclusions trapped inside these diamonds can shed light on the composition, redox state, and evolution of the fluids related to UHPM diamond formation while the carbon isotope ratios of the diamond itself can inform us about the source of carbon. The purpose of this review is to provide a brief history on the discovery of microdiamonds starting with work that began in the mid-1960s in Kokchetav massif, Kazakhstan, through to the present day. Particular attention will be on more recent micro-diamond discoveries in the last decade. The current state of understating of the mechanisms of UPHM diamond formation, the misidentification of microdiamonds due to contamination from sample extraction/preparation, and the future of UHPM diamond research are discussed. The paper also considers the controversial topic of the occurrence of lonsdaleite within the population of microdiamonds from UHPM terranes as well as recently reported ophiolite- and volcanic-hosted diamonds.

1529-6466/22/0088-0004$10.00 (print)
1943-2666/22/0088-0004$10.00 (online)
http://dx.doi.org/10.2138/rmg.2022.88.04

A multitude of geological and geodynamic events are recorded in collisional orogens where large-scale processes such as deep subduction of lithospheric plates, mantle convection, and mountain building occur. Continental collision is accompanied by the subduction of continental materials into the Earth's deep interior. The exhumation of these materials back to the Earth's surface is one of the largest natural processes that occur on the Earth. These rocks contain minerals formed under pressures that are higher than the pressures that occur within the crust and they provide a considerable amount of information about processes that occur in the Earth's mantle. Evidence of mineral reactions and deformation, fluid and melt migrations, phase transformations, and geochemical recycling are recorded in these rocks. On a regional scale continental collision zones release "energy" through earthquakes and volcanic eruptions.

In the early stages of the theory of plate tectonics several concepts were established; one such concept was that the continental crust is buoyant and will always remain floating above the oceanic crust. Therefore, this early version of plate tectonic theory did not provide a mechanism for the subduction of continental lithosphere into the Earth's deep interior. This paradigm was significantly challenged in 1984 with two discoveries of coesite, first in the Dora Maira Massif, Alps (Chopin 1984) and the second, published only three months later, in the Western Gneiss Region, Norway (Smith 1984). Soon after these exciting discoveries, graphite pseudomorphs after diamond in the Beni Bousera alpine peridotite massif (Pearson et al. 1989) and then true diamonds, "microdiamonds" were discovered in the Kokchetav massif, Kazakhstan (Sobolev and Shatsky 1990). These startling revelations ushered in an entirely new discipline, ultra-high-pressure metamorphism (UHPM).

Crustal rocks of that have experienced recrystallization within or above the coesite and diamond stability fields (≥ 2.7–4.0 GPa, ~700–1000 °C) implying subduction to a depth of ≥ 90–120 km are considered as UHPM rocks. The presence of coesite and/or diamond in metamorphic rocks of continental affinities has become the standard for defining UHPM terranes. UHPM research flourished due to the detailed studies of outcrops and mineral/rock thin-sections in laboratories with the aid of advanced state-of-art analytical and synchrotron assisted instruments and technologies. This led to the establishment of more than 20 coesite- and nine diamond-bearing localities (Fig. 1) (e.g., Ogasawara 2005; Dobrzhinetskaya 2012; Schertl and Sobolev 2013; Liou et al. 2014 and references therein). By combining all the results of this research, an integrated picture of the processes operating in the deep Earth at converging plate boundaries is realized. Moreover, a greater understanding of how crustal materials are recycled into the deep mantle environment and incorporated into large-scale mantle dynamics is also gained from these studies.

Diamond is an important index-mineral of UHPM events. Since diamond is chemically inert and stable over geological timescales it is the perfect "geological container" where gas, fluid, and solid inclusions can be preserved. These inclusions can provide detailed information about the conditions and chemistry of diamond forming media as well as mantle mineralogy and geochemistry. Moreover, diamond, which is often included in zircon, can be a precise geochronological indicator of the peak of UHP metamorphism. Aside from the inclusions, $\delta^{13}C$ values of the diamond itself can provide information about the carbon reservoir from which it crystallized. The type of nitrogen aggregation in diamond can shed light on the residence time of diamond in the environment where the diamond crystallized.

There are many types of reviews published in international forums that discuss impact of UHP mineralogy and UHP metamorphism studies on refining thermobarometry and plate tectonic modelling (e.g., Ernst and Liou 1999, 2008; Chopin 2003; Liou et al. 2004, 2009, 2014; Green 2005; Gerya 2010; Beltrando et al. 2010; Green et al. 2010; Guillot et al. 2008; Schertl and Sobolev 2013; Shirey et al. 2013; Faryad and Cuthbert 2020). However, comprehensive reviews of the studies of UHPM diamonds as well as their detailed studies with modern state-of-the-art instruments and technologies are still scarce (e.g., Ogasawara 2005; Dobrzhinetskaya 2012).

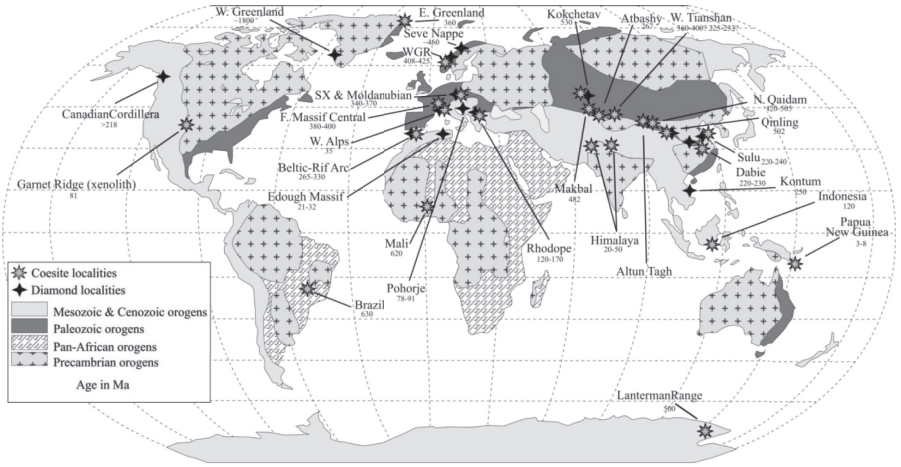

Figure 1. World map of coesite and non-cratonic microdiamond occurrences within Precambrian, Pan–African, Paleozoic and Mezozoic orogens. Numbers indicate age of UHP metamorphism in Ma. Sx–Saxoturingian area of Bohemian massif. Map is modified after Dobrzhinetskaya and Faryad (2011).

The goal of this review is to provide an update of new diamond discoveries that led to the establishment of new UHPM terranes, and to summarize and critically analyze existing concepts of diamond formation in orogenic belts, ophiolites and volcanic sources. An additional objective is to specifically emphasize certain aspects of knowledge from studies of diamonds which have been missed before and/or less highlighted in current research projects. The review outlines new constraints from many well-known collisional orogens which will lead to the improvement of geotectonic modelling that is currently being developed for very deep subduction of continental rocks, and their exhumation.

DIAMONDS FROM ULTRA-HIGH-PRESSURE METAMORPHIC TERRANES

The history of microdiamond discoveries in the Kokchetav massif, Kazakhstan

In the mid-1960s several detrital grains of diamond ranging in size from 7 to 200 mm were found in the Tertiary detrital deposits of titaniferous sands in the vicinity of the Kokchetav massif, northern Kazakhstan (Kashkarov and Polkanov 1964). The alleged source of the detrital material was determined to be the Precambrian metamorphic rocks of the Kokchetav massif (Essenov et al. 1968). By the 1970s extensive geological mapping and exploration for mineral resources began in Kazakhstan, led by A. A. Zaychkovsky from the Kokchetav Geological Survey. They collected nearly 10 m^3 of rocks from the eclogite lenses enclosed in garnet–biotite gneisses that were exposed at the shore of Kumdy Kol lake, Akmola Region, Kazakhstan. After crushing the rocks, the heavy minerals separation and flotation techniques were applied and, several microdiamonds were recovered from the residua (Rozen et al. 1972). It was concluded that these diamonds had formed under unusual crustal metamorphic conditions (Rozen et al. 1979).

The first detailed geological and petrographic descriptions of microdiamonds found *in situ* together with their host minerals was reported in Russian publications by Sobolev and Shatsky (1987, 1988). However, these unusual diamonds remained unknown to Western scientists until Sobolev and Shatsky (1990) published their results in *Nature*. They provided a detailed description of diamond morphologies and presented credible and convincing images of diamonds *in situ.* They were the first who postulated that these diamonds had formed in regional metamorphic rocks of continental affinities during deep subduction. They emphasized

that new models are needed to explain how crustal rocks can be subducted to depths greater than ~100–120 km and subsequently returned to the Earth's surface with preserved mineralogical relicts of ultra-high-pressure metamorphic (UHPM) events.

Following the efforts of the international community, the Kokchetav diamond-bearing metamorphic terrane became the "classic locality" of ultra-high-pressure metamorphism (e.g., Ernst and Liou 1999; Ogasawara 2005; Dobrzhinetskaya 2012; Schertl and Sobolev 2013; Liou et al. 2014). The "classic UHP rocks" of Kokchetav massif include metamorphic rocks with sedimentary and volcanic protoliths. They consist of varying lithologies of felsic gneisses, calc-silicate rocks, schists, quartzites, marbles, eclogites and garnet pyroxenites. Microdiamonds ranging in size from ~10 to 100 μm (rare up to 150–300 μm) with an average size ~40–50 μm occur in all the above-mentioned lithologies (Fig. 2) in high concentrations (e.g., Dobrzhinetskaya 2012; Schertl and O'Brien 2013). According to Pechnikov and Kaminsky (2008) the Kokchetav microdiamond reserves are calculated to be as large as ~2.5 billion carats, with the average content of ~20 carats per metric tonne. The Kokchetav diamonds have varying morphologies such as rose-like and dendritic-like crystals (Fig. 3A), platy skeletal-like and shapeless single crystals (Fig. 3B,C), or polycrystalline aggregates (Fig. 2D), hopper-like cuboidal, or cuboidal and octahedral-like with truncated corners, and sometimes slightly rounded single crystals (Fig. 3E,F). They are often observed as inclusions in refractory minerals such as zircon and garnet where they remain well-preserved and protected from complete transformation to graphite during exhumation of the UHPM rocks accompanied by retrograde metamorphism. While zircon and garnet protect diamond inclusions from graphitization, the radiation damage (metamictization) of microdiamonds included in zircon is a common phenomenon. Several studies (e.g., Orwa et al. 2000; Shimizu and Ogasawara 2014) have reported that the radiation damage of the Kokchetav diamonds occurred due to α-particle emissions from radiactive decay of U and Th in host zircon. This damage can be qualitatively probed with Raman spectroscopy, the Raman mode of diamond in the core of zircon is broadened and shifted to lower wavenumbers relative to pristine diamond (Shimizu and Ogasawara 2014), additionally two Raman modes at 1490 cm^{-1} and 1630 cm^{-1} have been observed and attributed to the vacancy and the split interstital, respectively (e.g., Prawer et al. 2004).

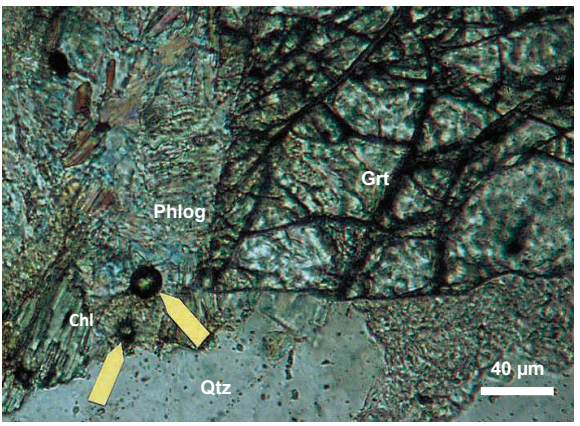

Figure 2. Photomicrograph of a standard petrographic thin section showing two diamond crystals (*in situ*) in quartz–calc–silicate rocks from Kumdy Kol lake locality, Kokchetav massif, Kazakhstan. Photomicrograph taken with a plane polarized transmitted light from an optical microscope equipped with a digital camera. **Yellow arrowheads** point to two diamond crystals situated at the phlogopite (Phlog)–chlorite (Chl) boundary; Grt–garnet; Qtz–quartz. Sample was collected by L. Dobrzhinetskaya from the abandoned underground mining gallery which crosses the diamond-bearing rocks of different lithologies; the petrographic thin section was prepared by L. Dobrzhinetskaya without any diamond abrasives.

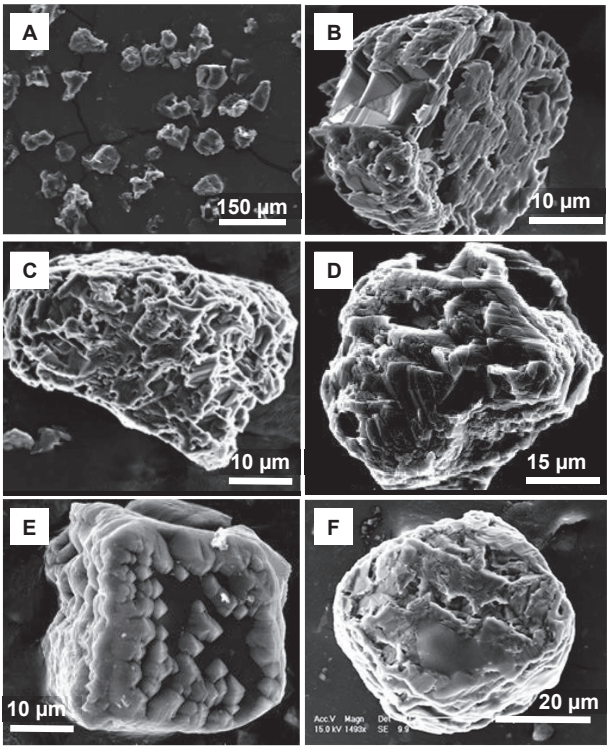

Figure 3. Secondary Electron Scanning Electron Microscope images of microdiamonds from Kokchetav massif, Kazakhstan (L. Dobrzhinetskaya's collection). **A**–diamonds separated from garnet–biotite gneiss; **B**–platy skeletal-like diamond single crystal from quartzite; **C**–shapeless diamond crystal from metacarbonate rocks; **D**–polycrystalline diamond from marble; **E**–truncated corners cuboid-like diamond with graphite (**black contrast**) from garnet–biotite gneiss; **F**–cuboidal diamond with truncated corners—from garnet–biotite gneiss.

The peak metamorphic conditions of the Kokchetav UHPM rocks are estimated by thermobarometry of the rock forming minerals to be P = ~4.5 GPa and T = 950–1000 °C(e.g., Ogasawara 2005). Studies of nanoinclusions in these diamonds suggest that the Kokchetav diamonds formed at a pressure range of 6–9 GPa, and a temperature range of 980–1200 °C (e.g., Dobrzhinetskaya et al. 2006a). The age of the UHPM event is Cambrian ~531 Ma whereas the protoliths of diamond-bearing rocks are as old as Precambrian ~2100–2700 Ma (Table 1).

Soon after Kazakhstan, similar microdiamonds (Fig. 4) were found in the Western Gneiss Region (WGR), Norway (Dobrzhinetskaya et al. 1995; van Roermund et al. 2002), the Erzgebirge Massif of Germany (Massonne 1999), in China in the metamorphic rocks of the Dabie mountains (Xu et al. 1992, 2003), and Qinling region (Yang et al. 2003), and the Kimi complex of the Greek Rhodope (Mposkos and Kostopoulos 2001, Perraki et al. 2006). Microdiamonds have also been discovered in UHP oceanic floor metasediments at Lago di Cignana, the western Alps, Italy (Frezzotti et al. 2011, 2014). The above-mentioned localities are unconditionally classified as UHPM terranes because aside from diamond other ultra-high-pressure minerals have been discovered there such as coesite, TiO_2-II (rutile with α-PbO_2 structure), majoritic garnet, Ca-Eskola-rich clinopyroxene (Ca-Eskola = $Ca\square Al_2Si_4O1_2$ where □ represents a cation vacancy in the pyroxene structure, see Vogel 1966 and others). Since the detailed reviews on UHPM diamonds were published by Ogasawara (2005), Dobrzhinetskaya (2012) and Liou et al. (2014) several new diamond-bearing metamorphic rock localities have been reported.

Table 1 summarizes the occurrences of microdiamonds in metamorphic rocks starting from their earlier descriptions (e.g., Dobrzhinetskaya 2012) to present. Within them are new diamond localities reported from granulite and garnet peridotites from the northern part of the Bohemian massive (Kotková et al. 2011; Naemura et al. 2011; Perraki and Faryad 2014), detrital diamonds from Erzgebirge (Schönig et al. 2019), from felsic granulites of the Betic Rif Cordillera, NW Africa and SE Spain (Ruiz-Cruz and Sanz de Galdeano 2012, 2013, 2014), from Straumen area of Western Gneiss Region, Norway (Smith and Godard 2013), from gneisses and eclogites of the Tromsø Nappe of Caledonides (Janák et al. 2013), from gneisses of Seve Nappe of Caledonides, Sweden (Majka et al. 2014; Klonowska et al. 2017), from oceanic metasediments of Lago di Cignana, Western Alps, Italy (Frezzotti et al. 2011; 2014; Frezzotti 2019), from garnet–kyanite–quartz–feldspathic gneisses of Pohorje, Eastern Alps (Janák et al. 2015), from amphibolites of Quinling region, China (Wang et al. 2014), from West Greenland (Glassley et al. 2014), and from garnet megacryst in mélange of the Edough Massif, NE Algeria (Bruguier et al. 2017).

Table 1. Microdiamonds occurrences in worldwide ultrahigh-pressure metamorphic terranes. This table contains part of information adopted from Table 1 (Dobrzhinetskaya 2012).

UHPM terrane/ locality	**Available data on diamond features**	**Age (Ma)**	***P* (GPa), *T* (ºC) estimate, and UHP index minerals associated with diamond**	**Data source**
Kokchetav massif, Kazakhstan (Kumdy-Kol, Barchi-Kol)	size of crystals: 10–100 μm (average ~40 μm); skeletal, imperfect; cubes with truncated corners single crystals, and polycrystalline diamonds	531 (UHPM) 2100–2700 (protolith)	P = 6–9; T = 980–1200 coesite, titanatite with exsolution lamella of coesite; diamonds with inclusions of aragonite + $MgCO_3$	Sobolev and Shatsky 1990; Claoué-Long et al. 1991; Ogasawara et al. 2000, 2002; Okamoto et al. 2000; Parkinson 2000; Katayama et al. 2001a; Dobrzhinetskaya et al. 2001, 2003, 2006a
Dabie-Sulu, China	Diamonds (~60–150 μm size) included in garnet from eclogite; in situ in polished thick sections	220–240	P > 2.7–5; T = 600–930 coesite, diamond	Xu et al. 1992, 2003
North Qaidam, China	Diamond inclusion in Zr recovered from garnet peridotite	420–450	P > 2.8–4; T = 620–740 coesite, diamond, majoritic garnet, relicts of stishovite	Song et al. 2005; Mattisson et al. 2006; Zhang et al. 2006; Liu et al. 2007; Liou et al. 2009; Katsube et al. 2009
North Qinling, China	Diamond (≤1 μm size) inclusions in zircon extracted from eclogite body	507	P > 2.6; T = 590–760 diamond	Yang et al. 2003
	Diamond inclusion in zircon extracted from amphibolite body	490.4 ± 5.8	P ~ 4.0 ± 0.5; T = 670–750	Wang et al. 2014

UHPM terrane/ locality	**Available data on diamond features**	**Age (Ma)**	***P* (GPa), *T* (ºC) estimate, and UHP index minerals associated with diamond**	**Data source**
Bohemian masif, Erzgebirge, Saidenbach, Germany	Diamonds (5–50 µm size) imperfect cubes, rose-like single crystals, and polycrystalline diamonds	360 (UHPM)	$P>7$; $T = 900–1200$ coesite, diamond, TiO_2 with αPbO_2 structure	Massonne 1999; Nasdala and Masssonne 2000; Hwang et al. 2000; Massonne and O'Brien 2003; Massonne et al. 2007
Bohemian massif, Moldanubian Zone, Ceské Stredohorí, Stráž nad Ohrí, Plesovice (Czech Republic)	Diamonds (~ 5–30 µm size) in situ graphitized diamond < 2 µm	340–380 (UHPM)	$P > 3.5$; $T = 1100$ diamond	Kotková et al. 2011; Naemura et al. 2011
Bohemian massif, Moldanobian Zone, Kutna Gora area, Czech Republic	Diamonds of ~7–8 µm Gföhl kyanite–bering granulites	~360 Ma (UHPM)	$P > 4.5$; T~680 Diamond, coesite, moissanite	Perraki and Faryad 2014
Western Gneiss Region, Norway (Fjortoft, Svartberget)	Diamons (1 nm–20 µm size) round-like crystals with "striation" and imperfect cubes with truncated edges	408–425 (UHPM)	$P > 3.2–4$; $T = 800$ coesite, majoritic garnet, diamond	Smith 1984; Dobrzhinetskaya et al. 1995; van Roermund et al. 2002; Spengler et al. 2006; Vrijmoed et al. 2006, 2008
Northern Norway, Tromso Nappe Caledonides	Diamond inclusions in garnet from kyanite–garnet–biotite–gneisses	452	$P = 3.5 \pm 0.5$; $T = 800$	Janák et al. 2013
Western Gneiss Region, Norway, Straumen	Diamond inclusion in zircon from eclogite	408–425	$P = 3.75 \pm 0.75$; $T = 750 \pm 150$	Smith and Godard 2013
Rhodope, Greece (Kimi and Sideronero)	Diamonds of 3–9 mm size inclusions in garnet (Kimi and Xanthi area) and in garnet from garnet–kyanite–mica schist, Sideranero area	202 (UHPM) 39–186	$P = 2.2$; $T = 750$	Mposkos and Kostopoulos 2001; Perraki et al. 2006; Schmidt et al. 2010, 2011; Liati et al. 2011
Western Alps (Lago di Cignana)	Diamond (1–2 µm size) inclusions in Mn-rich garnet; associates with fluid inclusions of HCO_3	35	$P \geq 3.2$; $T \leq 600$ (cold subduction)	Frezzotti et al. 2011; 2014; Frezzotti 2019
Eastern Alps, Pohorje	Diamond + SiC inclusions in garnet	92–95	$P \geq 3.5$ GPa, $T = 800–850$	Janák et al. 2015

UHPM terrane/ locality	**Available data on diamond features**	**Age (Ma)**	***P* (GPa), *T*(ºC) estimate, and UHP index minerals associated with diamond**	**Data source**
Betic Rif Cordilleras, Ceuta (NW Africa and SE Spain)	Diamond (5–15 μm size) intergrown with coesite; diamond inclusions in garnet, kyanite, apatite	330	$P > 4.3–7$; $T \rightarrow 1150$	Ruiz Cruz and Sanz de Galdeano 2012, 2013, 2014
Snasahögarna Mt., Seve Nappe, Sweden	Diamond (~1 μm size) diam + carbonate + graphite inclusions in garnet	441–445	$P = 4.1–4.2$; $T = 830–840$	Majka et al. 2014; Klonowska et al. 2017
Nagssugtoqidian Orogen, West Greenland	Diamond is partly replaced by graphite, majorite, reconstructed ringwoodite	1800	P ~7; T ~970	Glassley et al. 2014

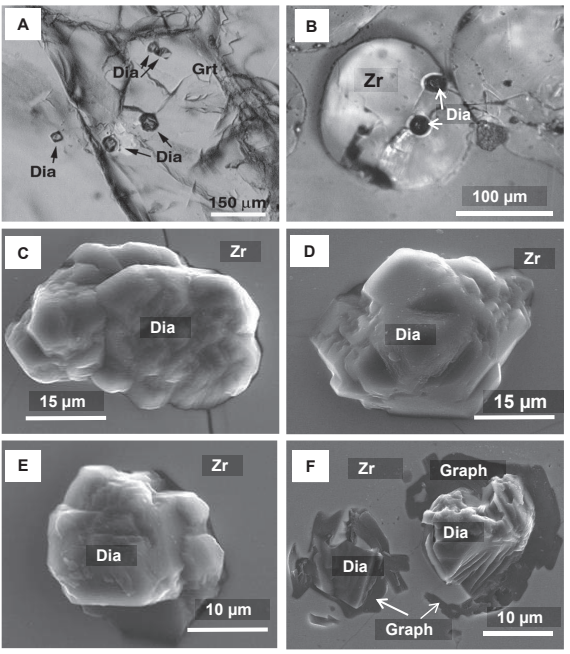

Figure 4. Diamonds from Erzgebirge UHPM terrane, Germany. Samples are collected by L. Dobrzhinetskaya from garnet–phengite–quatz–feldspathic gneisses occurred as small outcrops on the eastern shore of the Saidenbach Water Reservoir, Saxonian Erzgebirge, Germany. **A**–Photomicrograph of diamond inclusions in garnet from garnet–biotite–quartz–feldspathic gneiss (optical microscope equipped with a digital camera, polished thin section, reflected light). **B**–Photomicrograph of diamond inclusions in zircon separated from garnet–quartz–feldspathic gneiss (optical microscope equipped with a digital camera, zircons are glued on the petrographic glass slide and slightly polished, reflected light mode). **C**–**E**–Secondary electron SEM images of diamond inclusions in zircon (zircon was polished with a special technique using colloidal silica polishing compound). **F**–Secondary electron SEM images of diamond partly replaced by graphite included in zircon (sample preparation technique is like C–E).

New microdiamond localities discovered between 2011 and 2020

České Středohoří, Strážnad Ohří, Plešovice and Gföhl areas of Bohemian massif, Central Europe. The first *in situ* microdiamonds were reported as inclusions in garnet from felsic gneisses exposed in vicinities of Erzgebirge, northwestern part of the Bohemian Massif, Germany (Massonne 1999). The Erzgebirge locality became the second classical example of an UHPM terrane supported by extensive studies and publications (e.g., Nasdala and Massonne 2000; Stöckhert et al. 2001, 2009; Massonne 2003; Massonne and Tu 2007; Massonne et al. 2007b; Dobrzhinetskaya et al. 2003, 2006b, 2013). Since 2011 several new microdiamonds localities (Table 1) in the northern part of the Bohemian massif have also been reported (Kotková et al. 2011; Perraki and Faryad 2014).

Kotková et al. (2011) unambiguously documented microdiamonds ranging in size from 5–30 μm *in situ* in thin sections (Fig. 5) prepared from drill cores of felsic granulites extracted from two boreholes at the České Středohoří Mountains and from an outcrop in Stráž nad Ohří (Czech Republic).

Microdiamonds from the felsic granulites of these new localities occur as inclusions in grt, zr, and ky included in garnet. The correctly performed polishing technique provided indisputable evidence that the microdiamonds are *in situ* (Fig. 5). The microphotographs show that diamond inclusions "protrude" above the host minerals (zircon and/or garnet) well-polished surface. Coesite inclusions in kyanite included in garnet were also found in felsic granulite (Kotková et al. 2011). The authors hypothesized that during subduction (>120–150 km) the K-feldspar- and qtz-rich continental crust had "amalgamated" with small fragments of mantle materials and the latter are now presented as sparse lenses of the garnet peridotite containing relicts of Cr-spinel.

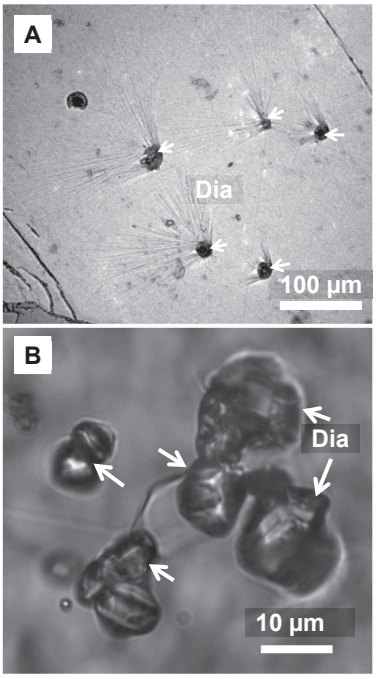

Figure 5. Diamonds from Saxony-type granulite of Bohemian massif (Kotková et al. 2011 with permission of Geology Research Czech Republic Moravia Periodicals). Photomicrographs from optical microscope: **A**–microdiamond (**white arrowheads**) inclusions in garnet (reflected light mode); polishing striation developed on the garnet surface around the microdiamonds. **B**–microdiamond (**white arrowheads**) inclusions in garnet (plain parallel light).

Kotková et al. (2011) emphasized that the protolith of these newly discovered diamond-bearing felsic granulites was "granitic crustal" rocks, which is different from the protolith of the Erzgebirge locality in Germany where the first diamond from this locality was reported by Massonne (1999). The Erzgebirge diamonds occur in garnet–biotite–phengite–quartz–feldspathic gneisses with a metasedimentary protolith. However, all these rocks belong to the same rock-unit of the Variscan orogeny, 340–380 Ma (e.g., Kröner and Willner 1998; Massonne and O'Brien 2003). Faryad and Cuthbert (2020) considered these diamond-bearing felsic granulites as former UHPM rocks that were overprinted by granulite facies metamorphism after their exhumation to the crust. Therefore, further studies of K-Fsp-rich felsic granulites with a primary granitic protolith may provide the opportunity to discover other UHPM minerals such as K-cymrite and/or K-wadeite which were first synthesized in laboratory (e.g., Fasshauer et al. 1997; Davies and Harlow 2002). Later K-cymrite was discovered in North Qaidam UHP eclogite, Western China (Zhang et al. 2009).

Perraki and Faryad (2014) discovered diamond, coesite, and moissanite inside of polished zircon grains. The zircons were extracted from the heavy minerals fraction that was separated from the crushed kyanite-bearing Gföhl granulite samples (the Moldanubian Zone of the Bohemian massif). The Gföhl kyanite-bearing granulites contain lenses and boudins of eclogites, garnet peridotites, and garnet pyroxenites. The thermobarometric calculations suggest that UHP metamorphism occurred at $P > 4$ GPa and $T = 680$ °C followed by granulite facies metamorphism and partial melting at $P < 2$ GPa and $T = 850$–950 °C. Perraki and Faryad (2014) agreed with Kotková et al. (2011) that the diamonds crystallized during UHP metamorphism of the Variscan Orogeny.

One novel aspect of the study of Perraki and Faryad (2014) is that they found SiO_2 (coesite) coexisting with diamond and moissanite (SiC). Moissanite formation requires extremely reducing conditions, e.g., 4.5–6 log units below the iron–wustite (IW) buffer, whereas diamond and SiO_2 (coesite) may coexist at an oxygen fugacity close to the diamond + CO fluid buffer (CCO) and the fayalite–magnetite–quartz (FMQ) oxygen buffers (e.g., Mathez et al. 1995; Frost and Frost 2014). Additional studies of the coexisting diamond, coesite, and moissanite inclusions in zircons from Gföhl granulites should be a high priority for future investigations, since such a study would shed light on the redox conditions of fluid–rock interactions and microdiamond formation in UHPM terranes.

Microdiamonds in detrital garnets from Erzgebirge, Germany. After several decades of the intensive studies motivated by the first discoveries of coesite and microdiamonds in rocks of continental affinities, it was shown that UHP metamorphism is not a rare phenomenon. However, despite the widespread exposure of presumably UHPM rocks in the continent–continent collisional orogens the mineralogical evidence of ultra-high-pressure metamorphism remains scarce, since during exhumation UHP minerals are typically overprinted with lower-grade metamorphism and partial melting. Schönig et al. (2019) proposed to study the distribution and characteristics of UHPM rocks by analyzing detrital garnets that have accumulated in surface sediments.

They collected detrital garnets from loose sediments deposited near the Erzgebirge massif where diamonds were described as inclusions in garnets and zircons (e.g., Nasdala and Massonne 2000; Dobrzhinetskaya et al. 2003). The sediments consist of sand from the creeks around the Saidenbach reservoir that have been draining the Erzgebirge UHPM rocks for a long time. After heavy mineral separation and examination of the residua with optical microscopy about 700 grains of garnets were chosen for further research. Out of the 700 inclusion bearing garnets they found 26 garnets containing 46 inclusions of monomineralic coesite, and 22 garnets containing 41 diamond inclusions, and they examined them with Raman spectroscopy (Schönig et al. 2019). These results provide undisputable evidence that the processes of erosion and weathering of UHPM rocks can relocate UHP minerals to sediments scattered around the hard

rock exposures. Therefore, this method may be used as an additional technique for discovering new UHPM terranes. Similar methodology has been successfully applied to single zircon grains that were separated from UHPM rocks and has been successfully used for more than a decade to identify microdiamonds and other UHPM mineral inclusions.

The Betic and Rif Cordilleras, NW Africa, and SE Spain. A new microdiamond-bearing locality was discovered within the felsic gneisses of granulite facies in the Betic–Rif arc (NW Africa) and in the SE of Spain (Ruiz-Cruz and Sanz de Galdeano 2012). This tectonically complicated domain belongs to the pre-Mediterranean Alpine orogenic zone formed during the Africa–Eurasia collision (e.g., Platt et al. 2013). It should be noted that almost two decades ago cubic graphite pseudomorphos after diamonds were discovered in peridotites of Beni Bushera massif (Morocco), situated within the Rif orogenic belt (Pearson et al. 1989). This discovery was the first report that mantle rocks can be tectonically emplaced into the crustal environment from a depth corresponding to the diamond stability field. However, unambiguous proof of this concept was emphasized by finding similar cubic graphite in the Ronda peridotite massif, Spain (Davis et al. 1993). They showed that the basal planes {0001} of graphite are parallel to the {111} of the octahedra which demonstrated distinctly that graphite is pseudomorph after diamond. Studies of carbon isotopes in cubic graphite of both Beni Bushera and Ronda massifs show that the precursor diamonds crystallized from a ^{13}C-depleted reservoir most likely originating from subducted crust (Pearson et al. 1991). A decade later, El Attrasi et al. (2011) reported finding of the 0.5–2 μm size diamond crystals included in large graphite flakes extracted manually from a garnet pyroxenite layer of the Beni Bousera massif, thereby providing unequivocal confirmation that these rocks were at some point in the diamond stability field.

Ruiz-Cruz and Sanz de Galdeano (2012) reported findings of octahedral, cuboid and cubo-octahedral microdiamonds of $<5 \times 10$–15 μm size (Table 1) as inclusions in garnet, kyanite, and quartz with relicts of coesite from felsic granulites exposed in the Ceuta area of the Northern Rif, NW Africa. The authors have estimated the metamorphic conditions of the Ceuta granulites as $P = 4.3$ GPa and $T = 1100$ °C (corresponding to a depth of >150 km) and suggested that the diamond-bearing crustal rocks and peridotites experienced a similar UHP metamorphic condition. They also suggested that the UHP metamorphism occurred ~330 Ma ago followed by partial melting and migmatization at ~265 Ma (Ruiz-Cruz and Sanz de Galdeano 2013). Given that the diamond-bearing garnet from felsic gneiss contains apatite' exsolution lamella and clusters, the authors calculated the phosphorus solubility in garnet and compared it with those obtained in high-pressure and high-temperature experiments (Konzett and Frost 2009; Konzett et al. 2012). Based on such a comparative analysis they concluded that the highest pressure reached during UHPM was 7 GPa, and temperature ~1150 °C (Ruiz-Cruz and Sanz de Galdeano 2013).

Straumen localiy, Western Gneiss Region, Norway. After the discovery of coesite inclusions in clinopyroxene occurring in the dolomite–eclogites from Grytting, Norway (Smith 1984) the Geological Survey of Norway (NGU) initiated a search in 1992 for possible microdiamonds in the WGR. Garnet–kyanite–phlogopite gneisses were collected at Fjørtoft island of WGR and crushed at the NGU laboratory. Several grains of microdiamonds (30–45 μm size) were separated from the heavy mineral concentrates extracted at the NGU chemical laboratory using a method of thermochemical decomposition (e.g., Dobrzhinetskaya et al. 1995). Later, microdiamonds were found *in situ* in thin sections prepared from hand-samples of garnet peridotite from Fjørtoft (van Roermund et al. 2002), and in Fe-Ti garnet peridotite from Svartberget (Vrijmoed et al. 2006, 2008).

In situ diamond has also been reported from two more localities in the central and northern parts of WGR, Norway (Smith and Godard 2013; Janák et al. 2013). Smith and Godard (2013) conducted Raman spectral point analysis and Raman mapping of the carbon-bearing inclusions in zircon from kyanite–phengite–coesite-bearing eclogites from the Straumen eclogite pod in the WGR, and they identified two graphitized diamonds. The authors noticed that the position of the

1st order Raman mode of the diamond inclusions varies from 1332 cm^{-1} (ambient value for single crystal diamond) down to as low as 1322 cm^{-1}. They observed additional features in the Raman spectra of these diamonds (doublets with peaks at 1328 cm^{-1} and 1322 cm^{-1}) which are like the Raman spectra of diamonds from the Kokchetav Massif. Given the Raman results and the *in situ* nature of the diamonds the geological origin of the Straumen diamonds is indisputable.

Tonsvika area, Tromsø nappe, the northern Norwegian Caledonides. Janák et al. (2013) documented microdiamonds (~10 μm) *in situ* in kyanite–garnet–biotite–gneisses exposed near Tonsvika, Tromsø nappe (452 Ma), in the northern part of the Norvegian Caledonides territory (Table 1). Microdiamonds were observed in thin sections with optical microscopy and confirmed with Raman spectroscopy. Microdiamonds occur as single crystals as well as multiphase inclusions of diamond + $MgCO_3$ and/or diamond + $CaCO_3$ in garnet. In addition to the diamond and diamond–carbonate inclusions, monocrystalline quartz with radial fractures was observed suggesting that this quartz is a product of decompression of coesite. Most of the Raman spectra collected from 21 microdiamonds in two petrographic thin sections have peaks that are observed between 1332 and 1330 cm^{-1} suggesting the presence of sp^3-hybridized carbon bonding (diamond). The presence of *G-bands* (1580 cm^{-1}) in Raman spectra indicate that sp^2-hybridized carbon bonding (graphite) is also present. The thermodynamic calculations reported by Janák et al. (2013) suggest that diamond crystallization took place at P = 3.5 ± 0.5 GPa and T = 770 ± 50 °C. The microdiamond discovery in Tromsø nappe combined with the previous discoveries of coesite, microdiamonds, majoritic garnets in the neighboring Western Gneiss Region extends this UHPM terrane by >100–120 km.

Jämtland and Årescutan areas, the Sweden Caledonides. Diamond inclusions are documented in 2014 for the first time in porphyroblastic garnets from garnet–sillimanite–biotite gneisses in the Seve Nappe Complex of northern Jämtland, Swedish Caledonides (Majka et al. 2014). Diamonds ranging in size from 4 to 7 μm with spheroidal and bleb-like forms occur inside of a multiphase assemblage of carbonate, quartz, and rutile (Fig. 6). The presence of sp^3 carbon bonding was confirmed with Raman spectroscopy, and scanning electron microscope (SEM) images acquired in secondary electron (SE) mode reveal negative relief of diamond inclusions with respect to the very flat, perfectly polished surface of the host garnet (Majka et al. 2014).

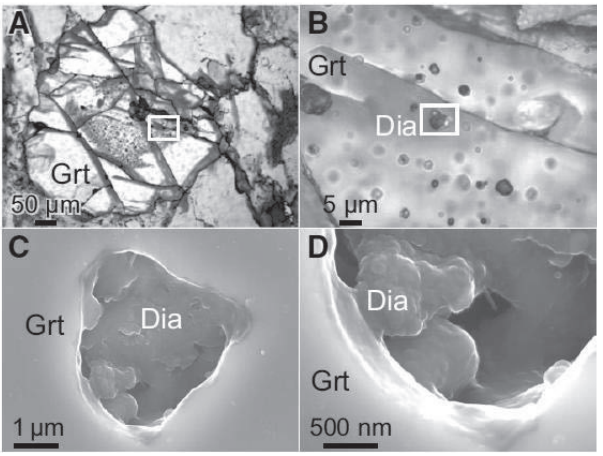

Figure 6. Microdiamond inclusions in garnet from garnet–sillimanite–biotite gneiss, Jämtland, Sweden Caledonides (Majka et al. 2014 with permission from the Geological Society of America). **A** and **B**–diamond (Dia) inclusion in garnet acquired at different magnifications (optical microscope: plane polarized transmitted light); **C** and **D**–Secondary electron SEM images of the same diamond shown in plates A and B (acquired at different magnifications).

Klonowska et al. (2017) discovered another microdiamond locality approximately 50 km from the locality described by Majka et al. (2014). Microdiamonds (~5 μm size) are found *in situ* as single and composite (diamond + carbonate) inclusions in garnet from garnet–phengite–kyanite–rutile gneisses in the Åreskutan area of the Seve Nappe Complex. Raman modes were observed at 1328 cm^{-1} and 1331 cm^{-1} confirming the presence of diamond (Solin and Ramdas 1970). Moreover, besides these diamonds, the gneisses contain textural relicts of decompressed coesite, observed as polycrystalline quartz surrounded by radial cracks. Thermodynamic calculations suggest that diamond crystallization took place at $P = 4.1–4.2$ GPa and $T = 830–840$ °C (Klonowska et al. 2017). The mineral assemblages of the UHP metamorphism were later overprinted under amphibolite and granulite facies conditions. The age of the UHP metamorphism recorded in the Åreskutan diamond-bearing gneisses occurred before ~445 Ma (Klonowska et al. 2017).

Diamonds from Lago di Cignana, Italy, Western Alps. Although UHP metamorphism in the Western Alps was proposed in the mid 1980s when coesite first was discovered by Chopin (1984) and later by Reinecke (1991), diamonds were not found in the Western Alps until almost two decades later (Frezzotti et al. 2011, 2014; Frezzotti 2019). Frezzotti et al. (2011) discovered microdiamond inclusions ranging from < 2–30 μm in size in Mn-rich garnets from garnetite nodules and boudins enclosed within mica–schists and quartzites that are spatially associated with eclogite facies metabasites. The upper part of this metamorphosed ophiolitic section belongs to the Lago di Cignana tectonic unit of the Western Alps and appears to be the first recognized UHPM terrane which originated as a fragment of the Thetyan oceanic lithosphere. The tiny diamond inclusions are closely associated with COH fluid inclusions, and tiny inclusions of magnesite and SiO_2 (quartz). There is no evidence that the quartz is a product of decompression of coesite during exhumation. Instead, the SiO_2 clusters are products of lower temperature post–metamorphic reactions that occurred in adjacent layers of the mica-schists (Frezzotti et al. 2011, 2014).

Detailed studies of diamond and COH fluid enclosed in garnets using Raman spectroscopy and C and O isotope geochemistry revealed that organic carbon dissolved in hydrous fluids was transported to a depth ~110 km together with oceanic sediments during Alpine oceanic subduction about 35 Ma ago. Frezzotti et al. (2011, 2014) and Frezzotti (2019) concluded that during subduction the UHP metamorphism led to diamond crystallization from COH fluid at respectively high oxidation state [fO_2 = 0–1.5 log units higher than the fayalite–magnetite–quartz (FMQ) buffer]. This UHP metamorphism took place at $P \geq 3.2$ GPa and $T \leq 600$ °C and is classified as a cold subduction metamorphism (e.g., Frezzotti 2019).

Diamonds from Pohorje (Slovenia) in the Austro-Alpine UHPM terrane, Eastern Alps. The Pohorje Mountains have been considered as an UHPM terrane since Janák et al. (2004, 2006) constrained the pressure and temperature ($P \geq 3.5$ GPa and T =800–850 °C) for eclogite and peridotite enclosed in meta-carbonaceous rocks, although at that time no UHP index minerals had been known in this locality. Later, Janák et al. (2015) discovered ~10 μm microdiamond inclusions in garnets from metapelitic gneisses that consist of layers rich in biotite, white mica, garnet and kyanite alternating with felsic layers, veins and segregations of quartz and feldspar. Inside of the host-garnets diamond occurs as single cubes or cubo-octahedral crystals and as a part of composite inclusions where it is associated with moissanite (SiC) and fluid inclusions containing abundant CO_2 and traces of CH_4. Diamonds, associated minerals, and fluid inclusions were confirmed with Raman spectroscopy. The authors concluded that diamond formed at depth > 100 km during Late Cretaceous (ca. 92–95 Ma) subduction of the continental slab from reduced supercritical fluids that formed during UHP metamorphism of carbonaceous sediments. This diamond-forming media is similar to that reported by Perraki and Faryad (2014) in the Gföhl granulites of the Moldanubian Zone of the Bohemian massif, where they documented polyphase inclusions of diamond+moissanite+coesite in zircon.

More diamonds from Qinling region, China. Though the Central Orogenic belt (COB) of China is a well-established UHPM terrane where coesite (e.g., Okay et al. 1988) as well as quartz paramorphs possibly after stishovite (Liu et al. 2007, 2018) and majoritic garnet with lamella exsolution of ortho- and clinopyroxenes (Ye et al. 2000) are well-documented, diamonds in these rocks are scarce. There are two reports of diamond occurrences in the Dabie Mountains (Xu et al. 1992, 2003) and the Qinling region of China as inclusions in zircons (Yang et al. 2003). However, these reports were not confirmed by others for more than a decade.

Wang et al. (2014) documented more microdiamonds as inclusions in zircons that had been separated from amphibolite rocks from the North Qinling region. To date, all microdiamonds reported from the COB have only been confirmed with Raman spectroscopy. Advanced electron microscopy studies of these diamonds such as FIB and TEM have not yet been reported. Nevertheless, both FIB and TEM research on these unusual diamonds is very important since it would likely shed light onto the geochemical conditions under which these diamonds crystallized. Considering that very few microdiamonds have been documented in the UHPM rocks of the COB it is understandable that researchers may be skeptical of these reports. It is possible that the low concentration of diamonds in the COB may be explained by geochemical conditions that would impede diamond crystallization. Hypothetically, such conditions could be: (i) low concentration of carbon in the bulk rocks and/or in small amounts of fluid/hydrous melt that can penetrate subducting slabs during UHP metamorphism; (ii) perhaps the concentration of carbon was high enough to start diamond nucleation, but the oxygen fugacity was extremely high which would prevent diamond crystallization; (iii) or all the diamonds were replaced by graphite during slow exhumation of the UHPM rocks accompanied by low-pressure and high-temperature regional metamorphism.

Graphitized diamond in West Greenland UHPM terrane. A new UHPM terrane was documented by Glassley et al. (2014) within the Nagssugtoqidian Orogen (Proterozoic age, ca. 1.8 Ga) of West Greenland. The Orogen consists of undifferentiated metasedimentary/metavolcanic rocks and amphibolites. They include strongly deformed quartzo-feldspathic granitic and dioritic gneisses, garnet–sillimanite–graphite–schists, and amphibolites; all which were traditionally considered as upper amphibolite to granulite facies from regional metamorphism (e.g., Davidson 1979; Glassley and Sørensen 1980; Mengel 1983).

The mineralogical confirmation of different UHP events includes (i) the presence of relicts of orthopyroxene exsolved from a supersilicic garnet precursor, (ii) exsolution lamella of rutile from garnet and pyroxenes, (iii) exsolution lamella of magnetite from olivine, and (iv) unusual quartz needles exsolved from olivine—a hypothetical ringwoodite. Glassley et al. (2014) showed that the Raman spectra of three mm-sized carbon-bearing inclusions in garnet exhibit modes at 1335 cm^{-1}, which unambiguously suggests the presence of sp^3-carbon bonds, e.g., the diamond structure. Broad peaks at ~1420–1450 cm^{-1} which are consistent with hydrogenated carbon on the diamond surfaces and well-pronounced Raman bands of graphite at 1580 cm^{-1} suggest that diamond probably gradually transformed to graphite. The authors hypothesized that these diamonds were encapsulated in the garnet during their growth and were transformed to graphite during decompression accompanied by metamorphism to granulite facies. The UHP metamorphic conditions suggest a pressure of ~ 7 GPa and a temperature of ~975 °C.

The Western Mediterranean orogen—the Edough Massif, NE Algeria, new UHPM terrane. Several microdiamond crystals were discovered by Caby et al. (2014) as inclusions in garnet megacryst (≥ 5 cm) collected from a mélange zone exposed at the northern margin of Africa (the Edough Massif, NE Algeria). The garnet megacrysts were adjacent to actinolite-bearing and ultramafic boudins associated with tectonic fragments of marbles occurring within a major mylonite–ultramylonite band. Several cuboid-like diamond crystals ranging from 3–50 μm in size were identified with Raman spectroscopy (Caby et al. 2014).

Later, a single diamond crystal approximately 50 μm in size intergrown with rutile enclosed in an almandine-rich garnet was studied in detail with the aid of SEM techniques (Bruguier et al. 2017). The secondary electron SEM image presented in Figure 3a from Bruguier et al. (2017) is unequivocal evidence that the diamond–rutile inclusion is indigenous (e.g., not from sample preparation or contamination) to the Edough massif. The image shows that the diamond is clearly "protruding above" the perfectly polished surface of the host mineral, which is very typical for a diamond–garnet interface. The contact zone between the diamond–garnet interface, appears intact which strongly suggests that the diamond is naturally occurring and not contamination from a cutting with a diamond-saw and/or polishing with diamond grit. Other garnets from the same area contain rutile, zircon, apatite, and plagioclase inclusions.

Thermodynamic calculations suggest that an UHP metamorphic event took place at $P \geq 3.6$ GPa and $T = 750$ °C (Bruguier et al. 2017; Caby et al. 2014). Studies of the zircon inclusions suggest that the Alpine age of UHP metamorphism of the West Mediterranean Orogen is between 32.4 ± 3.3 Ma and 20.7 ± 2.3 Ma (Bruguier et al. 2017). This was followed by exhumation as slab rollback occurred in the Oligocene (Brun and Faccenna 2008; Tirel et al. 2013). Additional studies of this locality should find more evidence of UHPM, such as UHP minerals and/or traces of their decompression products and/or proof of retrograde metamorphism.

Diamonds from Nishisonogi unit, Nagasaki metamorphic complex, western Kyushu, Japan. Nishiyama et al. (2020) report the discovery of microdiamond aggregates in the matrix of a metapelite from the Nishisonogi unit, Nagasaki metamorphic complex, western Kyushu, Japan. The Nishisonogi unit represents a Cretaceous subduction complex which has been considered as an epidote–blueschist subfacies metamorphic unit, and the metapelite is a member of a serpentinite mélange in the Nishisonogi unit (Nishiyama et al. 2020). The glaucophane and phengite ages are reported to be 95–90 Ma using the $^{40}Ar/^{39}Ar$ method (Faure et al. 1988) and 85–60 Ma using the K–Ar method (Hattori and Shibata 1982). The aggregates of diamonds range in size from 10 to 50 μm and they are embedded in dolomite, phengite, and albite (see Fig. 4 in Nishiyama et al. 2020). The diamonds are not sticking out above the polished surface of the sample. However, it should be noted that they are surrounded by soft minerals. Using SiC and Al_2O_3 abrasives as the main polishing abrasives, one would expect to see the diamonds "standing above" the flat surface of the surrounding softer minerals (see Fig. 4 in Nishiyama et al. 2020). This is because of the hardness of diamond itself, and it would not be "eroded" or 'flattened" by either SiC or Al_2O_3 abrasives since these abrasives are not as hard as diamond. Unfortunately, images where the diamonds are completely enclosed by the host minerals are not presented in this publication.

The authors characterized the microdiamonds with electron diffraction and Raman spectroscopy and carefully discussed both possibilities of metastable and stable conditions of diamond crystallization in metapelites of the epidote–blueschist subfacies from a Cretaceous subduction complex in Western Kyushu, Japan. They considered several lines of evidence for HP to UHPM conditions such as the presence of quartz pseudomorphs after coesite and high Si content in phengite. They speculate that almost all other HP–UHPM mineral assamblages have beed oblitered due to the retrograde metamorphism. Ultimately the authors hypothesized that the diamond crystallized from a COH fluid at $P > 2.8$ GPa and $T = \sim 450$ °C.

The authors specify that no diamond abrasives were used for sample polishing, and that ony Al_2O_3 and SiC were used. However, they did not specify if any diamond-bearing tools were used to extract or cut the samples prior to their polishing. Though Nishiyama et al. (2020) used FIB-TEM techniques they did not carefully examine the diamond–host mineral interfaces. In Figure 5a,b from Nishiyama et al. (2020) they show STEM images at different magnifications aquired from a FIB milled foil from the sample area contaning microdiamond aggregate. In Figure 5 plate c, Nishiyama et al. (2020) show a *d*-spacing = 2.06 Å (direction [111]) for the inner spot. Importantly, these data neither prove nor disprove that the diamond is indigeneous.

To unambiguously classify the metapelites from a Cretaceous subduction complex in Western Kyushu, Japan as a new UHPM terrane more FIB-TEM research is required on both the existing samples and/or new samples from this locality, and studies of the diamond–host mineral interface are necessary to confirm that the diamond is indigenous.

Lonsdaleite from WGR, Norway and Kokchetav massif, Kazakhstan, and a problem with its identification

Since lonsdaleite, a hexagonal polymorph of diamond, has been reported to occur in UHPM terranes as well as in meteorites and impact craters, a short discussion is warranted. At General Electric Company Bundy and Kasper (1967) synthesized a wurtzite like polymorph of carbon at $P = 13$ GPa and $T = 1000$ °C, and they named it hexagonal diamond. In nature hexagonal diamond was first identified from the Canyon Diablo iron meteorite and Goalpara ureilite (e.g., Frondel and Marvin 1967; Hanneman et al. 1967). It was named lonsdaleite in honor of the distinguished crystallographer Professor Kathleen Lonsdale (Frondel and Marvin 1967). Following this initial report lonsdaleite has been found in many other meteorites and impact craters (e.g., Daulton et al. 1996; Clarke et al. 1981; Kvasnitsya et al. 2013; Nakmuta and Toh 2013; Nestola et al. 2020). It has been reported to occur in the following terrestrial impact craters: Ries Crater, Germany (e.g., Rost et al. 1978), Popigai impact structure (e.g., Masaitis et al. 1972; Koeberl et al. 1997; Murri et al. 2019), Sudbury impact structure, Ontario, Canada (e.g., Masaitis et al. 1997), and Lappajärvi structure, Finland (e.g., Masaitis et al. 1998). There is also one report of lonsdaleite occurrence in nodules from Pipe 50, Fuxian kimberlite field, China (Leung and Winston 2002). These discoveries led to the hypothesis that lonsdaleite forms during impact events and very high pressure and temperatures are needed. However, it has also been reported to occur in UHPM rocks which would require alternative hypothesis to explain their existence.

Lonsdaleite has been reported in WGR, Norway (Godard et al. 2003, 2004; Smith et al. 2004) and in Kumdy Kol, Kokchetav massif, Kazakhstan (Smith 2004; Smith et al. 2004, 2011; Dubinchuk et al. 2010; Shumilova et al. 2011). Since these localities have been proven to be UHPM terranes by numerous studies, which clearly showed that they did not form during impact events, alternative hypotheses are required to explain the existence of lonsdaleite in UHPM rocks. One hypothesis is that the formation of hexagonal polytypes such as lonsdaleite could be cumulative with the metamictization of diamond (Smith et al. 2011; Smith and Godard 2013). Another hypothesis, which will be discussed in greater detail below, is that they formed during an impact event with a comet (Tretiakova and Luykin 2016, 2017).

Raman spectroscopy has been one of the most common techniques for confirming the presence of natural lonsdaleite since it is non-destructive, and mm-sized samples can be studied *in situ* (Smith and Godard 2009; Shumilova et al. 2011; Goryainov et al. 2014). Lonsdaleite has a 2H structure (spacegroup $P6_3/mmc$) which has three theoretically predicted Raman active modes, the transverse optical oscillations of the E_{2g} mode, and the longitudinal A_{1g} and transverse E_{1g} optical modes. Wu and Xu (1998) report the following theoretically predicted active modes E_{2g} 1193 cm^{-1}, A_{1g} 1312 cm^{-1}, and the E_{1g} 1305 cm^{-1}, while Denisov et al. (2011) predict them to be at 1221, 1280, and 1338 cm^{-1} respectively. The E_{2g} mode is predicted to have very low intensity so the A_{1g} and E_{1g} modes are typically used to identify lonsdaleite. Since the predicted lonsdaleite modes occur near the cubic diamond Raman active T_{2g} mode it should be noted that the peak position and width of the cubic diamond mode can vary significantly. As discussed by Nasdala et al. (2016) the peak position of the Raman active diamond mode can be downshifted and broadened by local heating through absorption of the laser (Herchen and Cappelli 1991), nanometer sized crystals (Lipp et al. 1997), substitution of ^{13}C for ^{12}C (Anthony and Banholzer 1992), incorporation of B-impurities (Pedroza-Montero et al. 2005) and accumulation of structural damage from nearby radioactive phases (Nasdala et al. 2013). Hence, one needs to be cautious when interpreting Raman spectra of natural diamonds since shifts in the cubic diamond Raman peak position and peak width could be misinterpreted as lonsdaleite.

Notably, there appears to be no consensus on the existence of lonsdaleite as a discrete mineral (e.g., Németh et al. 2014). Németh et al. (2014) point out that despite extensive efforts lonsdaleite has never been produced as a pure material and they show that defects in cubic diamond provide an explanation for the characteristic *d*-spacings and reflections reported for lonsdaleite. Natural lonsdaleite has been described as stacking disordered diamond where cubic and hexagonal sequences are interlaced in a complex way (e.g., Salzmann et al. 2015; Murri et al. 2019). Thus, while numerous studies of lonsdaleite have been reported from UHPM terranes, more studies of natural lonsdaleite using high-resolution techniques are needed to resolve this controversy.

ISOTOPIC STUDIES OF UHPM DIAMONDS

Carbon and nitrogen isotopes, and nitrogen content in UHPM diamonds

Carbon isotopic composition (expressed as $\delta^{13}C$, see Stachel et al. 2022, this volume for definition) is a key parameter used to constrain the origin and formation environment of a diamond. Since UHPM diamonds formed *in situ* in subducted continental lithologies, their carbon isotope ratios should reveal the origin of carbon, and the isotope fractionation of the COH fluids from which UHPM diamond formed. These carbon isotope ratios record the formation conditions both before and during diamond crystallization.

Among the reports on carbon isotopic compositions, E-type (eclogitic) and P-type (peridotitic) diamonds (e.g., Harris et al. 1975; Cartigny 2005; Stachel et al. 2022, this volume) found in kimberlites clearly show sfome similarities; both types of diamonds have a peak at approximately −5‰, which is similar to mantle-derived carbon observed in mid-ocean ridge basalts (MORBs), carbonatites, and kimberlites (Table 2, Fig. 7). The E-type diamond carbon isotopes are also spread towards lighter carbon to −41‰ (De Stefano et al. 2009; Smart et al. 2011), suggesting their crustal origin (Fig. 7).

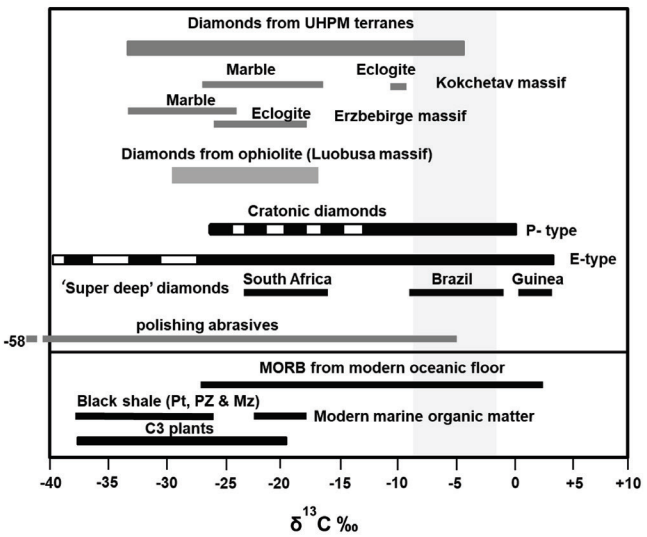

Figure 7. $\delta^{13}C$ characteristics of diamonds from UHPM terranes, diamonds from ophiolite (Luobasa chromitite massif), E-type and P-type of cratonic diamonds; modified after Liou et al. (2014), see Table 2 for references. $\delta^{13}C$ values of MORB, black shale of Proterozoic, Paleozoic, and Mesozoic ages and C3 plants adopted from Kohn (2010) and Meyers (2014).

Table 2. Carbon ($\delta^{13}C$) and nitrogen ($\delta^{15}N$) characteristics of diamonds, bulk rocks and carbon-bearing minerals from Kokchetav massif, Kazakhstan and Erzgebirge massif, Germany, kimberlitic xenoliths and ophiolitic chromitites.

Locality	Mineral/rock type	$\delta^{13}C$ value (‰)	$\delta^{15}N$ value (‰)	N content (ppm)	References
Kokchetav massif, Kazakhstan	diamonds-bulk measurements	−10.2 to −26.9			Chopin and Sobolev 1995; Lavrova et al. 1997
	diamond from garnet–clinopyroxene rocks;	−10.5			De Corte at al. 2000
	diamonds from marble	−10.2			
	diamond from garnet–clinopyroxene rock	−10 to −11	+5.9 (mean)	11,150	Cartigny et al. 2001
	diamond from marble	−8.5 to −10.19		2,650	
	S-diamond (outer rim) inclusion in garnet from dolomitic marble	−17 to −27			Imamura et al. 2013
	S-diamond (core) inclusion in garnet from dolomitic marble	−9 to −13			
	R-diamond inclusion in garnet from dolomitic marble	−8 to −15			
	Dolomite mineral from dolomitic marble	−4 to −7			Ohta 2003
	Dolomitic marble (bulk)	−2			
Erzgebirge Massif, Germany	Diamond inclusions in zircon (bulk analysis) from garnet–phengite gneiss	−24 to −33			Massonne and Tu 2007
	Diamond inclusions in zoned garnet (outer rim) from garnet–phengite–quartz–feldspathic gneiss	−22 to −26		740– 3,370	Dobrzhinetskaya et al. 2010
	Diamond inclusions in zoned garnet (core zone) from garnet–phengite–quartz–feldspathic gneiss	−17 to −19			Dobrzhinetskaya et al. 2010

Locality	Mineral/rock type	$\delta^{13}C$ value (‰)	$\delta^{15}N$ value (‰)	N content (ppm)	References
Worldwide UHPM terranes	UHPM metamorphic rocks	−3 to −30	−1.8 to +12.4		Cartigny 2005
Worldwide kimberlite-derived diamonds	Eclogitic diamonds	−40.7 to +2.5	−13.1 to +16.9	≤5 to 3833	Stachel et al. 2022
	Peridotitic diamonds	−34.5 to +2.3	−39.4 to +15	≤5 to 1923	Stachel et al. 2022
Luobusa ophiolitic massif (Tibet)	Chromitite	−18 to −28		20–670	Yang et al. 2013

A typical feature of UHPM diamonds is their yellow color (e.g., Schertl and Sobolev 2013) due to the presence of isolated nitrogen, which is the main substitutional impurity in diamond. Nitrogen has an extra electron compared to carbon, and the incorporation of a few ppm of isolated nitrogen atoms and their accompanying electrons changes the energy band gap in diamond to a level equivalent to absorption of blue and violet lights, resulting in a yellow color. The concentration of nitrogen, which is the main substitutional diamond impurity, is also an important parameter when it is combined with $\delta^{13}C$ to constrain the origin of metasomatic COH fluids and therefore diamond formation conditions (Table 2, Fig. 8). As noted by Cartigny et al. (2014), the behavior of nitrogen during diamond formation is unclear since nitrogen in diamond may be both compatible and incompatible (Smart et al. 2011; Palot 2013). On the contrary, if nitrogen compatibility is experimentally constrained, it would shed light on the composition, redox state, and evolution of the fluids related to UHPM diamond formation.

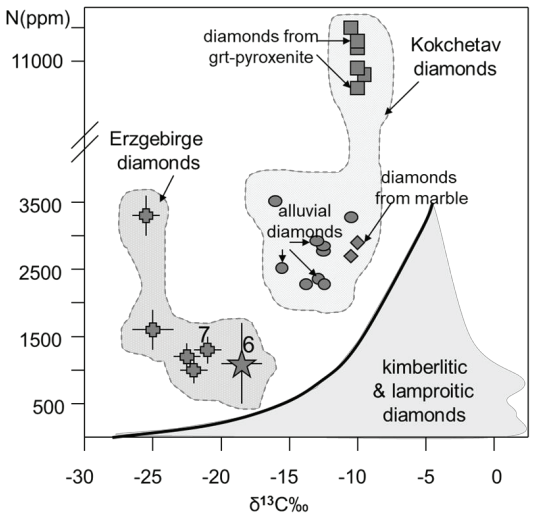

Figure 8. Nitrogen content versus $\delta^{13}C$ in the Erzgebirge microdiamonds included in garnets (Dobrzhinetskaya et al. 2010 with the Springer Nature permission #5034451417904). Diamonds #6 (**star**) and #7 (**cross**) are situated in the same garnet crystal in the core and the rim respectively. The fields of kimberlitic and lamproitic diamonds, and diamonds from garnet pyroxenite (**square**), marbles (**diamond**) and from alluvial deposits of the Kokchetav massif, Kazakhstan are adopted from Cartigny et al. (2001, 2003).

Nitrogen isotopic composition (expressed as $\delta^{15}N$, see Stachel et al. 2022, this volume for definition) also provide a clue to the origin of diamonds. Crustal nitrogen is enriched in ^{15}N, by approximately +5‰ compared with the atmosphere ($\delta^{15}N = 0$‰), whereas mantle nitrogen is depleted in ^{15}N by approximately −5‰. Being different to carbon, nitrogen isotopes are fractionated by only a few per mill during their incorporation into diamond, so nitrogen that is incorporated into diamond during crystallization is representative of the growth medium. Most E-type diamonds have a mantle-like $\delta^{15}N$, which is inconsistent with their origin from subducted organic carbon. On the other hand, UHPM diamonds systematically exhibit heavy $\delta^{15}N$ values ranging from +2 to +12 ‰ (Cartigny et al. 2001, 2014), suggesting their sedimentary source because devolatilization during sediment subduction would preferentially release ^{14}N, resulting in further enrichment of subducted material in ^{15}N (Bebout and Fogel 1992; Busigny et al. 2003). For thorough discussion on the origin of carbon and nitrogen isotopic compositions of diamond, the reader is refered to Stachel et al. (2022, this volume).

Carbon isotopes characteristics of the Kokchetav diamonds. Carbon isotopic composition studies of UHPM diamonds are limited due to their mm-size. One approach involves separating and grouping tens of thousands of microdiamonds and processing them together so that there is enough CO_2 to be analyzed with a conventional isotope-ratio mass spectrometer, this approach provides the average $\delta^{13}C$ ratio. For instance, Cartigny et al. (2001) reported $\delta^{13}C = -11$ ‰ to −10 ‰ in diamonds from garnet–clinopyroxene rocks and nitrogen contents of 11,150 ppm, while diamonds from marbles of the Kokchetav massif, Kazakhstan have a $\delta^{13}C = -10.2$‰ to −8.5‰ and 2650 ppm of nitrogen (Table 2, Fig. 8). Based on possible carbon isotope fractionation between coexisting carbonate and diamond, Cartigny et al. (2001) estimated diamond crystallization conditions as $T \leq 700$ °C and $P = 3$ GPa, e.g., slightly below the peak of UHPM, and concluded carbon and nitrogen stable isotopes strongly support their metasedimentrary origin. If Cartigny et al. (2001) data is combined with earlier $\delta^{13}C$ bulk measurements of the Kokchetav diamonds, they fall in range of −10.2 ‰ to −26.9 ‰ (e.g., Lavrova et al. 1997; Chopin and Sobolev 1995; Ogasawara 2005).

Later, Imamura et al. (2013) using Secondary Ion Mass Spectrometry (SIMS) technique analyzed carbon isotopes in diamonds (10–25 μm in size) included in garnet from dolomite marble of the Kokchetav Massif. These diamonds were subdivided on to morphological types: S-type consisting of single-crystal core and polycrystalline rim, and R-type presented by single crystal with rugged surfaces. In S-type diamonds the rim exhibits lighter $\delta^{13}C = -17$ to −27‰, whereas the core is much heavier, with $\delta^{13}C = -9$ to −13‰. The R-type diamonds fall into narrow ranges of $\delta^{13}C = -8$ to −15‰, which are like those in the core of the S-type diamond. This suggests that the R-type diamonds probably formed at the same stage as the core of the S-type, whereas rim growth during the second stage did not occur, or occurred, very weakly in R-type microdiamonds. Therefore, carbon isotopic data corroborate a two-stage growth of microdiamond in the Kokchetav dolomite marbles (Imamura et al. 2013).

Interestingly, the $\delta^{13}C$ value of dolomite from the host rocks ranges from −4 to −7‰, whereas the bulk dolomitic marble exhibits $\delta^{13}C = -2$‰ (Ohta et al. 2003). The marginal range of $\delta^{13}C = -8$ to −27‰ in S-type and R-type diamonds is different than that in mineral dolomite ($\delta^{13}C = -4$ to −7‰) and dolomitic marble host rock ($\delta^{13}C = -2$‰). It is difficult to attribute these differences to isotopic fractionation considering that the metamorphic temperature was very high (~1000 °C; e.g., Ogasawara et al. 2000). Under such conditions, the diamonds in dolomitic marble would not have been in carbon isotopic equilibrium with the dolomite. There appears to be no good candidate material or process that could occur in the dolomitic marble that would explain the origin of the very light $\delta^{13}C$ values between −17 and −27‰, measured in the rim of the S-type diamonds. Imamura et al. (2013) speculated that perhaps a fluid with a light carbon isotope ratio infiltrated into the dolomite marble from the surrounding gneisses, which might contain light carbon of organic origin. With regards to this explanation, it will

be discussed below that the Erzgebirge microdiamonds from felsic gneiss have a similar light carbon, e.g., $\delta^{13}C = -17$ to $-27‰$ (Dobrzhinetskaya et al. 2010). However, Imamura et al. (2013) have not discussed these data because no carbon isotope measurements in diamonds from felsic gneisses of the Kokchetav massif have been reported.

Carbon isotope characteristics of the Erzgebirge diamonds. Massonne and Tu (2007b) used a bulk analysis approach to obtain the carbon isotope ratios of diamond inclusions in zircons from the Erzgebirge UHPM terrane, and they reported that lighter carbon was involved ($\delta^{13}C = -24‰$ to $-33‰$) in diamond formation where the precursor was graphite.

Dobrzhinetskaya et al. (2010) used SIMS to analyze the $\delta^{13}C$ and nitrogen contents in ~5 to 10 μm diameter diamonds included in garnet from the garnet–quartz–feldspathic gneiss of the Erzgebirge massif (Fig. 9). They showed that the diamonds situated within the garnets closer to the garnet rim zone showed some $\delta^{13}C$ variations up to 10‰, with average values ranging from −22 to −26‰ (Table 2, Fig. 9). Their nitrogen contents vary heterogeneously between each individual measurement and between all diamonds without any systematics, ranging from 240 to 4600 ppm. On the other hand, the diamonds situated closer to the central part of the zoned garnet exhibits $\delta^{13}C = -17$ to $-19‰$, with an average value of −17.8‰. The latter is heavier than another diamond in the intermediate zone of the same garnet ($\delta^{13}C = -23‰$) and the other diamonds situated closer to the outer zone of the garnet (Fig. 10). Nitrogen in the diamonds from intermediate zone varies from 100 to 1200 ppm, with an average value of 820 ppm; and average value of nitrogen in diamonds from outer garnet zone is 1,838 ppm. The nitrogen content data plotted versus $\delta^{13}C$ show a weakly pronounced tendency to increase with the increase of lighter carbon isotope content in the diamonds (Fig. 8).

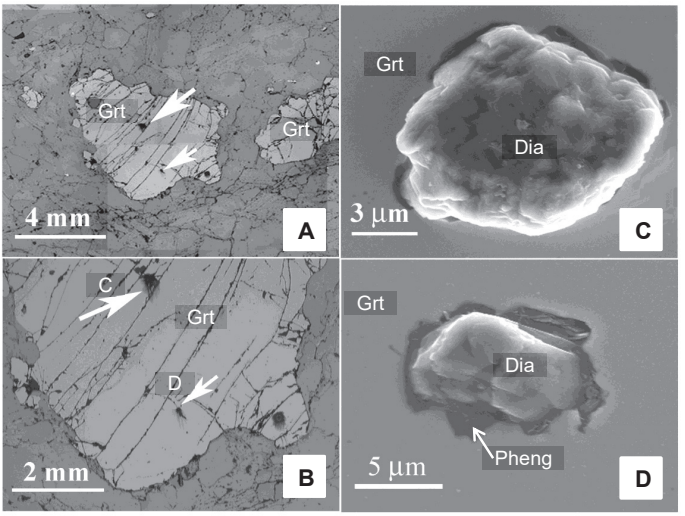

Figure 9. Carbon isotope characteristics in Erzgebirge diamonds (Dobrzhinetskaya et al. 2010, copyirght 2010 with the Springer Nature permission #5034451417904)**. A** and **B**–optical microscope digital microphotograph shows (reflected light) the polished slide from Erzgebirge garnet–quartz–feldspathic gneiss. Garnet contains inclusions of microdiamonds (indicated by **white arrowheads**). Plates **C** and **D**–Secondary Electron SEM images of diamonds (shown as C and D in plate B) inclusions in garnet. Diamond in plate C which is situated in the central part of the garnet (see A) has $\delta^{13}C = -17$ to $-19‰$, whereas diamond D situated at the outer part of the zoned garnet is characterized by $\delta^{13}C = -22$ to $-26‰$.

Based on relationships between the diamond inclusion in the garnet (Fig. 10), diamond formation can be constrained by the chemical zoning of the host garnet, and $\delta^{13}C$ values of two diamonds. Dobrzhinetskaya et al. (2010) argued that there were two stages of diamond crystallization from a COH fluid rich in biogenic carbon and diverse in minor elements of crustal origin. The $\delta^{13}C$ of the first stage of crystallization falls within the range of −17 to −19‰, while the second stage of crystallization is characterized by $\delta^{13}C$ = −22 to −26‰. Both $\delta^{13}C$ ranges strongly suggest that the carbon from which they crystallizedbelongs to the same biogenic reservoir. Graphite from the 3.7 Ga-old turbidite greywacke and slate from West Greenland have primary $\delta^{13}C$ = −19‰, which is similar to the range of biologically reduced carbon, and it is within the range of reduced-carbon compositions found in most modern marine sediments (e.g., Rosing 1999). Dobrzhinetskaya et al. (2010) suggest that the 1st-stage of diamond crystallization was from a more reduced carbon than the second stage of crystallization. This work indicates that within Erzgebirge diamond populations there are two $\delta^{13}C$ signatures which are distinguished from each other not only by $\delta^{13}C$ values but also by the positions of the diamond within the garnet where different zones in the garnets are related to recrystallization events during UHP metamorphism. It also suggests that the carbon-rich fluid that deeply infiltrated the subducted sediments was probably reduced during an earlier stage, producing diamonds with slightly heavier isotopes than the diamonds that crystallized during the second stage.

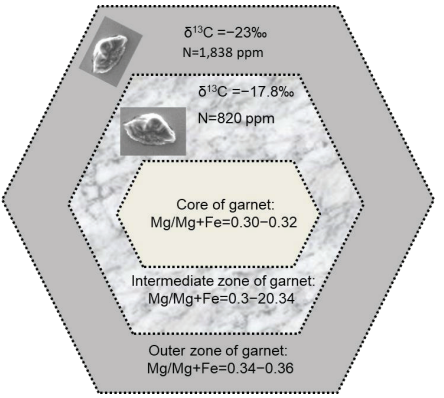

Figure 10. Sketch of the slightly zoned garnet with microdiamond inclusions situated within the intermediate zone between the core and the outer rim and close to the outer zone of garnet. Microdiamonds located in the intermediate zone of the garnet (Mg/Mg+Fe = 0.32–0.34) are characterized by "heavier" isotopes of carbon $\delta^{13}C$ = −17.8‰ and a N concentration of 820 ppm, whereas diamonds from outer garnet zone (Mg/Mg+Fe = 0.34–0.36) are characterized by "lighter" isotopes of carbon $\delta^{13}C$ = −23‰ and a N content of 1838 ppm (data are adopted from Dorzhinetskaya et al. 2010).

Additional carbon isotope analysis of UHPM diamonds from both Kokchetav and Erzgebirge UHPM terranes and any of the new UHPM localities at small scales (μm to nm) with SIMS are necessary to shed light on the evolution of carbon-bearing fluids in subducted continental lithologies before and during diamond formation.

Noble gas isotopes in diamonds from UHPM terranes

Noble gas isotopes in mantle-derived samples are key tracers of chemical heterogeneity of the Earth's mantle and the origin of the atmosphere (e.g., Ozima and Podosek 2002; Porcelli and Ballentine 2002). Samples of MORBs (quenched glass of mafic minerals) and

ocean island basalts (OIB) have provided the most comprehensive understanding of mantle noble gases. MORBs show relatively uniform $^{3}He/^{4}He$ ratios around 1.1×10^{-5} and a trend in $^{22}Ne/^{22}Ne$–$^{20}Ne/^{22}Ne$ ratios toward a composition more enriched in nucleogenic ^{21}Ne. In contrast, OIB samples, which are derived from a deeper region of the mantle, exhibit higher $^{3}He/^{4}He$ ratios of up to 7×10^{-5} and less nucleogenic Ne isotope compositions (Honda et al. 1991; Trieloff et al. 2000; Graham 2002; Stuart et al. 2003). The latter characteristics are believed to be evidence for a mantle source in which primordial He, with $^{3}He/^{4}He$ of $(1.4–4.6) \times 10^{-4}$, and Ne ("solar" or "Ne–B" composition, Honda et al. 1991; Trieloff et al. 2000; Ballentine et al. 2005) has been less diluted by the addition of radiogenic ^{4}He and nucleogenic ^{21}Ne produced by decay of U- and Th-series elements. The primordial noble gas source is considered to have been isolated from whole mantle convection over geological timescales and sampled by upwelling mantle plumes (Jackson et al. 2010; Mukhopadhyay 2012). However, the reasons for the less radiogenic/nucleogenic character of the plume source are still under debate; it may be "undegassed" (e.g., Allègre et al. 1983; Kaneoka 1983; Kurz et al. 1982; Porcelli and Ballentine 2002; Porcelli and Elliott 2008; Mukhopadhyay 2012), or it may be depleted in U and Th by ancient melt extraction events (Parman 2007; Porcelli and Ballentine 2002; Jackson et al. 2010). The main advantage of analyzing noble gases contained in diamonds is their great potential to constrain the noble-gas state of the deep mantle because they are formed deeper than 150 km and act as chemically/mechanically stable "capsules". Most noble gas studies are focused on kimberlitic diamonds (e.g., Basu et al. 2013; Timmerman et al. 2018).

"Unprecedentedly" high Helium-3 content in the Kokchetav diamonds: myth or reality? Although currently there are dozens of UHPM diamond-bearing terranes that are known, only a few noble gas studies of microdiamonds from the Kokchetav massif have been reported (Begemann 1994; Pleshakov and Shukolyukov 1994; Shukolyukov et al. 1993; Verchovsky et al. 1993; Sumino et al. 2011). Due to the small (micrometer) size of UHPM diamonds, noble gas analyses were conducted using several tens-of-thousands (or even a greater number) of microdiamonds that were separated from their host rocks/minerals by treatments with HF and oxidizing acids. Pleshakov and Shukolyukov (1994) and Shukolyukov et al. (1993) reported "unprecedentedly" high $^{3}He/^{4}He$ ratio during in vacuo stepwise heating of Kokchetav microdiamonds with a maximum value of 0.47 in the low temperate release, which was the highest He content known among terrestrial diamonds (Pleshakov and Shukolyukov 1994; Shukolyukov et al. 1993). Moreover, this high $^{3}He/^{4}He$ value exceeds the maximum values reported for any terrestrial mantle-derived sample of $\leq 7 \times 10^{-5}$ (Stuart et al. 2003) and even the primordial $^{3}He/^{4}He$ value of $(1.7–4.6) \times 10^{-4}$ (Porcelli and Elliott 2008).

The most plausible source of the high $^{3}He/^{4}He$ ratio is nucleogenic ^{3}He production via the $^{6}Li(n, \alpha)^{3}H$ (β) ^{3}He reaction (Kurz et al. 1987). However, this requires an anomalously high Li content of ~100 ppm either in the diamonds, or within a ~20 μm vicinity in the host rocks (Begemann 1994; Verchovsky et al. 1993). Moreover, the host rock would need to contain more than 1% of U (Th/U = 3.3 is assumed) to provide a neutron source sufficient to produce the levels of ^{3}He observed (Begemann 1994; Verchovsky et al. 1993). An important feature of the Kokchetav diamonds was that high $^{3}He/^{4}He$ values were obtained from gas released over the relatively low temperature range of 200–1100 °C during in vacuo stepwise heating (Pleshakov and Shukolyukov 1994; Shukolyukov et al. 1993). These temperatures are significantly lower than the diamond graphitization temperature (over 1700 °C), and lower than the temperatures at which noble gases trapped in the diamond lattice are released. This suggests that the high $^{3}He/^{4}He$ component was not hosted by the diamond itself. Although Verchovsky et al. (1993) confirmed release of He with high $^{3}He/^{4}He$ (2.4×10^{-4}) during in vacuo heating of the Kokchetav diamonds at 820 °C. However, He released during diamond combustion under a controlled oxygen atmosphere showed a rather low $^{3}He/^{4}He$ ratio of $\leq 3 \times 10^{-6}$. Additionally, Verchovsky et al. (1993) showed that the amount of 'excess' ^{3}He (as well as $^{3}He/^{4}He$ ratio) strongly depends on the grain-size of diamond fractions: the coarser the fraction the less (by orders of magnitude) the

^{3}He concentration. These findings were interpreted to indicate that the high ^{3}He/^{4}He component may reside in Li-rich contaminants, which are quite resistant to treatments with HF and oxidizing acids during diamond separation from their host minerals/rocks, and therefore not trapped within the diamond itself (Begemann 1994; Verchovsky et al. 1993).

To clarify this "unprecedented" ^{3}He/^{4}He value Sumino et al. (2011) focused their attention on the presence of abundant nanometer-sized fluid inclusions in Kokchetav microdiamonds (Dobrzhinetskaya et al. 2001, 2005, 2006a), which could provide potential sites for preserving the noble gas signature of the diamond-forming COH fluid. Sumino et al. (2011) employed in vacuo sequential dynamic crushing extraction with which sample grains are mechanically crushed in vacuum in order to selectively extract noble gases from fluid/melt inclusions with significantly less noble gas release from the diamond lattice and any associated mineral inclusions (Kurz 1986; Kurz et al. 1987).

The crushing technique results were compared with those obtained from a conventional vacuum stepped heating method which releases noble gases from fluid and solid inclusions and the diamond lattice. According to Sumino et al. (2011) the diamond crushing process extracts most of the ^{3}He, indicating that ^{3}He occurs within inclusions trapped during the Kokchetav diamond formation. The inclusion-hosted ^{3}He/^{4}He of (3.3–6.5) × 10^{-5} is significantly higher than that of the MORB-source mantle (1.1 × 10^{-5}), but close to the maximum value observed in OIBs (~7 × 10^{-5}) containing noble gases enriched in a primordial component and delivered from the deep mantle by plumes. On the other hand, very low ^{3}He/^{4}He (5.0 × 10^{-8}) obtained by heating of the crushed powder supports the presence of radiogenic ^{4}He in the diamond lattice, resulting from α-particle implantation from U- and Th-series radioactive elements in the diamond-bearing minerals, which is consistent with the combustion results by Verchovsky et al. (1993). The results of Sumino et al. (2011) clearly indicate that the fluid inclusions in the Kokchetav diamonds preserve primordial He similar to those observed in OIBs and that abundant He with "unprecedentedly" high ^{3}He/^{4}He ratio reported by previous works (Shukolyukov et al. 1993; Pleshakov and Shukolyukov 1994) should be attributed to Li-rich contaminants resistant to separation treatments of the diamonds from their host rocks/minerals (Verchovsky et al. 1993; Begemann 1994).

Sumino et al. (2011) showed that isotope compositions of Ne (^{20}Ne/^{22}Ne and ^{21}Ne/^{22}Ne ratios) extracted from the Kokchetav diamonds during relatively low-temperature heating steps are on the trend defined by OIBs from deep-mantle-derived hotspots (e.g., Hawaii, Iceland, and Galapagos) which are enriched in primordial Ne (Honda et al. 1991; Trieloff et al. 2000; Kurz et al. 2009) but deviate from the trend defined by MORB data (Sarda et al. 1988) (Fig. 11). The Ne-isotope data indicate that deep-mantle-derived, primordial Ne is an intrinsic feature of the microdiamonds, but at higher temperatures during diamond graphitization, the Ne released shows a nucleogenic contribution. The Ne isotope data indicate that primordial Ne is an intrinsic feature of the microdiamonds, but at higher temperatures during diamond graphitization, the Ne released shows a nucleogenic contribution. The nucleogenic Ne resides in the diamond lattice as a result of implantation by recoiling Ne isotopes mainly produced during the reaction of α-particles (from U–Th decay) with oxygen and fluorine atoms in surrounding rocks (Kurz et al. 1987; Lal 1989; Verchovsky et al. 1993). The nucleogenic Ne composition released from the microdiamonds requires a very high F/O ratio of 0.02 (Fig. 11B) compared with the average crustal values of 0.0013 (Ballentine and Burnard 2002).

The observation that deep-mantle-derived, plume-like noble gases are contained in the Kokchetav microdiamonds paradoxically requires that deep-mantle-derived volatiles be present in the relatively shallow mantle wedge at 190–280 km depth. To solve this paradox, Sumino et al. (2011) suggest a few possible processes which are either capable of bringing deep-mantle-derived noble gases to the relatively shallow mantle: (i) a plume tapped from the lower mantle or core–mantle boundary; and/or (ii) a large-scale mantle convection cell which entrained a fragment of the deep mantle, and subsequently added it to the mantle wedge at depths of 190–280 km.

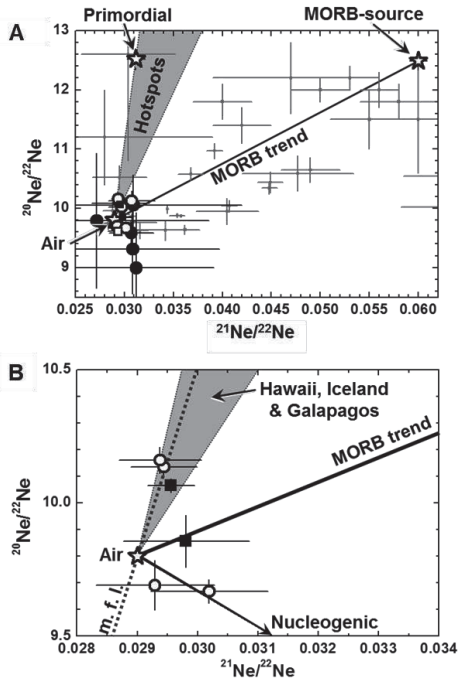

Figure 11. A–Neon three-isotope plot for the Kokchetav microdiamond, and plate **B** is a magnification of plate A. **Solid and open circles** were obtained by crushing and heating of the Kokchetav microdiamonds, respectively. Total isotope ratios of the heating steps (**solid squares**) and that of the crushed–powder heating (**open square**) are also shown. Reported data for kimberlitic diamonds (**solid small squares**, Gautheron et al. 2005; Honda et al. 1987, 2004; Ozima and Zashu 1988, 1991; Wada and Matsuda 1998; Broadley et al. 2018) are shown for comparison. End-member compositions (air, primordial, and MORB-source mantle) are shown as designated stars. Primordial and MORB-source mantle compositions and a trend which is formed by the data for hotspots (Hawaii, Iceland and Galapagos) enriched in the primordial component are taken from Trieloff et al. (2000), Sarda et al. (1988) and Kurz et al. (2009). Data point uncertainties are 1σ. Reference lines for nucleogenic production assuming the average crustal composition and F/O = 0.02 (Ballentine and Burnard 2002) and mass fractionation line (m.f.l.) of atmospheric Ne (Ozima and Podosek 2002) are shown as **solid and dotted lines**, respectively. Adapted from Sumino et al. (2011) with permission of Elsevier #5036211173353.

To date there is no geological evidence in the vicinity of the Kokchetav massif of mantle plume activity at the time of diamond formation (~530 Ma). A plume may have interacted with the subcontinental lithosphere which was beneath metasedimentary rocks before the Kokchetav slab was subducted and microdiamonds formed. To clarify the origin of the plume-like, deep-mantle-derived noble gases in the Kokchetav microdiamonds, more investigation is required particularly on UHPM diamonds from other localities. If metasomatism by plume-derived volatiles is essential for subduction and exhumation of continental crust as proposed by Seno and Rehman (2011), and the metasomatic volatiles play an important role in UHPM diamond formation, then plume-like noble gas is expected to be observed in UHPM diamonds from other localities.

MECHANISMS OF METAMORPHIC DIAMOND FORMATION

It is generally agreed upon that during a continent–continent collision crustal rocks can be subducted to depths of >150 km, which leads to the formation of UHPM terranes, however readers may be surprised to learn that there are countless hypotheses for the origin of microdiamonds found in these terranes. The debates are primarily focused around the crystallization conditions of diamond, some of the hypotheses include (i) from carbon-rich supercritical fluids vs. hydrous silicate and/or carbonatite melts, (ii) oxidation state of the media (e.g., see reviews: Ogasawara 2005 ; Frezzotti et al. 2011, 2014; Dobrzhinetskaya 2012; Schertl and Sobolev 2013; Liou et al. 2014; Zhang et al. 2017; Frezzotti 2019), (iii) stable vs. metastable conditions (e.g., Pechnikov and Kaminsky 2008, 2011; Simakov 2010), and/or (iv) from meteorite impact (Tretyakova and Luykin 2016, 2017). These hypotheses will be discussed individually in greater detail below.

During the last decade there have been attempts to resolve some of these disagreements which have resulted in considerable progress in our understanding of the formation conditions of microdiamonds. Particularly advancements in high resolution instruments such as STEM, FIB, a 'Structural & Chemical Analyser' (SCA) probe and 'inVia' Raman spectrometer (a Renishaw trademark) combined with SEM system (e.g., O'Bannon et al. 2020), μm and sub-μm monochromatic and white beam synchrotron X-ray diffraction (e.g., Stan et al. 2020) and synchrotron infrared (IR) micro-spectroscopy (e.g., Dobrzhinetskaya et al. 2006b) have all made it possible to perform analyses at the nano-scale of solid and gas/liquid inclusions in microdiamonds. Table 3 presents summarized information on nanoscale inclusions detected in diamonds from UHPM terranes by different techniques.

As new instruments and technology are adopted by researchers it has led to many other important discoveries and increased our knowledge about the origins of microdiamond. Moreover, the integration of high-pressure devices such as multianvil presses and diamond anvil cells into synchrotron X-ray facilities has enabled a wide range of experiments to study UHPM diamond crystallization at varying pressures, temperatures, fO_2, X_{H_2O}, organic/inorganic carbon and different bulk chemistry of the starting materials (e.g., Akaishi and Yamaoka 2000; Yamaoka et al. 2000; Kumar et al. 2001; Pal'yanov et al. 2002, 2013; Dobrzhinetskaya et al. 2004; Dobrzhinetskaya and Green 2007a; Zhang et al. 2011). These experiments have demonstrated that the kinetics of diamond crystallization varies depending on different experimental conditions such as hydrous or anhydrous, oxidation states, and if the pressure and temperature are high enough to stabilize sp^3 carbon bonding.

Table 3. Inclusions reported in microdiamonds from different UHPM terranes

Diamond locality	Rock type	Inclusions in diamonds	Identification method	References
Kokchetav massif, Kazakhstan	Garnet clinopyroxenite	CO_3^{2-}; H_2O; OH^-	IR spectroscopy	de Corte et al. 1998
	Garnet–biotite–gneiss	crystalline inclusions (40–80 nm)*: $Fe_2Si_2O_6$; TiO_2; Cr_2O_3; Fe_xO_y; SiO_2; $MgCO_3$; $ZrSiO_4$; $BaSO_4$; Th_xO_y ; almost all inclusions show trace components of: Si, Cr, Fe, Ti, Mg, Ca, Al, K, Na, S, P, Nb, Cl, Zn, Ni	FIB-TEM, SEM, EDX	Dobrzhinetskaya et al. 2001, 2003
	Garnet–biotite–gneiss	Si, K, P, Cl glass (1–5 nm)	AEM, EDX	Hwang et al. 2006
	Dolomite marble	Ultrapotassic fluid inclusions (<500 nm); low in SiO_2	AEM, EDX	Hwang et al. 2006
	Garnet–quartz–clinopyroxene	K rich Si poor fluid/melt in intergranular pockets within a microdiamond aggregate	AEM, EDX	Hwang et al. 2006
	Dolomite marble	$CaCO_3$ (Fe, Mg) aragonite (10–100 nm) along with COH fluid inclusions	FIB-TEM, EDS	Dobrzhinetskaya et al. 2005
	Dolomite marble	$CaCO_3$ (aragonite), $CaCO_3$, $MgCO_3$; N-bearing phase (5–250 nm)	FIB-TEM, EDS	Dobrzhinetskaya et al. 2006a

Diamond locality	Rock type	Inclusions in diamonds	Identification method	References
Erzgebirge, Germany	Gneiss lenses within migmatites of gneiss–eclogite	Silicates, apatite, rutile and diamond, altogether are included in a former fluid/melt pocket	SEM, EDS, EBSD	Stöckhert et al. 2001
	Quartz–feldspathic gneiss	Solid inclusions (20–60 nm)*: SiO_2, Al_2SiO_5, KH_2PO_4, Pb_xO_y or $PbCO_3$; unknown stoichiometry phases*: Si, K, P, Ti, O or Si, O; Si, Fe and O	FIB-TEM, SEM, EDX	Dobrzhinetskaya et al. 2003
	Quartz–feldspathic gneiss	P/K rich silica glass	AEM, EDS	Hwang et al. 2005
	Quartz–feldspathic gneiss	Molecular H_2O, OH^-, CO_3^{2-} and SiO_2; Pb_xO_y or $PbCO_3$; Al_2SiO_5	Synchrotron IR spectroscopy	Dobrzhinetskaya et al. 2006b
	Quartz–feldspathic gneiss	Silicates, apatite, rutile and diamond are included in former fluid/melt pockets located inside of garnet	SEM, EBSD, EDS	Stöckhert et al. 2009
	Garnet–phengite–quartz–feldspathic gneiss	Solid inclusions (5–20 nm)*: $KAlSi_3O_8$; Na_2SO_4; SiO_2; $KAlSi_3O_8$; $CaCO_3$; $ZrSiO_4$; $BaCO_3$ occurring inside of the diamond or at the diamond–diamond interface, almost all inclusions show trace amounts of some of these elements: Fe, Al, Cl, Mg, Ti, Pb, K, Ca, P, Cr	FIB-TEM, SEM, EDS, EELS	Dobrzhinetskaya et al. 2013
Lago di Cignana, western Alps, Italy	Oceanic metasedimentary rocks	Mg-calcite, rutile, graphite like amorphous carbon, SO_4^{2-}; HCO_3^-; CO_3^{2-}; $Si(OH)_4$ monomer; deprotonated monomers $SiO(OH)_3^-$ and $SiO_2(OH)_2^{2-}$	Raman and electron microprobe	Frezzotti et al. 2011

Note: *crystal structure was not determined due to the extremely small size of inclusions.

UHPM diamonds crystallized from a multicomponent supercritical COH fluid or a hydrous silicate melt. Studies of nanometric fluid and solid inclusions in microdiamonds (Table 3) have revealed important information on the crystallization conditions of microdiamonds. Conventional infrared (IR) spectroscopic studies revealed the presence of molecular H_2O and CO_3^{2-} radical from Kokchetav microdiamonds occurred in garnet clinopyroxenite, calc-silicate, garnet–pyroxene–quartz rocks and gneisses (e.g., de Corte et al. 1998, 2002; Sitnikova and Shatsky 2009). Dobrzhinetskaya et al. (2006b) carried out synchrotron IR spectroscopic studies of the Erzgebirge diamonds separated from garnet–phengite–quartz–feldspathic gneisses using a thermochemical microwave digesting method. They collected synchrotron IR spectra from two diamond crystals (Fig. 12).

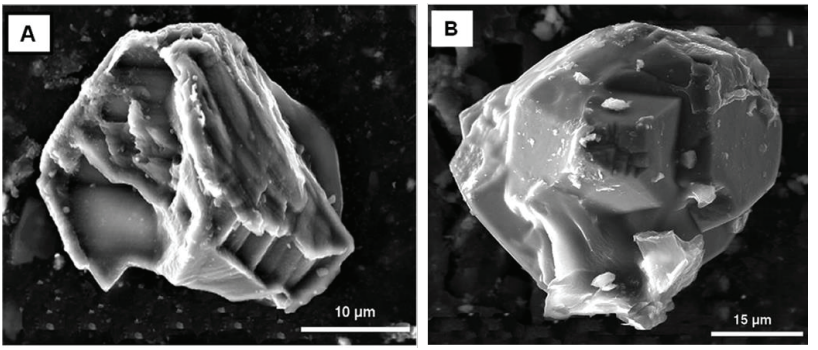

Figure 12. Secondary electron SEM images of diamonds extracted from garnet–phengite–quartz–feldspathic gneiss from the Erzgebirge massif, Germany: (**A**) diamond #1, (**B**) diamond #2 (Reprinted from Dobrzhinetskaya et al. 2006b, copyright 2006 with the permission of Elsevier # 5035711034058).

Both spectra (Fig. 13) show the presence of nitrogen impurities, molecular H_2O, OH^- hydroxyl radical, CO_3^{2-} radical, and silicate inclusions in addition the C–C diamond phonon absorption bonds. Dobrzhinetskaya et al. (2006b) intentionally studied the same samples with synchrotron IR that had been previously studied using FIB-TEM techniques (Dobrzhinetskaya et al. 2003). Abundant nanometric solid crystalline inclusions were found in the diamond FIB-foils; some of the identified phases are: (i) SiO_2-containing traces of K, P, Ti, Fe; (ii) inclusion of unknown stoichiometry which consists of three elements, K, P, and O, (iii) oxide Pb_xO_y, (iv) carbonate (Pb_2CO_3), and (v) Al_2SiO_5. Due to the extremely small size of these inclusions and their random orientations, their lattice parameters could not be determined by selected-area electron diffraction (SAED), however, all of them yield Bragg diffraction spots confirming their crystalline nature.

Besides the presence of crystalline nano-inclusions a considerable amount of nanometric-size euhedral cavities representing traces of decrepit fluid were documented. Many of these cavities were associated with dislocations related to diamond growth and are evidence of diamond nucleation and growth that took place in a COH fluid-rich media (Dobrzhinetskaya et al. 2003). The presence of larger scale diamond-bearing multiphase inclusions (or "pockets") inside of garnets and zircons (Fig. 14) observed in polished slides with optical microscopy and scanning electron microscopy corroborate perfectly with the nanoscale observations (Stöckhert et al. 2001; Dobrzhinetskaya et al. 2003, 2006a). Moreover, direct TEM observations of fluid-filled nanometric inclusion-bubbles preserved in FIB foil prepared from the Kokchetav diamond, and the serendipitous measurement of their contents immediately after bursting, showed that the fluid consists of C, H, O, Cl, S, Ca, Fe and K (Dobrzhinetskaya et al. 2005). This well-documented direct observation of residual fluid bubbles in microdiamonds unambiguously establishes their fluid growth medium.

Polycrystalline microdiamonds appear to be the best samples to study nano-fluid inclusions. There are several types of polycrystalline diamonds from the Kokchetav massif: (i) "spiral diamonds" which formed from a metal–sulfur–COH–silicate fluid (Hwang et al. 2003), (ii) S-type (star-shaped) and R-type (rugged face) diamonds that crystallized from a fluid during two stages (Ishida et al. 2003; Ogasawara 2005), and (iii) "overgrown" diamonds which crystallized from an aqueous-carbonate and aqueous-silicate fluid/melt (Sitnikova and Shatsky 2009). Polycrystalline diamond has also been described as daughter crystals associated with larger diamonds included in garnets from Erzgebirge felsic gneisses (Stöckhert et al. 2001, 2009). Stöckhert et al. (2009) concluded that the tiny daughter crystals precipitated from a supercritical COH + K-, Na-rich silicate fluid.

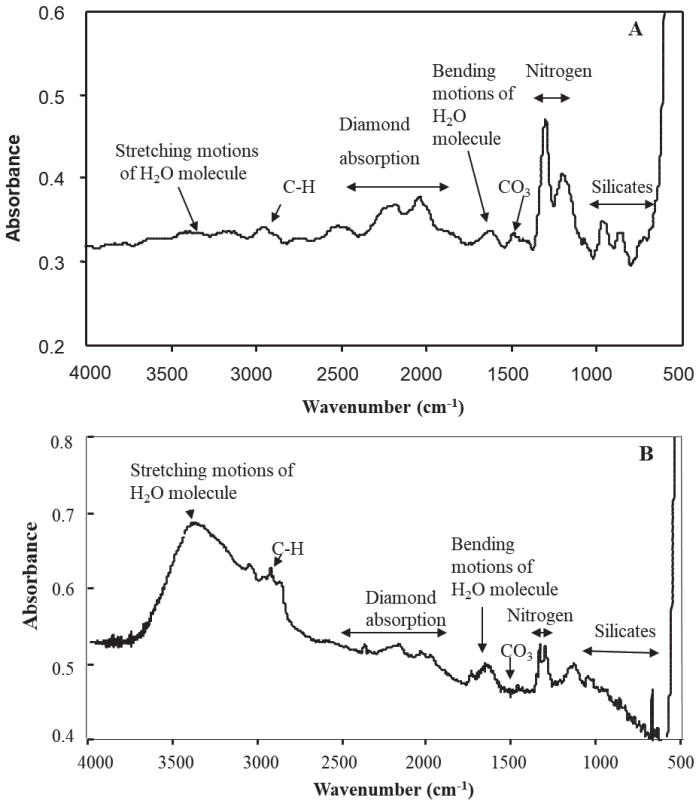

Figure 13. Synchrotron IR spectra (beam line U2A, Brookhaven National Laboratory, USA) obtained from Erzgebirge diamond #1 (**A**) and diamond #2 (**B**); diamonds are shown in plates A and B of Fig.12 (Reprinted from Dobrzhinetskaya et al. 2006b, copyright 2006 with the permission of Eslsevier # 5035711034058).

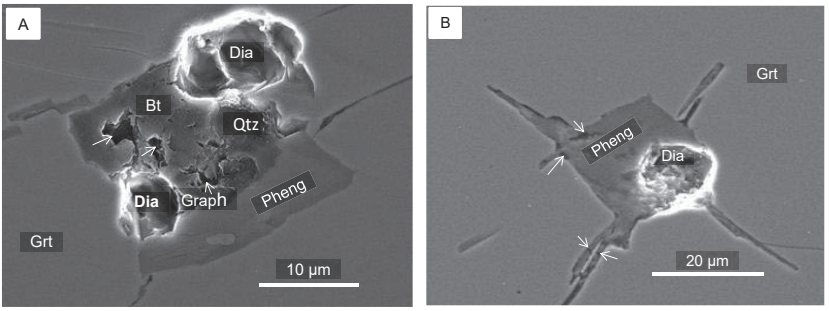

Figure 14. SEM secondary electron images of multiphase pockets in garnet from garnet–phengite–quartz–feldspathic gneiss, Erzgebirge, Germany (Reprinted from Dobrzhinetskaya et al. 2010, with the permission of Springer Nature #5034451417904). **A**—the multiphase pocket contains biotite (Bt), diamond (Dia), phengite (Pheng), quartz (Qtz), and graphite (Graph) shown by **arrowheads** (adapted from Dobrzhinetskaya et al. 2010); **B**—the phengite–diamond pocket contains abundant tiny cavities (**arrowheads**), e.g., traces of fluid inclusions decrepitated during sample preparation.

Dobrzhinetskaya et al. (2013) conducted SEM and FIB-assisted TEM studies of the Erzgebirge polycrystalline diamond inclusions in zircons (Fig.15). They studied five polycrystalline diamonds and found that they consist of 5–15 single crystals ranging in size from 0.3–5 μm with irregular sharp-angled grain boundaries (Fig. 16). Numerous triangular nanoscale voids situated along the diamond–diamond interfaces were filled with a COH fluid containing traces of Al, Co, F, V, Zn, Si, Cl, S, Ca, Mg, Fe, K in varying combinations and concentrations. The latter, if considered along with the "spider-like" dislocations, sharp-angled grain boundaries, and stacking faults that were observed in these diamonds, suggests that they rapidly nucleated and grew from a fluid media under an internal stress. These observations combined with previous results provide an additional constrain for the formation conditions of these UHPM microdiamonds. They likely crystallized from a supercritical fluid with a composition that was close to one of two end members, (1) a carbon-rich hydrous-silicic fluid and (2) a hydrous-saline fluid (Dobrzhinetskaya et al. 2006a, 2013; Jacob et al. 2014).

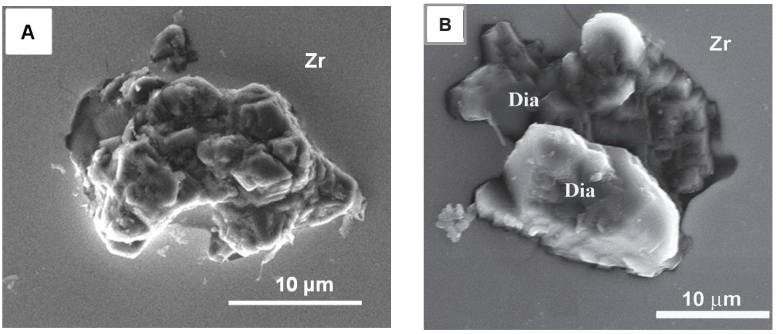

Figure 15. A and **B –** Polycrystalline diamond inclusions in zircons from garnet–phengite–quartz–feldspathic gneiss, Erzgebirge, Germany (Secondary Electron SEM images).

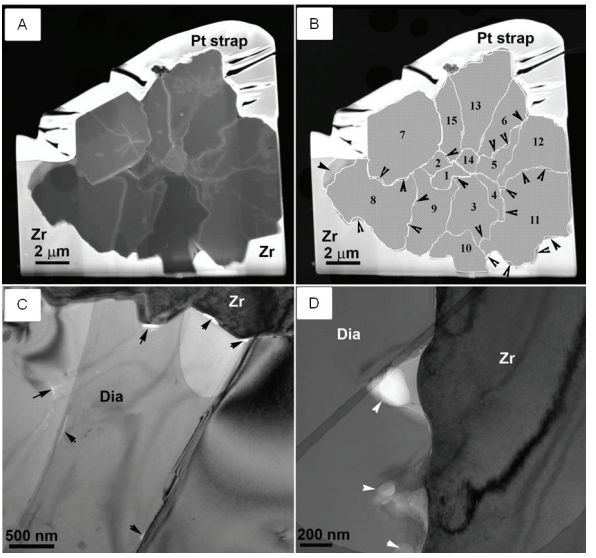

Figure 16. Bright Field TEM images of polycrystalline diamond inclusions in zircon (adapted from Dobrzhinetskaya et al. 2013). **A –** a FIB foil cut through the central part of a diamond shows that the polycrystalline diamond consists of at least 15 individual monocrystals situated closely together; **B –** a sketch of the individual monocrystals shows that the smaller crystals (#1, 2, and 14) are situated in the central part of the diamond whereas the large crystals have curved boundaries with each other and with the surrounding zircon. Plate **C** shows the "zig–zag" character of the diamond–zircon and diamond–diamond interfaces containing fluid pockets and a fluid film which are shown by the **black arrowheads**. Plate **D** shows triangle-like cavities at the diamond–zircon interface which are filled with fluid; these fluid pockets are marked by **white arrowheads**.

Zhang et al. (2017) also conducted studies of polycrystalline diamonds in zircons separated from quartz–feldspathic gneisses at Saidenbach water reservoir, Erzgebirge, Germany. Their conclusions confirm the studies by Dobrzhinetskaya et al. (2013), and unconditionally support the concept of UHPM diamond crystallization from a multicomponent COH fluid or COH fluid–hydrous silicate melt media.

Frezzotti et al. (2011) studied fluid inclusions associated with UHPM diamond formation in metamorphic schists from Lago di Cignana, Western Alps where the protolith of these rocks was likely oceanic sediments. Based on studies of the fluid geochemistry they concluded that the carbon was released from the subducting oceanic sediments at relatively shallow depths through the dissolution process (Frezzotti et al. 2011, 2014; Frezzotti 2019). Furthermore, their detailed investigation convincingly demonstrated that the deep subduction of oceanic sediments leads to a continuing saturation of the shallow fluid with carbon and precipitation of diamonds at UHPM conditions occurred. The Lago di Cignana diamond's nucleation from a COH fluid at UHPM conditions is unambiguously supported by the presence of coesite inclusions located in the same garnet growth zones where the primary fluid inclusions are located (Frezzotti et al. 2011, 2014; Frezzotti 2019). This is also in good agreement with thermodynamic calculations reported by Sverjensky et al. (2014) who investigated the stability of COH fluids as a function of pressure, temperature, and oxidation state.

A literature survey on UHPM diamond crystallization reveals that sometimes discussions are oriented around "fluid vs. melt" or "fluid vs. hydrous melt." Without clear a definition of how one should distinguish a silica-rich fluid from a hydrous silicate melt at high pressures and high temperatures, this controversy simply reflects a semantic issue. For example, experiments conducted by Bureau and Keppler (1999) suggest that there is a complete miscibility between silicate melt and water in most of the upper mantle, except at very shallow depths. In these experiments, the hydrous melt and silicate-bearing vapor coexisted separately at low T, whereas at higher T they mixed to become a single-phase supercritical fluid that was stable at $P = 1.5–2.5$ GPa. Experiments and direct studies of fluid inclusions in natural rocks conducted by others (e.g., Akaishi and Yamaoka 2000; Pal'yanov et al. 2002; Manning 2004; Ferrando et al. 2005; Frezzotti et al. 2007) also demonstrated that at $P \geq 4$ GPa and $T \geq 800$ °C there is no distinction between aqueous fluids and silicate melts because volatile-rich chemical systems are in a supercritical state.

A melt concept for Erzgebirge diamond crystallization was proposed by Massonne (2003) which was motivated by their studies of melting events in the bulk rocks of both Kokchetav and Erzgebirge diamond-bearing UHPM terranes which were constrained by zircon geochronology (Massonne et al. 2007a; Massonne and Fockenberg 2012). The cathodoluminescence images (Figs. 3 and 4 from Massonne et al. 2007a) clearly show that the cores of the zircons are typically eroded. The eroded zone of the zircon core is interpreted as being caused by a melting event. The second zone overgrew the eroded core and contains diamonds, while the third zone at the outer rim of the zircon grain does not contain any diamond inclusions. The authors report the following ages: metamorphic zircon core 337.0 ± 2.7 Ma (21 analyses); diamond-bearing zone of zircon 336.8 ± 2.8 Ma (23 analyses); and the outer rim zone of zircon 330.2 ± 5.8 Ma (12 analyses). Indeed, zircon ages combined with petrological observations could provide some constraints on the pressure–time history of these rocks, however there would be uncertaintnies in the pressure–time history that is derived from this approach. Moreover, the presence of an eroded core of zircon enveloped by diamond-bearing zircon zone does not provide any direct evidence that the diamonds originated from a melt; it can be interpreted as a metasomatic "erosion". We believe that information about the origin of the diamonds is still "hidden" inside these diamonds since Massonne et al. (2007a) did not study their inclusions. Thus, the media which these diamonds crystallized from, whether it be a carbon-rich silicate melt, and/or a COH fluid or a multicomponent fluid is not well constrained. Additional studies using high resolution techniques (e.g., synchrotron IR spectroscopy and FIB-assisted STEM or TEM coupled with nanoSIMS) would provide better constrains on the melt vs. fluid origin of these unique microdiamonds enclosed in zoned zircons.

Korsakov et al. (2004) suggested that diamonds from the Kokchetav UHPM terrane should be classified as "intragranular" type A (diamonds included in garnet, clinopyroxene and zircon; e.g., high-pressure minerals) and "intergranular" type B (diamonds occurring within pseudomorphs after high-pressure minerals), and "intergranular" type C which occur within the granitic-like material with a quartz+feldspar composition. They observed that type C "intergranular" diamonds occur in high concentrations within the quartz–feldspathic material (e.g., they could be called "granitic melt injections" or "migmatitic material") along the contact zone between the garnet–biotite–quartz and clinopyroxene–calcite layers. They proposed that these diamonds formed during the interaction of pelite–derived hydrous melt with a granitic composition with carbonate rocks during UHPM events. Korsakov et al. (2004) suggest that a granitic melt could act as a crystallization medium as well as a transport medium for type C "intergranular" diamonds. If one hypothesizes that three geologic events could have taken place, then three generations of diamonds could have formed, and they would have different ages, formation mechanisms, and media from which they crystallized.

To prove such a hypothesis, one should collect diamonds of each type along with: (i) geochronological data of diamond formation, (ii) type of inclusions preserved in diamonds (fluid, gas, solid matter) and their geochemical and crystal structure parameters, and (iii) morphology of diamonds. Until such data become available, the "three different type of diamonds" proposed by Korsakov et al. (2004) can more straightforwardly explained by one crystallization event that occurred during the same geological process (supercritical fluid/melt at the peak of the UHP metamorphism) which would imply that the diamonds all have the same age. Since diamond is chemically stable it may survive a retrograde metamorphic event, whereas other UHP minerals such as coesite, majorite, phengite, super Si-titanite, high Ca-Esk clinopyroxene and others can become re-equilibrated or replaced by their lower-pressure phases, e.g., pseudomorphs. Therefore, the same diamond (type A) which formed under peak UHP metamorphic conditions can be preserved within former UHPM minerals subjected to retrogressive metamorphism. However, in this case such a diamond would be classified type B according to Korsakov et al. (2004). If diamonds of type C are formed due to interaction between Si-rich and C-rich layers during their partial melting at UHPM conditions, such diamonds are expected to contain inclusions with chemistry that would support this origin hypothesis. Until such data are collected, the concepts of three types of diamonds (A, B and C) crystallizing during different UHPM events remain unproven.

Korsakov and Herman (2006) have also proposed that carbonate melt can be a medium where diamond crystallization occurred in the Kokchetav dolomite marbles. However, this hypothesis has been questioned by Imamura et al. (2013). They note that it is difficult to explain the extremely negative $\delta^{13}C$ values by diamond crystallization from a carbonate melt, because strong isotopic fractionation is not expected between diamond and carbonate melt at high pressures and temperatures (Bottinga 1968; Reutsky et al. 2015).

Oxidation state during UHPM diamond crystallization. Another important aspect of diamond crystallization is the oxidation state of the diamond-forming media. Association of Erzgebirge polycrystalline diamonds with carbonate ($CaCO_3$) inclusions suggests that they formed in an oxidizing environment close to the CCO buffer (Fig. 17) (e.g., Dobrzhinetskaya et al. 2013; Jacob et al. 2014). This is also supported by synchrotron infrared spectra of Erzgebirge diamond inclusions which show a well pronounced absorption band at 1430 cm^{-1}, which corresponds to the CO_3^{2-} radical (e.g., Dobrzhinetskaya et al. 2006b). Nanoinclusions of $MgCO_3$ and $CaCO_3$–aragonite were directly observed with TEM in diamonds from garnet–biotite gneiss and metacarbonate rocks of the Kokchetav massif (Dobrzhinetskaya et al. 2001, 2005, 2006a). This allows one to hypothesize that the Kokchetav diamonds also formed in an oxidizing environment close to the CCO buffer (Jacob et al. 2014).

Frezzotti et al. (2014) suggested that the Lago di Cignana (Western Alps) diamond nucleation began when the H_2O-rich fluid reached the excess concentration of carbon required for spontaneous nucleation of diamond. They showed that at high pressures the interaction of rock buffered fO_2 and the prograde *P–T* path may control the carbon saturation. The thermodynamic modeling (Frezzotti al. 2014) suggested that the diamond crystallized from COH fluids with a water concentration of about $0.992 < X_{H_2O} < 0.997$, and that the fO_2 was at the level required for EMOD (enstatite + magnesite = olivine + diamond) equilibrium (Fig. 17).

However, there are two cases where microdiamonds were found together with SiC as multiphase inclusions in zircon from Gföhl granulite samples of the Moldanubian Zone, Bohemian massif (Perraki and Faryad 2014) and in garnet from metapelitic gneisses of Pohorje, the Austro-Alpine UHPM terrane, Eastern Alps (Janák et al. 2015). Notably, Perraki and Faryad (2014) stated that they used SiC abrasives for one step of the polishing procedure, but to eliminate the possibility of contamination they removed the polish with an ultrasonic cleaner and polycrystalline-type diamond spray was used for the polishing of the thin section surface. Additionally, the occurrence of SiC and diamond grains beneath the polished surface was checked with both transmitted and reflected light microscopy.

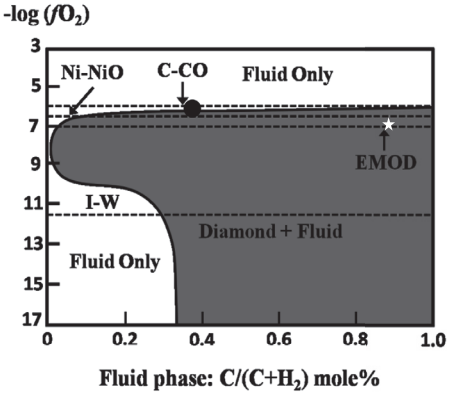

Figure 17. Diagram of –log fO_2 v. fraction of (C ⁄C + H_2) mole % for COH fluids in equilibrium with diamond at 5 GPa and 1400 K (adopted from Jacob et al. 2011; Taylor 1990 and Dobrzhinetskaya et al. 2013). C–CO, Ni–NiO, EMOD (enstatite + magnesite + olivine + diamond), and IW (iron–wustite) are known buffer curves adopted from Eggler and Baker 1982, and Sokol et al. 2000. **Gray field** corresponds to conditions at which diamond coexists with a fluid (Diamond + Fluid); **blank fields** above and outside of the left part of the **black curve**, marked as Fluid Only, correspond to that oxidation state and concentrations of C and H_2 where diamond is not stable. The **black dot** corresponds to the position of the Erzgebirge diamonds within the C–CO buffer curve; **white star**—fluid oxidation state for diamonds from Lago di Cignana, Western Alps (Frezzotti et al. 2014).

Though Janák et al. (2015) hypothesized that diamond + moissanite inclusions in garnet from metasedimentary rocks of Pohorje were crystallized from a reduced COH fluid, they concluded that further detailed studies are needed to fully understand the oxidation state during their formation. Certainly, these unusual findings of diamond + SiC inclusions in garnets from UHPM terranes deserve additional close attention.

UHPM diamond formation under metastable conditions. Shortly after the discovery of diamonds in UHPM rocks, crystallization under metastable conditions was considered as an alternative to the classical concept of diamond formation in the Earth at *P* ~ 4.0–6.0 GPa and *T* ~ 900–1400 °C (Bundy 1980; Boyd et al. 1985).

Throughout the 1980s and into the mid of 1990s the concept of metastable diamond formation at low-pressure conditions of crustal metamorphism was proposed (e.g., Letnikov 1983; Lavrova 1991; Ekimova et al. 1992; Lavrova et al. 1995). Even at that time it was considered controversial to the new concept of diamond crystallization during UHP metamorphism of crustal rocks subducted to a depth ≥120 km (Sobolev and Shatsky 1988, 1990; Shatsky and Sobolev 1993; Shatsky et al. 1995). It has since been shown unambiguously that the Kokchetav massif is an UHPM terrane through the documentation of numerous UHPM mineral phases by hundreds of high-quality studies involving state-of-art and synchrotron assisted instruments (see reviews: Ernst and Liou 1999; Ogasawara 2005; Dobrzhinetskaya 2012; Schertl and Sobolev 2013; Liou et al. 2014). Despite all these convincing observations the concept of diamond crystallization outside of the diamond stability field has still occasionally appealed as a formation mechanism for diamonds found in UHPM terranes (e.g., Pechnikov and Kaminsky 2008, 2011; Simakov et al. 2008; Simakov 2010, 2015, 2018). Since this hypothesis has been invoked to describe the formation conditions of microdiamonds a short discussion about what is known from experiments on metastable diamond growth is warranted.

Pechnikov and Kaminsky (2008) focused their attention on the geometry of the "productive" diamond-bearing ore body using detailed mapping completed by the local Kokchetav Geological Survey, and they combined this information with their petrographic observations. They concluded that the diamonds were formed under crustal conditions (e.g., metastable) from crustal fluid–metasomatic processes that were active along the fault-zone superimposed on the Precambrian gneisses. They accepted the diamond bearing zircon age of 527–537 Ma (Claoué–Long et al. 1991; Jagoutz et al. 1990, 1991; Hermann et al. 2006) as the age of diamond formation and therefore the age of the fluid–metasomatic activities along the fault zone. The authors believe that the micrometer size of the diamonds, along with their isotopic signatures ($\delta^{13}C = -8.9$ ‰ through −27 ‰), support diamond formation under metastable crustal conditions. On the other hand, Pechnikov and Kaminsky (2008) note that their concept does not exclude the occurrence of episodes of UHP metamorphism and they accept the presence of coesite and other UHP minerals in the diamond-bearing rocks. However, their concept fails to explain when the UHP metamorphic episodes took place, and the authors did not discuss that fact that zircons containing diamonds and/or coesite, or pyroxene with high Ca-Eskola component and other UHP phases have the same age (e.g., Katayama et al. 2000, 2001a,b, 2002; Ogasawara 2005). Though the prevalent light carbon isotope characteristics of diamonds prove that such carbon has a crustal origin it does not reject the possibility of the subduction of crustal rocks to depths ≥ 120–150 km where the pressure and temperature are high enough to stabilize carbon in the form of diamond. Indeed, the arguments of Pechnikov and Kaminsky (2008) on the metastable origin of the Kokchetav diamonds are contrary to the conclusions reported by most other scientists who have collected and studied diamonds from this locality.

Simakov (2010) reports that they synthesized nano-diamonds from a water–alcohol solution which was the source of free carbon C, in a high-pressure reactor (volume ~500 cm^3) at $P = 0.1$ GPa and $T = 500$ °C. They directly applied the results of this experiment to explain the origin of mm-sized diamonds from UHPM terrane of the Kokchetav massif without taking into consideration all of the other UHP minerals associated with these diamonds (e.g., Katayama et al. 2000, 2001b, 2002; Ogasawara et al. 2002; Ogasawara 2005).

Furthermore, Simakov (2015, 2018) also discussed the metastable formation of diamond from a COHN fluid and applied this idea to explain the origin of UHPM diamonds. They discussed that nitrogen interaction decreases the total energy of diamond nuclei formation and the equilibrated methane pressure stabilizes the diamond, and they confirmed this by the hydrothermal synthesis of nano-diamond from nitrogen bearing organics at metastable P–T conditions (Simakov et al. 2008). Synthesis of nano diamonds at high temperatures and/or ambient–low pressure (e.g., metastable) are well-known in materials sciences processes such

as laser ablation, chemical vapor deposition (CVD), autoclave synthesis from supercritical fluids, ion irradiation of graphite and ultrasound cavitation (e.g., Krueger 2008; Derjaguin and Fedoseev 1994; Fedoseev et al. 1971) as well detonation techniques (e.g., Danilenko 2004), which requires extremely high pressures. However, before invoking any of the processes mentioned above to explain how diamonds form in UHPM terranes, would require a critical evaluation of all the existing data that have been collected by many research groups. Thermodynamic calculations for *PT*-conditions of diamond-bearing rocks and the presence of UHP minerals associated with diamond are important petrological evidence indicating that the diamonds from Kokchetav formed under UHPM conditions and their formation does not easily fit to the models/experiments proposed by Simakov (2010, 2015, 2018). Additionally, experiments conducted by other groups using a starting material that is close to the bulk chemistry of the Kokchetav diamond-bearing rocks, under both hydrous and anhydrous, and at varying oxidation states have produced run products that are a good fit to the data collected from the rocks, diamond itself and other associated minerals (e.g., Hong et al. 1999; Pal'yanov et al. 1999, 2000, 2013; Akaishi and Yamaoka 2000; Yamaoka et al. 2000; Kumar et al. 2001; Hwang et al. 2003; Dobrzhinetskaya et al. 2004; Dobrzhinetskaya and Green 2007a,b). Therefore, while the models/experiments proposed by Simakov (2010, 2015, 2018) do, indeed, explain diamond formation outside the diamond stability field, they cannot be applied to diamonds from the Kokchetav massif or for diamonds from other well established UHPM terranes.

It should be emphasized that if diamond formation under metastable conditions is proposed the following data are expected to be presented for consideration: (i) thorough geologic mapping of the area where the sample was collected to find any other UHPM indicator minerals other than diamond; (ii) unambiguous proof of the indigenous origin of the diamond, the diamond should be *in situ* so that the interface between the diamond and its host mineral can be examined in detail with high resolution techniques, and (iii) all available thermodynamic data has been reviewed.

Comet impact hypothesis for the origin of diamonds from Kumdy Kol Lake, Kokchetav Massif. Recently a new impact–cosmic–metasomatic genesis of the Kokchetav diamond deposit was proposed (Tretiakova and Lyukhin 2016, 2017). It was provoked by an impact event followed by metamorphism and alteration of the rocks. The authors note that the ring structure of Kumdy Kol Lake, where most of the diamond-bearing metamorphic rocks of the Kokchetav massif are situated, has the form and size (~4 km diameter) resembling a small impact crater. They suggest that the diamond-bearing terrane formed by comet impact under an oblique angle which generated shock wave compression with peak pressures reaching > 50 GPa.

They argue that there is evidence of impact metamorphism, (1) presence of UHPM minerals diamond–lonsdaleite, coesite, omphacite, (2) the delivery by comet moissanite (SiC) and graphite spherules as well as "meteoritic matter" such as magnetite, hematite, iocite, troilite, ∝-Fe, Ni–Fe, (3) annealed metallic globules are observed having various fanciful forms (globules, small dump-bells, drops, spherules and so on) in host rock and rock-forming minerals, and (4) dislocation and birefringence in diamonds, planar structure in quartz, inclusions UHP minerals in rock forming minerals. The authors suggested that collision of huge velocity comet and the Earth generated rapid shock wave compression (pressure peak > 50 GPa) forming diamond, coesite and other UHPM minerals which later together with so-called "meteoritic matter' were subjected to regional metamorphism and metasomatism.

Additionally, they hypothesize that the "unprecedentedly" high $^{3}He/^{4}He$ isotopic ratios of the Kokchetav diamonds reported by Shukolyukov et al. (1993) are, indeed, due to the formation of these diamonds outside of the solar system. However, new measurements by Sumino et al. (2011) revealed that $^{3}He/^{4}He$ value of the Kokchetav diamonds are close to the values found for OIB, and that the extremely high $^{3}He/^{4}He$ ratio likely originated from Li-rich contaminants.

The "impact–cosmic–metasomatic" origin remains unproven based on the following evidence: (i) Sumino et al. (2011) have shown that the "unprecedentedly high" $^{3}He/^{4}He$ isotopic ratios are not likely a true feature of the Kokchetav diamonds, (ii) the authors have not presented unambiguous evidence of the claimed "oblique" impact (e.g., asymmetrical ejecta deposits), (iii) the authors do not propose that any of the other dozens of similar shaped lakes around Kumdy-Kol lake were caused by impact events, and (iv) and they do not report that the Kokchetav diamonds show unique moiré fringes which are well-known features observed in impact-formed diamonds (e.g., Langenhorst 2003; Ohfuji et al. 2015).

OPHIOLITE-HOSTED AND VOLCANIC DIAMONDS

Ophiolite-hosted diamonds

Liou et al. (2014) provided a comprehensive review of the history of the discovery of ultra-high-pressure minerals in ophiolitic chromitites and peridotites. To avoid unnecessary repetition here, we focus our reader's attention on the studies of diamonds and specifically *on the methods used for confirmation of whether the diamond is indigenous or not.* This topic is still highly controversial as is evidenced by several recent critical *comments* and *replies* on a few recent publications that have reported ophiolite-hosted diamonds. The crux of the matter is the indigenous nature of these reported diamonds. In this section we will discuss our vision and approach for how the community can reach a consensus about whether these diamonds are myth or reality.

To present ophiolite-hosted diamonds have been reported from more than a dozen geographic localities in the World (Fig. 18). Most of them have been found in the Tertiary Yarling-Zangbo suture zone of Tibet which formed during the India–Asia continental collision. The ophiolite complex situated along this suture zone is mainly composed of remnants of the Neo-Tethys ocean floor. Within them the Luobusa massif encompasses diamond-hosted chromitite and harzburgite (e.g., Fang and Bai 1981; Bai et al. 1993, 2001; Yang et al. 2007a), and the Purgan, Xigaze, Dongbo, Burang, Dangqiong, and Dongqiao massifs enclose diamond-hosted chromitites and peridotites (e.g., Yang et al. 2011, 2013, 2014; Lian and Yang 2019). Other worldwide ophiolite hosted diamond-bearing localities include podiform chromitites and/or peridotites in the Sartohai massif, NW China, Ray-Iz massif, Polar Ural, Russia (Yang et al. 2007b, 2015a); Hegenshan massif of Inner Mongolia, China (Huang et al. 2015); Mirdita massif, Albania (Wu et al. 2017, 2019; Xiong et al. 2017); Pasani-Karsanti massif, Turkey (Lian et al. 2017); Nidar ophiolite, India (Das et al. 2017); Myikyina massif, Myanmar (Chen et al. 2018), Tehuitzingo, Puebla State, southern Mexico where diamonds was documented *in situ* in chromitite-bearing serpentinites (Farré-de-Pablo et al. 2018), and diamond inclusions in magmatic olivine from ophiolite section of the Moa-Baracoa ophiolitic massif, eastern Cuba (Pujol-Solà et al. 2020).

Ophiolitic diamond formation hypotheses

Since the formation conditions for diamond and ophiolites are incompatible with each other several hypotheses have been put forward to explain their existence and some of them are very controversial (e.g., Arai 2013; Yang et al. 2014, 2015a,b; Zhou et al. 2014; McGowan et al. 2015; Robinson et al. 2015; Griffin et al. 2016; Rollinson 2016; Ballhaus et al. 2017; Dilek and Yang 2018; Lian and Yang 2019). We summarize them as three main hypotheses:

(i) Diamond is formed at depth in the mantle at high-pressure and high-temperature conditions with the source of carbon coming from the deep subduction of oceanic lithosphere fragments. These diamonds are then transported to the shallow mantle by mantle convection (e.g., Arai 2013; Mcgowan et al. 2015); and/or they are transported by mantle plumes to the shallow upper mantle (e.g., Xiong et al. 2015, 2017; Yang et al. 2015b; Griffin et al. 2016; Lian and Yang 2019).

(ii) Diamond crystallization at low T and low P (metastable conditions) from carbon-rich fluids that form during alteration of chromitites and other fragments of oceanic crust at shallow depths (Farré-de-Pablo et al. 2018, 2019, 2020; Pujol-Solà et al. 2020).

(iii) Diamond (and super-reduced alloy and minerals) formation from lightning strikes (Ballhaus et al. 2017, 2021).

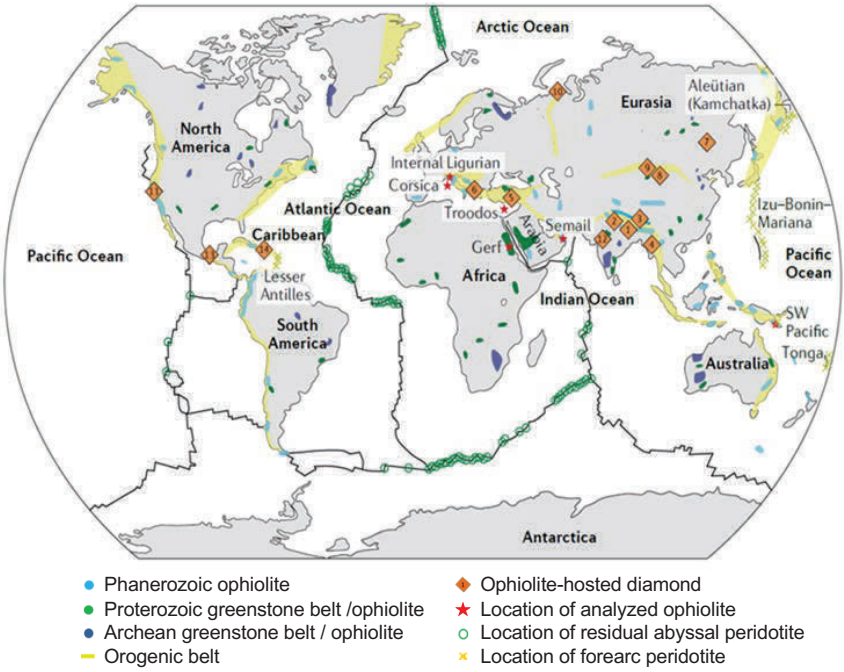

Figure 18. Global distribution of ophiolite belts and diamond-bearing ophiolites (Yang et al. 2021, with the Elsevier permission #5035651046919). Diamond-bearing ophiolites are typically located close to orogenic belts. The location of Archean (4–2.5 Ga) and Proterozoic (2.5–0.54 Ga) greenstone belts, Phanerozoic (<0.54 Ga) ophiolites and orogenic belts are from Dilek and Furnas 2011; Furnas et al. 2014 2015. Locations of known ophiolite-hosted diamonds: Liobasa, Zedang and Xigaze ophiolite (1) (Bai et al. 1993; Yang et al. 2014; Guo et al. 2015); Purang, Dongbo and Dangquong ophiolite (2) (Yang et al. 2011; Xu et al. 2015); Dingqing ophiolite (3) (Xiong et al. 2018); Myitkyina opiolite (4) (Chen et al. 2018); Pozanti–Karzanti ophiolite (5) (Lian et al. 2017); Mirdita ophilite (6) (Wu et al. 2017, 2019; Xiong et al. 2017); Hegenshan phiolite (7) (Huang et al. 2015); Qilian ophiolite (8), Sartohay ophiolite (9) (Tian et al. 2015); Ray-Iz ophiolite (10) (Yang et al. 2015); Josephine ophiolite (11), Nadar ophiolite (12) (Das et al. 2017); Tehuitzongo ophilite (13) (Farré-de-Pablo et al. 2018); Moa–Baracoa ophiolite (14) (Pujol-Solà et al. 2020). **Red stars** show locations discussed in Yang et al. 2021. **Open green circle** indicates locations of residual abyssal peridotites (Warren 2016). **Yellow crosses** show locations of the forearc peridotites (Dien et al. 2019).

Localities of ophiolites-hosted diamonds formed at mantle depth

Diamonds from ophiolites of the Yarling-Zangbo suture zone, Tibet. The first diamonds were found in Tibet during the examination of the heavy mineral separates retrieved from mechanically crashed chromitites using optical microscopy (Fang and Bai 1981). The heavy minerals separation techniques have different protocols and procedures in different countries; however, all are used for the exploration of industrial mineral deposits, which in the case of chromitites are platinum group elements (PGE) metals and alloys. Fang and Bai (1981) reported that 20 diamonds were recovered from the Luobusa chromitite and hargburgite, and six

diamonds from similar rocks collected from Donqiao massif of the Bangong-Nujiang ophiolite belt situated 500 km northwest from the Luobusa massif (Bai et al. 1989, 1993). These diamonds were characterized as colorless and transparent euhedral/octahedral-like morphology; their sizes fall in range of 100–500 μm, though some broken crystals of 200–250 μm and diamonds as large as 900–1000 μm were also reported (Bai et al. 1989). Other than diamonds, additional minerals which are "unexpected" to occur in chromitites, such as SiC, graphite, Ni–Fe alloys, and Cr^{+2}-bearing chromium spinel were also documented in the heavy minerals separate.

These first reports of diamond findings in Tibetan chromite were eventually disproved by an international group of kimberlitic diamond experts who concluded that these diamonds *"…are consistent with synthetic contamination introduced at some stage during the sampling or concentration of heavy minerals from these ultramafic bodies*" (Taylor et al. 1995). After this report a new effort commenced to carefully process and separate heavy minerals from the Luobusa and other chromitite deposits of the Yarling-Zangbo suture zone, Tibet. The Institute of Geology, Chinese Academy of Geological Sciences, the Tibetan Geological Bureau, and international collaborators all participated in this effort. As a result, dozens of diamond crystals ranging from ~100–600 μm in size were documented again (Fig. 19) as well as more unusual new minerals including native Cr, Os–Ir–Ru alloys, Ir–Ni–Fe alloys, Pt–Fe alloys and others were recognized (e.g., see reviews Yang et al. 2007a 2014; Liou et al. 2014).

Additional explorations for ophiolitic diamonds in Tibetan and other worldwide ophiolitic terranes began; they used the same protocol, e.g., the collection of ~200 to 1000 kg of chromitites or peridotites, mechanical crushing and sieving of the rocks followed by heavy minerals separation including vibration, magnetic, heavy liquid floatation, and electrical conductivity techniques. Most Tibetan diamonds and diamonds from other ophiolitic belts were found in mineral separates processed in the Institute of Multipurpose Utilization of Mineral Resource, Zhengzhou, China. The diamonds retrieved from other Tibetan ophiolites (Purgan, Xigaze, Dongbo, Burang, Dangqiong, and Dongqiao massifs) share morphological similarities with those of Luobusa massif (Fig. 19), and they are always associated with of ultra-reduced minerals, metallic alloys and native elements (e.g., Liou et al. 2014; Yang et al. 2014; Xiong et al. 2017; Lian and Yang 2019).

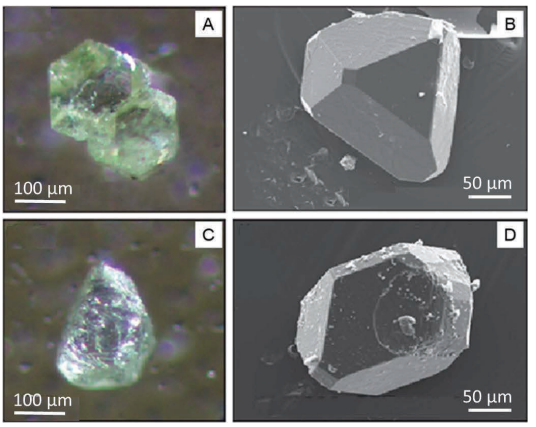

Figure 19. Topography of microdiamonds from chromitites and mantle peridotites (Xu et al. 2018, published under the terms of the CC–BY–NC license). **A –** Polycrystalline diamond from chromitite (Luobusa ophiolite, Tibet) exhibits cuboctahedral morphology and in light yellow color under a binocular microscope. **B** – Scanning electron microscope (SEM) image of diamond from chromitite (Luobusa ophiolite, Tibet) displaying octahedral-dominated cuboctahedron crystal habit. **C –** Colorless diamond from mantle peridotite (Luobusa ophiolite, Tibet) showing cuboctahedral morphology under a binocular microscope. **D –** SEM image of diamond from mantle peridotite (Luobusa ophiolite, Tibet) displaying hexoctahedron crystal morphology.

Tibetan diamond in situ, unusual UHP minerals and highly reduced minerals and alloys. A small diamond of ~6 μm size was found as an inclusion in an Os–Ir alloy that was recovered from heavy mineral separates from Luobusa chromitite. This diamond was confirmed using Raman spectroscopy and the first order Raman mode was reported to be centered at 1332.2 cm^{-1} (Yang et al. 2007a). The position of this diamond in the thin section (polished without diamond abrasives) was observed with both optical microscopy and with SEM in secondary electron mode. Although the authors claim this satisfies the minimum requirements for the diamond to be considered in situ, the diamond was not observed below the surface of the host mineral before it was exposed to the surface by polishing. Alsothe samplewas not studied with FIB-TEM technique to confirm the nature of the Os–Ir-alloy–diamond interface and to find/analyze any inclusions that may be encapsulated inside this diamond (Yang et al. 2007a). Observation of the diamond below the surface of the host mineral and detailed analysis of the diamond host mineral interface with FIB-TEM would have unambiguously proved this diamond is indigenous. It has been suggested that the *in situ* Tibetan diamonds were likely formed at depths of 150–300 km (Yang et al. 2007a, 2014) or even deeper than 380 km (Xiong et al. 2018).

Detailed studies were conducted on another unusual recovered mineral fragment, an Fe–Ti alloy which was retrieved from the same mineral separates as the Os–Ir alloy containing diamond (Yang et al. 2007a). The fragment of Fe–Ti alloy had a small portion of a silicate rock which contained coesite after stishovite and kyanite suggesting that coesite after stishovite and diamond, might be incorporated into the chromitites in the deep upper mantle, or that they have an impact origin with a prevalence of evidence for the deep mantle origin (Yang et al. 2007a).

Later Dobrzhinetskaya et al. (2009 2014b) studies of the same sample using the state-of-the-art FIB-TEM analytical techniques showed that the coesite and kyanite contained mm-sized inclusions of native iron, cubic–BN (qingsongite), TiC (osbornite) and TiO_2-II (rutile with α-PbS structure). The authors discussed two possible explanations that these data support: (i) the UHPM minerals have been encapsulated within chromitite at mantle depth, or (ii) they were formed by shock events due to a meteorite bombardment (Dobrzhinetskaya et al. 2009 2014b). Since the microstructures of UHPM minerals in the studied fragment are inconsistent with those formed due to shock metamorphism (e.g., Martini 1991; Stähle et al. 2008) the mantle origin of the fragment was deemed more plausible (Dobrzhinetskaya et al. 2009, 2014b). Dobrzhinetskaya et al. (2009, 2014b) have clearly informed the readers that the studied fragment of these metamorphic rocks, contained cubic-BN (quingsongite), TiC-osbornite, TiO_2-II, coesite after stishovite and some high Si-Al-rich amorphous material, all recovered from these Tibetan chromitites by "crushed rocks–minerals separation" technique.

Although Tibetan chromitites contain more than a dozen different native elements, alloys, and minerals only a few of them may be classified as UHP minerals (diamond, coesite, TiO_2 II). Most of the other reported minerals are highly reduced minerals (e.g., SiC-moissanite and FeO-wustite), native elements (e.g., Fe, Si, Ti, Cr), alloys (e.g., Os–Ir–Ru, Ni–Fe, Ir–Ni–Fe Pt–Fe), carbides [e.g., WC-qusongite, $(Cr,Fe,Ni)_9C_4$-yarlongite] and silicides (e.g., Fe_5Si_3-xifengite, $TiFeSi_2$-zanboite) to mention a few (see reviews: Robinson et al. 2004; Liou et al. 2014; Lian and Yang 2019; Yang et al. 2019a). Importantly verification of their stability field *at high pressures and high temperatures* requires further experimental studies.

Diamonds in situ from Rai-Iz ophiolite, Polar Ural, Russia. New reports of ophiolitic diamonds and ultra-reduced minerals in other countries of Euro-Asian continent (Russia, Albania, Turkey, India, and Myanmar) confirm that they are widespread and that new concepts are required to explain their occurrences in ophiolite formations. Some interesting results came from recent studies of Nano-inclusions in ophiolitic diamonds from the Ray-Iz massif, which is an early Paleozoic ophiolitic belt in the Polar Urals, Russia. Yang et al. (2015a) recovered 1000 grains of loose diamonds (~200–500 μm in size) from heavy mineral separates processed from 1500 kg of Ray-Iz chromitite samples. They were processed at the same facilities as the Tibetan diamonds.

To search for diamond *in situ* they cut 40 pieces of rock that were roughly 4 cm^2 in area and encased them in epoxy. The samples were grinded down in 100 μm increments using a diamond-coated disk with a maximum grain size of 37 μm. Optical microscope images show that two diamonds remained enclosed in chromite (Fig. 20, plates A and C). On plate B of Fig. 20 (sample Y–5B–17– 2) one can see a sub-euhedral diamond crystal that is ~ 300 μm in diameter surrounded by thin patch of amorphous carbon. Sample Y5B-16-2 (plate D) exhibits a well-shaped hexagonal platy-like diamond crystal with dimensions of ~300 × 400 μm surrounded by an irregular-shaped mass of amorphous carbon—all are inside of a host chromite (Yang et al. 2015a).

Though the authors concluded that both crystals are diamonds, they provided only one spectrum (e.g., plate E shows only one Raman spectrum with band at 1330.8 cm^{-1}, see caption to Fig. 8, page 469, Yang et al. 2015a). Furthermore, the nature of the amorphous carbon remains unclear. The authors claim that it is amorphous based the absence of a Raman modes in the areas where elemental mapping showed that carbon was present (Yang et al. 2015a). However, even amorphous carbons with very little graphitic ordering show the presence of *G*-

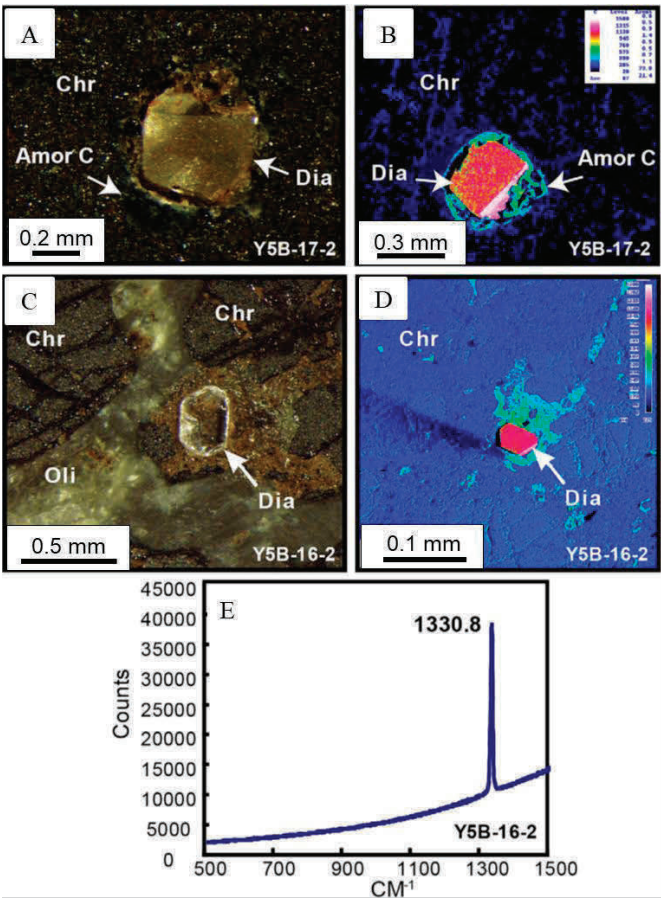

Figure 20. Photomicrographs (**A**, **C**) and, carbon element maps (**B**, **D**) of diamonds from the Ray-Iz ophiolite and (**E**) laser Raman pattern of diamond (reprinted from Yang et al. 2015a, copyright 2015 with the permission of Elsevier #5035691008088). The in–situ diamonds are hosted in spherical (sample 05B–17–2) to irregular (sample 05B–16–2) patches of amorphous carbon within chromitite of the Ray-Iz ophiolite. Chr–chromite, Oli–olivine, Dia–diamond. The **dark blue** color is chromite and olivine and the **light blue** color is amorphous carbon.

and *D*-like features in their Raman spectra (e.g., Ferrari and Robertson 2000). So, it remains a mystery as to why Yang et al. (2015a) did not observe any Raman peaks, they do not show these spectra and they do not report any instrument details from their Raman measurements (e.g., laser wavelength, spectrometer focal length, spectrometer resolution etc.). Moreover, presence of coesite inclusions in ophiolitic diamond is not an undisputable feature that can be used as a criterion to sort out if diamond is synthetic or indigenous. Milledge (1961) reported that they found coesite inclusions in one of the synthetic diamonds produced by the General Electric Company (G.E.C.) Laboratories in Schenectady county NY, USA. Therefore, careful characterization of sp^3-carbon (diamond), sp^2-carbon (graphite), and disordered or amorphous carbon should be provided in the future by Yang et al. (2015a) to prove unconditionally that the Ray-Iz diamonds are indigenous. They also need to show the differences between their so-called "amorphous carbon" and epoxy resin, which was used for this sample preparation.

Several loose diamonds were studied with FIB-TEM technique (Yang et al. 2015a,b). The results showed that the diamonds contain several ~2–10 μm inclusions of NiMnCo alloys, graphite and one inclusion of coesite. Further studies of inclusions in diamonds recovered from ophiolites are needed so that we can start to better understand the formation conditions of these diamonds.

Diamonds from the Skenderbeu chromitite massif of the Mirdita ophiolite, Albania. Wu et al. (2017) collected 600 kg of chromitite rocks from the Skenderbeu massif of the Mirdita ophiolite, Albania, the western part of Neo-Tethys ocean. After processing these samples at Institute of Multipurpose Utilization of Mineral Resources, Zhengzhou, China, the authors found 20 loose diamonds (100–200 μm in size) of octahedral, cubo-octahedral and irregular shapes (Fig. 21). Diamonds were confirmed with Raman spectroscopy and studied with TEM.

TEM studies of two FIB-prepared foils revealed that the Skenderbeu diamonds contain inclusions of NiMnCo alloy, traces of S and Cl, indicated escaped fluid, and $Ca_{0.81}Mn_{0.19}(SiO)_3$— which has a structure similar to wollastonite. They hypothesized that this phase may be a product of the decompression of a Ca-perovskite, although no undisputable data to support

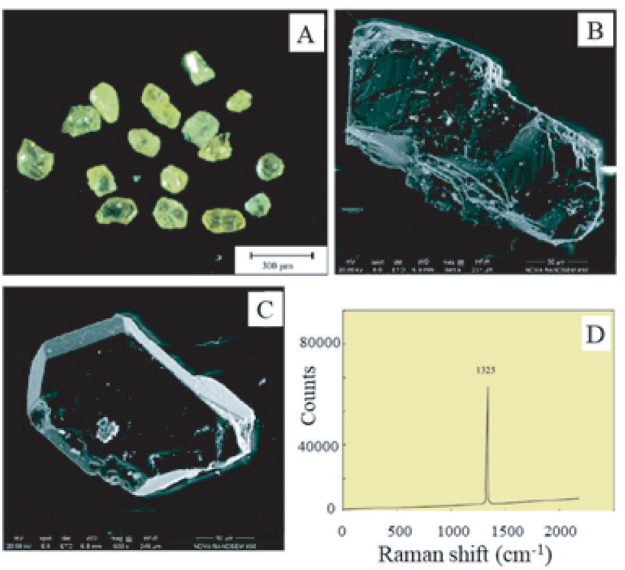

Figure 21. Phographs of diamonds recovered from Skenderbeu chromitites (Reprinted from Wu et al. 2017, copyright 2017, with the permission of John Wiley and Sons #5036200875863). **A –** a microphotograph showing yellow–light yellow diamonds. **B –** SEM image of irregular damond grain. **C** – SEM image of octahedral diamond. **D** – Raman spectrum showing typical diamond Raman shift around 1335 cm^{-1}.

this interpretation was provided. The authors proposed that diamonds were formed in the deep mantle from a carbon-saturated NiMnCo-rich melt acquired from a subducted slab of oceanic crust and lithosphere (Wu et al. 2017, 2020).

Diamonds from Pozanti-Karsanti podiform chromitite, Turkey. The Pozanti-Karsanti ophilite complex occurs within the eastern Tauride belt, in southern Turkey, and consists of well-preserved sections of mantle peridotite, ultramafic and mafic cumulates, podiform chromitites, gabbros, sheeted dikes, and basalts (Dilek et al. 1999). Lian et al. (2017) reported that they recovered more than 100 grains of euhedral and irregular shaped diamonds (50–250 μm in size) from heavy minerals separates from the Pozanti-Karsanti podiform chromitite. The rocks were processed at the same facilities in Zhengzhou, China, as all other ophiolitic diamonds described above. The authors also found SiC and many "crustal" minerals such as zircon, rutile, hematite, magnetite, quartz, sulfides, chlorite, monazite, and also olivine, pyroxene, and an unusual octahedral silicate pseudomorph with a complex chemistry (Mg, Si, Al, Cr, Fe, O and Mg,Si,O). Lian et al. (2018a) showed that the diamonds contain nanometric inclusions of Ni–Mn–Co alloys and $(Ca,Mn)SiO_3$ with triclinic symmetry similar to wollastonite. The authors have hypothesized that wollastonite may be a product of the decompression of $(Ca,Mn)SiO_3$-perovskite, and concluded that the diamonds may have crystallized from carbon-rich fluids in the mantle at a depth of more than 250 km and that they were rapidly transported to a shallower depth by an asthenospheric melt (Lian et al. 2017 2018a,b). Interestingly their interpretation is similar to what was proposed by Wu et al. (2017) for $Ca_{0.81}Mn_{0.19}(SiO)_3$ wollastonite inclusions in Skenderbeu diamonds from Albania.

Diamond in situ from Nadar ophiolites, India. The Nadar ophiolites are situated within the Indus suture zone, southeast Ladakh Himalaya, marking a collision zone between India and Asia. Das et al. (2017) discovered diamond in situ in a polished petrographic thin section of peridotite collected from the lower section of the Nadar ophiolites. Peridotite consists of olivine (50%), orthopyroxene (30%), clinopyroxene (10%), Cr-spinel (5%) and serpentine (5%). A diamond of ~50 μm in size is included in orthopyroxene; a Raman spectrum of the diamond exhibits a well-pronounced Raman band at 1326.7 cm^{-1} (characteristic of disordered sp^3-carbon bonding) and broad feature centered at 1583.2 cm^{-1} (sp^2 disordered graphite carbon bonding often referred to as the *G-band*). Some grains of olivine in this thin section contain numerous 2–5 μm size inclusions of graphite associated with fluid inclusions of C–H and H_2. For those grains of olivine which exhibit well-oriented exsolution lamellae of Cr-spinel and blebs of α-Fe_2O_3, the β-Mg_2SiO_4 was inferred to be a precursor. Das et al. (2017) suggested that diamond crystallized from C–H fluids that were derived from the bottom of the upper mantle—top of the mantle transition zone (depth ~ 410 km). Although 1, 3 and 6 μm diamond grits were used for sample preparation, Das et al. (2017) deduced that their diamond inclusion size (~50 μm) exceeds the size of diamonds from the polishing source, and therefore the diamond inclusion in orthopyroxene from Nadar peridotite is indigenous.

Carbon isotopes, nitrogen content and nitrogen aggregation in UHPM ophiolitic diamonds

According to Xu et al. (2018) carbon isotope characteristics of ophiolitic diamonds from chromitites are comparable with a light carbon reservoir: $\delta^{13}C = -29.0‰$ to $-16.9‰$ (Luobusa chromitite) and $\delta^{13}C = -28.7‰$ to $-18.3‰$ (Ray-Iz, Polar Urals, Russia). The carbon isotope values of ophiolitic diamonds bear similar features as metamorphic diamonds from UHPM terranes, and they are significantly different from cratonic diamonds (Fig. 7). Nitrogen content in Luobusa diamonds varies from 152 to 428 ppm, whereas in Ray-Iz diamonds it varies from 108 to 499 ppm, and both are significantly lower than the nitrogen content reported in diamonds from UHPM terranes and cratonic settings (see Table 2 for comparison). Nitrogen isotope characteristics for Tibetan ophiolite-hosted diamonds ranges from $\delta^{15}N = -28.4‰$ to $-18.8‰$ (e.g., Xu et al. 2018; Lian et al. (2018a) studied carbon and nitrogen isotope values

in diamonds from Posanti-Karsanti chromitites, Turkey. The Pozanti-Karzanti diamonds are characterized by $\delta^{13}C = -28.4‰$ to $-18.8‰$ and $\delta^{15}N$ values ranging from $-19.1‰$ to $16.6‰$ with nitrogen contents ranging from 7 to 541 ppm. All these parameters are similar to those from diamonds of Loubasa and Ray-Iz ophiolites (Table 2) and their strongly ^{13}C-depleted more than likely originated from a subducted crustal carbon-reservoir.

Howell et al. (2015) studied nitrogen aggregation in Luobasa diamonds. They show that these diamonds contain nitrogen impurities in the form of singly substituted C centers (Type Ib diamond). According to Taylor et al. (1996) natural diamonds with similar nitrogen characteristics have a short residence time and they are rare in nature because isolated nitrogen aggregates to form nitrogen pairs (A centers–Type IaA diamond) and more aggregated nitrogen (B centers–Type IaB diamond). Type IaAB is most typical for cratonic diamonds which have long-term (~0.5 to 3 billion year) upper mantle residence, whereas Type Ib is a nitrogen aggregation characteristic, which is typical for synthetic diamond (Taylor et al. 1996). Thus, if ophiolitic diamonds are indigenous, their low aggregation state (Ib) would reflect a short residence time (millions of years' time scale) at temperatures < 900 °C (e.g., Xu et al. 2018). However, a literature survey shows that Ib diamonds were found within their cratonic populations (e.g., Hainschwang et al. 2013; Smit et al. 2016; Smith et al. 2016; Timmerman et al. 2018). Therefore, the nitrogen aggregation parameters do not allow us to unambiguously classify ophiolitic diamonds as either synthetic or indigenous.

Litasov et al. (2019a,b) have suggested that all ophiolitic diamonds are due to anthropogenic contamination. The main arguments are that the composition of the metallic inclusions in type Ib cuboctahedral diamonds in ophiolitic chromitites and peridotites is similar to the composition (Ni:Mn:Co = 70:25:5) of the catalyst used in industrial diamond synthesis. Yang et al. (2020) commented on Litasov et al. (2019b) stating that they have ignored the petrologic context related to microdiamond occurrences and inclusion assemblages discovered in ophiolite-hosted diamonds. Yang et al. (2020) also claim that they ignored the wide occurrence of ophiolite-hosted diamonds discovered in different locations by different research groups. Litasov et al. (2020) replied to this comment and made a simple thermodynamic and kinetic argument against the co-existence of diamond, moissanite, native elements, corundum, wadsleyite, coesite, and quisongite with major ophiolite minerals, they re-emphasized that the metallic inclusions have a similar composition to the catalysts used in industrial diamond synthesis, and they argue that the in situ findings discussed by Yang et al. (2019a) do not meet the basic requirements for in situ mineral grains (they were not observed below the surface before being exposed).

Yang et al. (2019a) also emphasized that the diamonds from ophiolites fall within the size ranging from 100–300 and ~500 μm, and they, therefore, are much larger than those which are used in typical laboratories as an abrasive material. Moreover, they asserted that the ophiolitic diamonds have well-developed crystal faces, whereas any other diamonds from drill bits, or stone-cutting saws would be presented by broken fragments of the crystals.

Shallow diamonds from ophiolites

Healed-crack diamond inclusions in chromite from altered ophiolitic chromitite pods in Tehuitzingo serpentinite (Southern Mexico). Farré-de-Pablo et al. (2019) report *in situ* diamond inclusions in chromite from ophiolitic chromitite pods hosted in the Tehuitzingo serpentinite, southern Mexico. They observed diamonds of 1 to 8 μm in size, quartz, clinochlore, serpentine, and amorphous carbon appeared as "healing-crack inclusions" in chromite. The authors concluded that diamond was formed at a shallow depth at T = 515–670 °C from reduced COH fluids, which infiltrated in during the shallow hydration of chromitite pods enveloped by serpentinite.

Yang et al. (2019b) and Massonne (2019) submitted comments on the Farré-de-Pablo et al. (2018) report raising different concerns. Yang et al. (2019b) specifically discuss that in suggesting

a shallow origin for ophiolite-hosted diamonds Farré-de-Pablo et al. (2019) ignore the presence of many other UHPM phases occurring as both inclusions in diamonds and as associated grains. Yang et al. (2019b) propose an alternative scenario in which the diamonds, along with a carbon-rich fluid and some silicate grains were incorporated into the chromite grain at the time it crystallized in the diamond stability field thus sealing the fracture. Massonne (2019) raised concerns that these diamonds are not indigenous, and they could be considered contamination from abrasives or diamond-bearing tools. Massonne (2019) point out that only show diamonds that have been exposed to the surface, and that the five exposed grains are clearly xenomorphic.

In their reply Farré-de-Pablo et al. (2019) address the concerns of both Yang et al. (2019b) and Massonne (2019). They first address the concerns of Massonne (2019) and stress that they provided many lines of evidence supporting the presence of natural diamonds in the Tehuitzingo chromitites. They discuss that diamonds formed from COH fluids may also exhibit irregular morphologies and they cite Dobrzhinetskaya et al. (2004). In their reply to Yang et al. (2019b) they point out that UHPM minerals other than diamond were not found in the Tehuitzingo chromitites as evidence that the diamonds formed under low P and T conditions. The reply from Farré-de-Pablo et al. (2019) has not unambiguously proved the indigenous origin of these diamonds nor has it clarified the crystallization conditions of these diamonds.

Notably, the submission of comments on published papers and replies to the comments indicates that articles are being read by the community and that the topics are controversial. Moreover, they facilitate discussion not only between the authors but also the readers. These controversies should be considered positive since they are one way that science moves forward.

From our standpoint, finding diamonds as healing–crack inclusions in chromite (Farré-de-Pablo et al. 2018) is extremely interesting, and it may expand our understanding of microdiamond formation. However, the most important information that would unambiguously prove that the Tehuitzingo diamonds are indigenous is still missing. The authors presented FIB-TEM images accompanied with EELS spectroscopy data confirming both sp^3 carbon bonding (diamond) and amorphous carbon. Farré-de-Pablo et al. (2018, 2019) emphasized that the Tehuitzingo diamonds exhibit "cohesive" contacts with the host minerals and particularly with enveloping amorphous carbon which contains hollows interpreted as evidence of the escaped fluid. We scrutinized their FIB-TEM data (Fig. 2 in Farré-de-Pablo et al. 2019, and Supplemental Materials) and strongly believe that higher quality HRTEM images of diamond–amorphous carbon and diamond–chromite interfaces are necessary to prove or disprove the indigenous origin of this diamond. The authors should continue to do TEM studies (maybe with additional FIB milling) on the same foil to acquire HRTEM images accompanied by selected area electron diffraction (SAED) patterns of each phase. These data would provide a better understanding of the relationships between all solid phases (lattice fringes, d-spacings) and traces of fluid (e.g., as an example see Fig. 6 d in O'Bannon et al. 2020).

Diamonds inclusion in magmatic olivine from gabbro and chromitite of the Moa-Baracoa ophiolitic massif, eastern Cuba. Pujol-Solà et al. (2020) report that they found *in situ* diamond hosted by magmatic olivine occurring in gabbro and chromitite of an upper mantle section of ophiolite. The authors described 200–300 nm sized diamonds associated with low-temperature and low-pressure minerals such as lizardite, chrysotile and magnetite and they are hosted by trails of the healed cracks and CH_4-rich fluid inclusions inside of olivine. The authors concluded that the observed diamonds were formed at a shallow depth from reduced carbon-rich fluid at $P < 200$ MPa and $T < 350$ °C during serpentinization of olivine in gabbro and chromitite. They also hypothesized that the presence of super-reduced phases together with metastable diamond is clear evidence of a widespread infiltration process of CH_4-rich fluids in the oceanic lithosphere, and therefore the ultra-high-pressure origin for other ophiolitic diamonds can be dubious (Pujol-Solà et al. 2020).

Since these samples were prepared with abrasive diamond material, we believe that there would be fewer concerns of contamination if they provided more detailed data of the diamond–host minerals interface. Special attention should be focused on Fig. 2a,b,c of Pujol-Solà et al. (2020) where ~400 nm diamond inclusion is enveloped by "soft" serpentine material; the latter is situated between olivine and magnetite. The diamond–serpentine interface shown in Figure 2c of Pujol-Solà et al. (2020) does not provide clear information about the diamond–serpentine interface. HRTEM images are needed to observe lattice fringes of the diamond inclusion and its host serpentine. HRTEM images would be helpful to investigate the material between the diamond and serpentine which looks like a darker line surrounding the diamond (see their Fig. 2 c). It also would be helpful to inspect both the diamond and serpentine for any nanometric fluid or solid inclusions. The SAED analysis (Fig. 2c) and EELS spectrum (Fig. 2e) shown by Pujol-Solà et al. (2020) do confirm the presence of diamond, however, they do not prove or disprove that this diamond is indigenous.

Ophiolite-hosted diamonds and super-reduced minerals and alloys formed from natural lightning strikes

Ballhaus et al. (2017) proposed a new concept for ophiolitic diamond and associated ultra-reduced minerals formation due to natural lightning strikes. They conducted laboratory experiments in which basalt rock was subjected to electrical discharge (T~5700 °C) to simulate a natural cloud-to-ground lightning strike (Uman 1986). Ballhaus et al. (2017) report that the high-electrical energy discharge into basalt created a plasma followed by melting and rapid crystallization of Fe–Si alloys, W–Ti alloys, metallic Ti, SiC, amorphous carbon and spherulitic ejecta. Though no diamond was produced by these experiments, the authors believe that they produced potential precursors to diamond. Ballhaus et al. (2017) hypothesized that diamond could nucleate in the cores of fullerenes, when they contract during cooling similar to that described in earlier experiments reported by Banhart and Ayajan (1996). Furthermore, Ballhaus et al. (2017) explicated that coesite and stishovite could also be formed during discharging experiments, though these minerals were not found in the run products of their experiment. Ballhaus et al. (2017) concluded that all existing models of ophiolites formation should be scrutinized because the diamond (and some ultra-reduced phases) have dubious origin.

The lightning origin of diamonds and associated ultra-reduced minerals, alloys and metals hosted by ophiolites has been met with criticism. Griffin et al. (2018) disagreed with Ballhaus et al. (2017) hypothesis because diamonds from ophiolites exhibit characteristics which are not comparable with the environment created in experiments by the high-electrical energy discharge (equivalent of natural lightning).

Yang et al. (2018) argued that Ballhaus et al. (2017) experiments have never produced diamond with solid inclusions, whereas diamonds from ophiolites contain wide variety of UHPM and highly reduced mineral inclusions of SiC, NiMnCo and other alloys, Mn-rich olivine, garnet, Mn-oxides, chromite, coesite and fluids (Yang et al. 2015b; Wu et al. 2017; Moe et al. 2018). Additionally, Yang et al. (2018) asserted that the lightning process cannot produce so many diamonds in such geographically different places (China, Turkey, Russia, India, Albania to mention a few), and in the rocks which have been situated at the mantle depth during diamond crystallization.

Volcanic diamonds from Kamchatka, Russian Federation

A sensational discovery of microdiamonds occurring in lava and ash of the modern Tolbachik volcanic eruption of 2012–2013 (Kamchatka peninsula, Russian Federation) was reported by Karpov et al. (2014) and Gordeev et al. (2014). Later Galimov et al. (2016) proposed that carbon dispersed during the eruption could be the perfect source of carbon for these diamonds. They suggested *"…that Tolbachik microdiamonds were formed as a result of cavitation during the rapid movement of volcanic fluid*" (Galimov et al. 2016). According to

this concept the ultra-high-pressure required for diamond formation is concentrated locally, e.g., inside of the carbon-rich fluid bubbles expelled by the volcano, while the external pressure remains not very high.

Further investigation of Tolbachik diamonds lead to conclusions that their geochemical and mineralogical data strongly support their origin from gases released during volcanic explosion (e.g., Galimov et al. 2020a; Galimov and Kaminsky 2021). They reported that Tolbachik diamonds are characterized by $\delta^{13}C = -22$ to $-29‰$, which are comparable with the $\delta^{13}C$ values of kimberlitic diamonds, and their $\delta^{15}N = -2.58$ and $-2.32‰$ are similar to $\delta^{15}N$ of volcanic gases, while atmospheric nitrogen has $\delta^{15}N = 0‰$ (Galimov et al. 2020a, b). The nanometric inclusions of Tolbachik diamonds are presented by Mn–Ni–Si alloys and silicides with compositions ranging from $(Mn,Ni)_4Si$ to $(Mn,Ni)_5Si_2$, Mn_5Si_2, and MnSi. These features resemble those in diamonds found *in situ* in ophiolitic chromitite and peridotite (e.g., Galimov et al. 2020a,b).

The Tolbachik diamonds existence as a product of a volcanic explosion was met with extreme criticism and suggestions that those diamonds and accompanied ultra-reduced minerals, alloys and metals are products of anthropogenic contamination (Litasov et al. 2019a,b, 2020; Pokhilenko et al. 2019). There is a series of Comments and Replies publications between those who considered Tolbachik diamonds (as well as their ophiolitic counterparts) as natural Earth materials (Galimov et al. 2020a,b; Galimov and Kaminsky 2021), and those who insisted that all of them are a result of anthropogenic contamination (e.g., Litasov et al. 2019a,b, 2020, 2021; Pokhilenko et al. 2019). It is clear from reading of these comments and replies that each group believes that their arguments are correct, and therefore they deny any disagreements.

Are diamonds from ophiolite and modern volcanic eruption myth or reality?

The narrative of discovery of both ophiolitic and volcanic diamonds to some degree reminds us of the story of ultra-high-pressure metamorphism. This was best described by Harry W. Green II as "a confused mixture of surprising, sometimes spectacular, discoveries and emotional reactions" (Green 2005, p.439). Green (2005) emphasized that science advances in a conservative fashion in a process where *accurate* ideas are added to the existing "library" of knowledge and *inaccurate* ideas are not. He also stressed that new ideas which attempt to shift the paradigm will be met with criticism proportional to how large a shift is needed (Green 2005). The example most relevant to the recent controversial reports of ophiolitic and volcanic diamonds, is the story of the discovery of microdiamonds in metamorphic rocks of continental affinities described at the beginning of this paper. First diamonds from Kokchetav massif, Kazakhstan became known to local geologists due to processing large volumes of the garnet–biotite gneisses using industrial scale methods for minerals separation (Rozen 1972; Rozen et al. 1979 and references therein). After Sobolev and Shatsky (1990) clearly demonstrated that diamonds from Kokchetav were indeed indigenous, Massonne (1999) reported the discovery of similar diamonds in metamorphic gneisses of Erzgebirge, Germany. This discovery was met with harsh criticism and denied at the 1999 Kimberlitic Conference (Green 2005), fortunately additional investigations were published soon after the conference supporting this new diamond find (Massonne 1999; Nasdala and Massonne 2000; Green 2005).

In general, the disbelief that diamond and other UHPM minerals could occur naturally in crustal metamorphic rocks was overcome by a step-by-step process which eventually disregarded the inaccurate observations and deductions. The process included major efforts of many scientific groups who organized an uncountable number of seminars and scientific schools associated with International meetings, where participants had the opportunity to see these "mysterious" diamonds *in situ* for themselves with the aid of an optical microscope. In parallel to these efforts more advanced analytical techniques were also being developed and presented to the scientific community. The resolution of SEM and FIB-TEM and the flux and brightness of synchrotron facilities continued to improve. As a result, there was a shift in the paradigm and diamond-bearing UHPM terrains are now well-documented and accepted by the community.

The main argument underlying the disbelief in ophiolitic and volcanic diamonds is that they have a lot of common characteristics with their synthetic counterparts which are widely used in industrial machines and tools. The increasing concerns arise because almost all worldwide ophiolite-hosted diamonds were separated at the same mineral processing facilities at the Institute of Multipurpose Utilization of Mineral Resources, Chinese Academy of Geological Sciences, Zhengzhou (e.g., Xu et al. 2009). There is, however, one encouraging report of an ophiolitic diamond that was extracted from the Luobasa chromitite by an individually developed method of minerals separation which excluded any possible anthropogenic/laboratory contamination (Howell et al. 2015; Griffin et al. 2016). This provides us evidence that some ophiolitic diamonds are indigenous.

We strongly believe that the indigenous origin of ophiolite-hosted diamonds can be unconditionally proven if diamond abrasives/tools are eliminated from every step of the samples preparation from extraction to polishing stages. The observations of the same diamond in a polished thin section surface should be conducted using a combination of techniques such as optical microscopy, Raman spectroscopy, and SEM, FIB-TEM confirmation of diamond–host mineral interface. The same approach should be applied to studies of volcanic diamonds. The critical samples should be shared between different research groups so that a wide range of analytical techniques can be utilized to study origin of these diamonds.

Once anthropogenic contamination can be ruled out, the community can move past this question and focus on more important aspects of these findings. This would include searching for natural processes that would be similar to the industrial diamond synthesis processes, as well as the formulation of new models that can adequately explain diamond growth in ophiolites and processes that can transport diamonds from elsewhere to the shallow mantle beneath spreading centers.

MISIDENTIFICATION OF MICRODIAMONDS DUE TO CONTAMINATION FROM SAMPLE PREPARATION

General precautions and examples

Since many diamonds from UHPM terranes as well as from ophiolites and volcanic sources are small ranging in size from ≤ 3–50 μm they can be misidentified with diamonds which were mechanically embedded into softer minerals during sample preparation (e.g., cutting, drilling, and/or polishing with diamond tools or abrasives). Recognition of possible contamination has been mentioned in the scientific literature as well as in numerous instruction manuals attached to polishing instruments. Microdiamond researchers are acutely aware that contamination from sample preparation can occur, and that distinguishing indigenous microdiamonds from diamonds embedded during sample preparation is not trivial.

Figure 22A–F contains a series of images showing the morphology of diamond particles found in a typical abrasive powder and those embedded in diamond saws. Figure 22G–H shows "loose" UHPM diamond crystals recovered from crushed rocks. If a diamond-bearing sample is properly polished (see detailed procedure in Dobrzhinetskaya et al. 2001), the diamonds will be elevated above the polished surface of host minerals (e.g., zircon and garnet) which is due to the difference in hardness between the diamond and host minerals (Fig. 23). Visual inspection of the images, especially those acquired with an optical microscope or SEM using low magnification, reveal that the morphology of diamonds from abrasive grits and natural diamonds are quite similar (Fig. 22). Therefore, the morphologies of the diamonds cannot always be used to distinguish between natural microdiamonds and diamonds from abrasive grits.

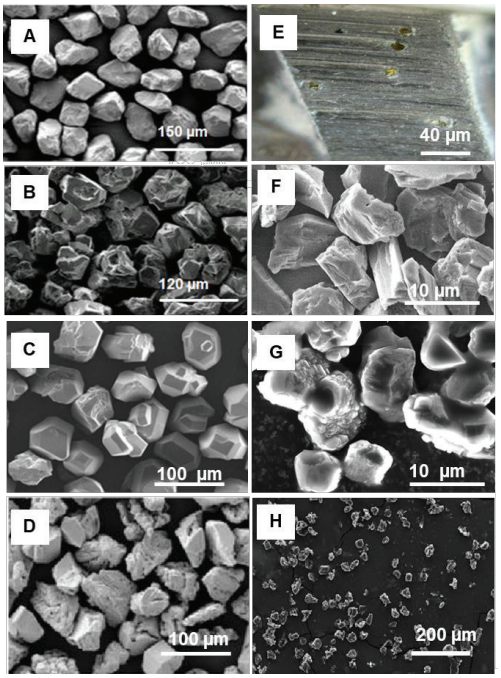

Figure 22. A–B: synthetic diamond abrasive powder, courtesy of Henan Baililai Superhard Material Co., Ltd; **C–D:** synthetic diamond grit, courtesy of Hiperion Materials & Technologies, France; **E**: a segment of a diamond saw blade, (Wiki Commons), **F:** synthetic diamond abrasive, TradeIndia Ltd (www.tradeindia.com); **G:** natural microdiamonds separated from Erzgebirge garnet–quartz–feldspathic gneiss (Dobrzhinetskaya's collection); **H:** natural microdiamonds separated from Kokchetav garnet–biotite gneisses (Dobrzhinetskaya's collection).

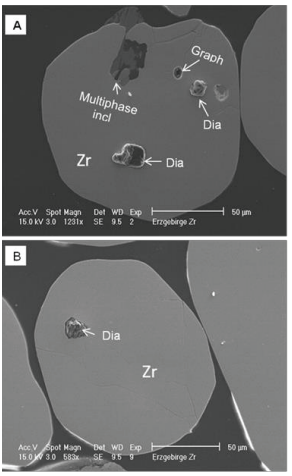

Figure 23. Secondary electron SEM images of zircon grains separated from the garnet–quartz–feldspathic gneiss from the Erzgebirge, Germany; zircons are mounted with Petropoxy on a standard petrographic glass slide and polished with SiC grit, Al_2O_3 and SiO_2–colloidal abrasive liquid (see polishing procedure protocol described in Dobrzhinetskaya et al. 2001). **A**: diamond inclusions are standing above the perfectly polished zircon surface, whereas graphite and multiphase inclusions (phengite + SiO_2 + $KAlSiO_3O_8$) remain flat; lattice parameters of SiO_2 and $KAlSi_3O_8$ are not measured due to the small size of inclusions. **B:** diamond inclusion in zircon; phengite (**black contrast**) occurs at the diamond–zircon interface.

Raman spectroscopy: indigenous diamond vs. its synthetic counterpart

One should be cautious when using Raman spectroscopy as the sole diagnostic for identifying indigenous diamonds. Diamond has a strong first order Raman mode at 1332 cm^{-1}, some abrasives show broadening of this mode as well as a strong shift of this mode to lower wavenumbers. However, Nasdala et al. (2016) show that the Raman parameters of diamond abrasives (collected from 11 different manufacturers) widely overlap with UHPM microdiamonds (Fig. 24A–C, E, F) making it nearly impossible to distinguish between a genuine UHPM relict or an introduced artefact based on Raman spectroscopy alone.

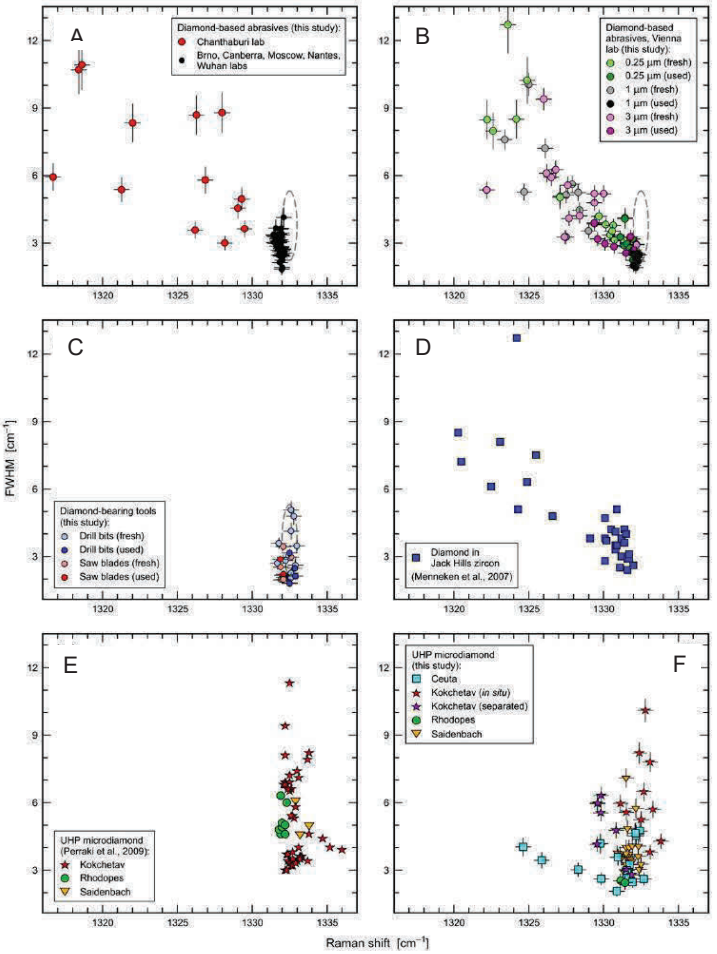

Figure 24. Plots of the FWHM as a function of peak position of the first–order Raman mode of diamond (LO = TO mode at 1332 cm^{-1} for ideal ambient single–crystal diamond), adopted from Nasdala et al. 2016—Fig. 5 (copyright 2016, reprinted with the permission of Elsevier #5032691073556). **A–C:** data from diamond-based abrasive and diamond tools (Nasdala et al. 2016's study), **dashed oval**—data from Perraki et al. 2009; **D:** Jack Hills diamonds in zircon (Menneken et al. 2007 Fig. 2); **E:** diamonds from UHPM terranes from Perraki et al. 2009; **F:** diamonds from UHPM terranes (Nasdala et al. 2016's study).

The study of Menneken et al. (2007) is a prominent example of diamond contamination during sample polishing. They reported the astonishing discovery of the oldest microdiamonds on Earth as inclusions in zircons from the Jack Hills conglomerate, Australia (~ 4.2–3.0 Ga, Nemchin et al. 2008). They used Raman spectroscopy as their primary diagnostic technique, particularly they relied on the FWHM of the diamond Raman mode to distinguish their diamonds from the diamond-based abrasive used for their sample preparation. Indeed, in Fig. 2 from Menneken et al. (2007) the plots of the FWHM vs. Raman shift show that the Jack Hills microdiamonds have larger FWHM's and are shifted to lower frequency than the abrasive diamonds used during their sample preparation. In addition to the Raman results Menneken et al. (2007) ruled out contamination from the diamond polishing powder based on (i) some of the diamonds are completely enclosed by zircon, and (ii) they argued that the size of the diamond inclusions are mostly larger than the size of the diamonds in the polishing materials.

However, several unreconciled discrepancies existed. One is that it does not matter if the zircons are considered as magmatic (Hopkins et al. 2008, 2010, 2012) or as metamorphic (Rasmussen et al. 2010, 2011, 2012) the oldest Jack Hills zircons have a shallow (<10 km) crustal origin. If diamond crystallized along with the zircon at these shallow depths, the diamonds would have formed outside the diamond stability field. Alternatively, the diamonds could have formed within the diamond stability field at a depth of ≥150 km and they were later transported to these shallow depths where they became incorporated into the zircons when they crystallized.

Another discrepancy is that other high-pressure minerals or evidence of their decompression have not been reported in the Jack Hills zircons, and that boundary between the diamond included in zircon is highly irregular and sharp, and even porous and filled with granular "debris" (Fig. 25A). Such "unusual" boundaries between two detached phases (diamond and zircon) look significantly different from the boundaries between an indigenous diamond and its host zircon. The contact zone in many samples generally shows that the diamond is intricately intergrown with its host zircon, which immediately makes it clear that such a diamond is indigenous (Fig. 25B and C).

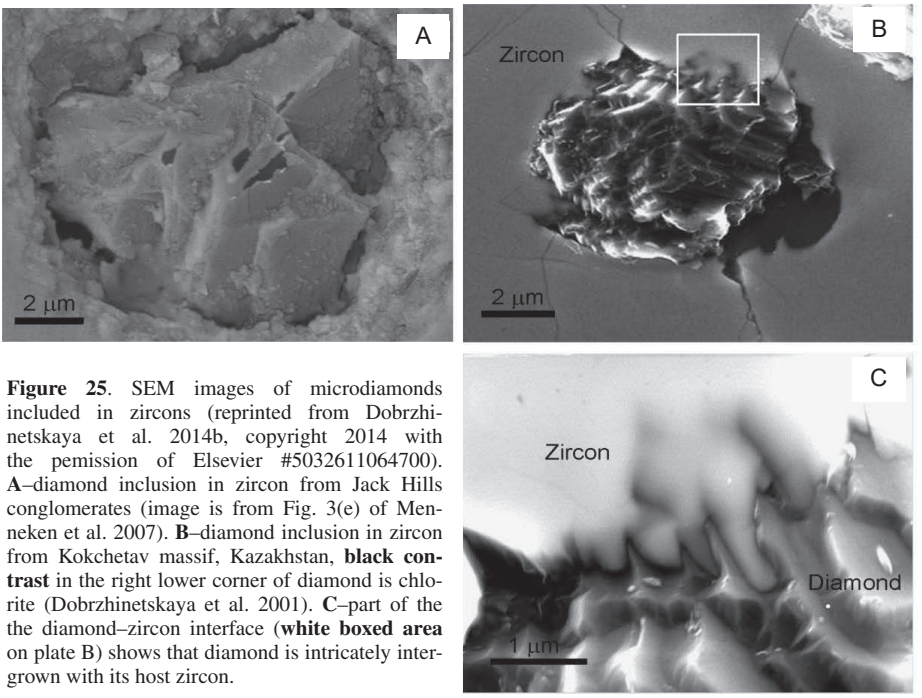

Figure 25. SEM images of microdiamonds included in zircons (reprinted from Dobrzhinetskaya et al. 2014b, copyright 2014 with the pemission of Elsevier #5032611064700). **A**–diamond inclusion in zircon from Jack Hills conglomerates (image is from Fig. 3(e) of Menneken et al. 2007). **B**–diamond inclusion in zircon from Kokchetav massif, Kazakhstan, **black contrast** in the right lower corner of diamond is chlorite (Dobrzhinetskaya et al. 2001). **C**–part of the the diamond–zircon interface (**white boxed area** on plate B) shows that diamond is intricately intergrown with its host zircon.

Considering these inconsistences, Dobrzhinetskaya et al. (2014a) examined the exact same diamond bearing zircon samples which were kindly provided by Menneken et al. (2007) and Nemchin et al. (2008). The SEM and TEM studies of FIB-prepared foils (Fig. 26 A,B,C) concluded that the "Jack Hills diamonds" are not indigenous, and that they are a product of contamination from the industrial diamond abrasive used for sample preparation (Dobrzhinetskaya et al. 2014a). Dobrzhinetskaya et al. (2014a) clearly demonstrated that fragments of broken diamond's ranging in size from ≤0.10–0.30 μm were mechanically embedded/inserted into surficial pores and cracks (Fig. 26 A), and they eroded softer minerals together with polishing dust and petropoxy resin all which occurred during sample preparation (Fig. 26 B,C).

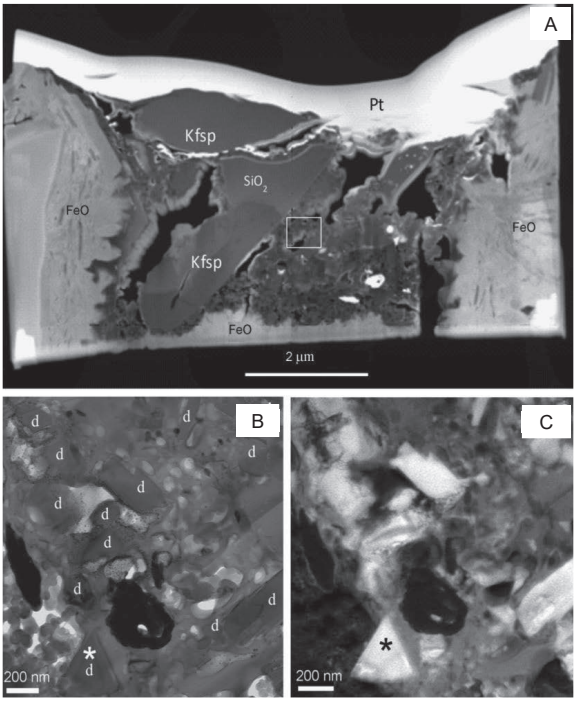

Figure 26. STEM–TEM images of FIB foils cut through inclusions identified by Raman spectroscopy as diamond (Dobrzhinetskaya et al. 2014b, copyright 2014 with the pemission of Elsevier #5032611064700). **A**–STEM image–overview of the place where diamond was identified with Raman spectroscopy (1st order diamond Raman mode observed at: 1332 cm^{-1}) shows the presence of Kfsp and amorphous SiO_2 inclusions. The platinum (Pt) film (**white contrast**) was deposited on the surface of the inclusion prior to the FIB foil preparation, and it has a concave–upward surface indicating that the material from the surface was preferentially eroded during the primary mechanical polishing, because the Kfsp inclusion is softer than the zircon. The **black contrast** areas between Kfsp and SiO_2 represent holes that were probably filled with volatile-rich solid materials or fluids that "evaporated" to the vacuum chamber during FIB milling. **B**–Bright Field TEM image of boxed area shown in plate (A) showing abundant diamond fragments (labeled as '**d**'); the dark contrasted grains with irregular shapes and surfaces are gold (from the previous gold sputtering). Note the unusual sharp–angle morphology of the diamond. The round bubble-like **bright–grey contrast** area is an epoxy resin mixed with the polishing debris. **C**–Image taken of the same area as (B) with characteristic X–rays of carbon (carbon–element map). Bright contrast indicates essentially pure carbon; * is labeled for an easy comparison with the diamond fragments shown on plates B and C.

Later, Menneken et al. (2014) used TEM and Raman spectroscopy on FIB cut sections of the embedded diamonds in their samples and they concluded that the embedded diamond particles originated from the diamond polishing powder. This study is evidence that diamonds that contaminated the sample during cutting and polishing can be misidentified as indigenous UHPM diamonds. In the case of the Jack Hills diamonds if this misidentification was not brought to the scientific forum, it could have had a profound impact on our understanding of the earliest phase of Earth's history. Since it is now known that the "Jack Hills diamonds" are not indigenous (Dobrzhinetskaya et al. 2014a; Mennekan et al. 2014, 2017) several new thorough systematic studies of synthetic diamonds from different manufacturers and microdiamonds from well-established UHPM terranes (Fig. 24) have been reported (Steger et al. 2013; Nasdala et al. 2016). Raman data from Jack Hills diamonds reported by Menneken et al. (2007) (Fig. 24 D) fit well with the Raman data from diamond-based abrasives and tools (Fig. 24A–C), and they partly overlap with Raman data collected from UHPM diamonds

(Fig. 24 E,F). As discussed above, Nasdala et al. (2016) demonstrated that Raman spectroscopy can be used as fast and nondestructive diagnostic method for diamond identification. However, they emphasize that Raman spectroscopy cannot unambiguously differentiate between natural diamonds and industrial diamond–abrasives. To avoid erroneous discoveries of new microdiamond localities one should avoid using Raman spectroscopic techniques as the *only* diagnostic for confirmation of the indigenous origin of the diamonds.

In an earlier chapter we discussed that microdiamond occurring together with SiC, moissanite (Perraki and Farayd 2014; Janák et al. 2015) would require ultra-reduced conditions. These samples are very important for future investigations since they imply a specific oxidation state of the diamond–moissanite inclusions in garnet. However, additional documentations are required that these SiC inclusions have indigenous origin. Nasdala et al. (2016) also note that the Raman spectra of geological moissanite and the Raman spectra of synthetic silicon carbide are not distinguishable (see their Fig. 4d). Consequently, the presence of moissanite in multiphase inclusions from UHPM assemblages should be confirmed in order to exclude any misinterpretation of contamination from SiC-based abrasives used for polishing materials.

How to prove that microdiamond is indigenous

In general, we believe that it should be a mandatory for acceptance of any new discovery of non-cratonic microdiamonds to demonstrate the nature of the diamond–host minerals interface to avoid misidentification with remnants of diamond-based polishing abrasives. In some cases, studies of the diamond–host mineral relationships with optical microscopy and their documentation with high resolution SE images from an SEM can be enough to confirm the indigenous nature of a microdiamond (e.g., Dobrzhinetskaya et al. 2001). For example, Figures 25 B and C present the secondary electron SEM images which demonstrate the intergrown features of zircon–diamond interface. Such relationships unconditionally confirm indigenous origin of the diamond inclusion in zircon. In other cases, it is necessary to use a TEM to investigate FIB-prepared foils that were cut through the diamond–host mineral interface (Fig. 26) (e.g., Dobrzhinetskaya et al. 2001, 2003, 2005, 2006a). As an example, see Figures 26 and 27 which demonstrate FIB-milled sample of the diamond–zircon interface. FIB-TEM techniques are the safest approach for avoiding the misidentification of industrial diamonds–abrasive as natural diamonds, especially if the diamond inclusions under question are smaller than 5 mm (e.g., Dobrzhinetskaya et al. 2003, 2006a).

Notably one robust approach for avoiding the misidentification of diamond and moissanite inclusions would be to not use diamond and SiC tools and abrasives during sample extraction and preparation, one could use corundum instead. Final finishing of the samples with colloidal SiO_2 liquid always provides a great polishing effect and makes diamond inclusions more visible on the flat polished surface of the host minerals.

FUTURE DIRECTIONS

Studies of UHPM microdiamonds have furthered our knowledge and understanding of geochemical and mineralogical processes during the deep subduction of crustal material and its interaction with the Earth's mantle. Despite their mm-size these diamonds have preserved solid, liquid, and gas inclusions over long time periods. These inclusions reflect pathways of the crustal rocks and organic carbon from the Earth's surface to its interior and back to the Earth's surface. The next decade of in situ microdiamond research may be focussed on the following:

(i) Confirmation of the indigenous nature of microdiamonds in newly discovered UHPM, ophiolites and volcanic localities requires the documentation of the diamond–host mineral interface with the aid of the high-resolution secondary electron SEM imaging, and/or TEM imaging and crystal structure data obtained from FIB-prepared samples.

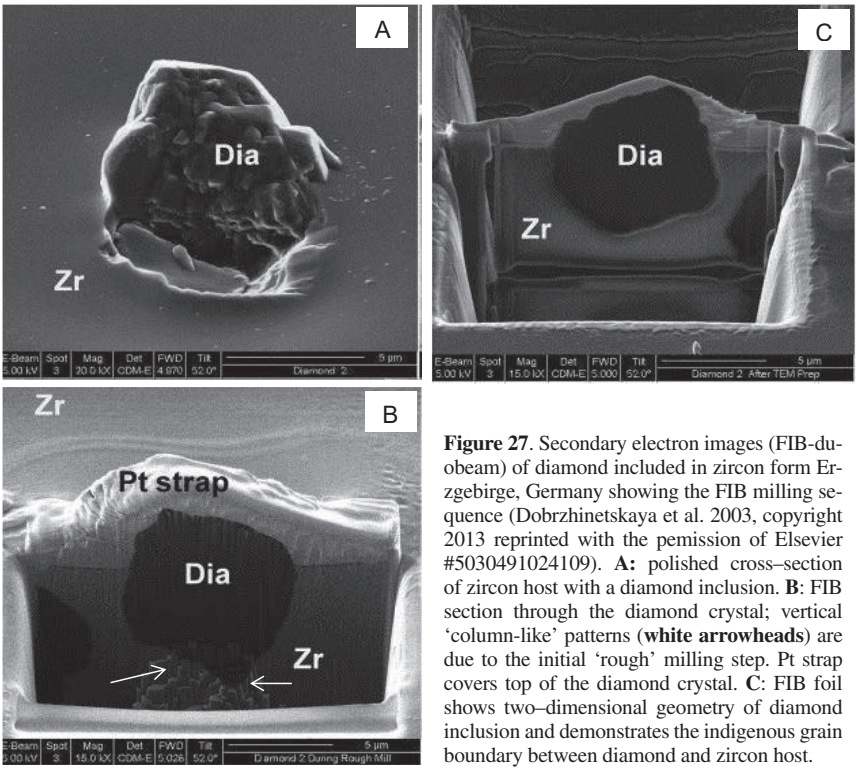

Figure 27. Secondary electron images (FIB-duobeam) of diamond included in zircon form Erzgebirge, Germany showing the FIB milling sequence (Dobrzhinetskaya et al. 2003, copyright 2013 reprinted with the pemission of Elsevier #5030491024109). **A:** polished cross–section of zircon host with a diamond inclusion. **B**: FIB section through the diamond crystal; vertical 'column-like' patterns (**white arrowheads**) are due to the initial 'rough' milling step. Pt strap covers top of the diamond crystal. **C**: FIB foil shows two–dimensional geometry of diamond inclusion and demonstrates the indigenous grain boundary between diamond and zircon host.

(ii) Studies of nanoscale inclusions in microdiamonds from different lithologies to improve our understanding of geochemical environments and PT conditions of diamond crystallization.

(iii) Raman studies of anomalies in microdiamonds which are interpreted as evidence of the "lonsdaleite structure" need to be investigated with FIB-TEM, and/or synchrotron assisted X-ray and spectroscopic techniques.

(iv) Studies of stable isotopes chemistry and noble gases from additional UHPM, ophiolite and volcanic diamond localities to increase our knowledge of processes that occur during continental crust–mantle interaction.

(v) Coordination of laboratory-assisted studies on microdiamonds with general questions of Earth's dynamics through studies of UHPM minerals assemblages associated with diamond formations.

(vi) Modeling and calculations of subduction and exhumation rates; and understanding of how much crustal materials have reached the "point-of-no-return" during deep subduction and remained in the Earth's deep interior being intermixed with the mantle.

ACKNOWLEDGEMENTS

LD research was performed as a part of the International Lithosphere Program, Task Force IV, project "Fate of the subducted continental lithosphere: insight through analytical mineralogy and microstructures", and were supported in different years by NSF grants EAR 0229666, EAR 0107118 and INT–EAR 0329596; Los Alamos National Laboratory through

Science and Technology Base Programs (grant 9949); the Consortium for Materials Properties Research in Earth Sciences (COMPRES); Pacific Rim Program of the University of California, and the University of California Lab Fee Research Grant. EFO acknowledges that a portion of this work was performed under the auspices of the US Department of Energy by Lawrence Livermore National Laboratory under Contract No. DE–AC52–07NA27344. HS research was supported by KAKENHI Grant Numbers JP20740314, JP23340169, JP24109702, JP26287139, and JP15KK0150 from MEXT/JSPS, Japan. Helpful discussions of several aspects of UHPM microdiamonds origin with C.V. Stan, M. Janák, J. Kotková and K. Naemura are acknowledged. Fruitful advices from the peer–reviewers H–P. Shertl, T. Tsujimori, S.W. Faryad and G. Pearson and editors K.V. Smit and S.B. Shirey of this special volume are greatly appreciated.

REFERENCES

Akaishi M, Yamaoka S (2000) Crystallization of diamond from C–O–H fluids under high-pressure and high-temperature conditions. J Cryst Growth 209:999–1003

Allègre CJ, Staudacher T, Sarda P, Kurz M (1983) Constraints on evolution of Earth's mantle from rare gas systematics. Nature 303:762–766

Anthony TR, Banholzer WF (1992) Properties of diamond with varying isotopic composition. Diam Relat Mater 1:717–26

Arai S (2013) Conversion of low–pressure chromitites to ultrahigh-pressure chromitites by deep recycling: a good inference. Earth Planet Sci Lett 379:81–87

Bai WJ, Zhou MF, Cai Y, Hu X (1989) The types andcharacteristics of basic and ultrabasic rocks from China. Bull Inst Geol Chin Acad Geol Sci (in Chinese) 20:51 –74

Bai WJ, Zhou M F, Robinson PT (1993) Possibly diamond-bearing mantle peridotites and podiform chromitites in the Luobusa and Dongqiao ophiolites, Tibet. Can J Earth Sci 30:1650–1659

Bai WJ, Yang JS, Fang QS, Yan BG, Zhang ZM (2001) Study on a storehouse of ultrahigh pressure mantle minerals—podiform chromite deposits. Earth Sci Front 8:111–121 (in Chinese, Abstr in English)

Ballentine CJ, Burnard PG, (2002) Production, release and transport of noble gases in the continental crust. Rev Mineral Geochem 47:481–538

Ballentine CJ, Marty B, Lollar BS, Cassidy M (2005) Neon isotopes constrain convection and volatile origin in the Earth's mantle. Nature 433:33–38

Ballhaus C, Helmy HM, Fonseca ROC, Wirth R, Schreiber A, Jöns W, Bragagni A, Nagel T, Dittrich S, Thome V, Hezel DC, Below R, Cieszynski H (2017) Ultra-high pressure and ultra-reduced minerals in ophiolites may form by lightning strikes. Geochem Perspect Lett 5:42–4

Ballhaus C, Helmy HM, Fonseca ROC, Wirth R, Schreiber A, Jöns N (2021) Ultra-reduced phases in ophiolites cannot come from Earth' mantle. Am Mineral 106:1053–1063

Banhart F, Ajayan PM (1996) Carbon onions as nanoscopic pressure cells for diamond formation. Nature 382:433–435

Basu S, Jones AP, Verchovsky AB, Kelley SP, Stuart FM (2013) An overview of noble gas (He, Ne, Ar, Xe) contents and isotope signals in terrestrial diamond. Earth Sci Rev 126:235–249

Bebout GE, Fogel ML (1992) Nitrogen-isotope compositions of metasedimentary rocks in the Catalina schist, California: implications for metamorphic devolatilization history. Geochim Cosmochim Acta 56:2839–2849

Begemann F (1994) Indigenous and extraneous noble gases in terrestrial diamonds. *In*: Noble Gas Geochemistry and Cosmochemistry. Matsuda J (ed.) Terra Scientific Publishing Company, Tokyo, p. 217–227

Beltrando M, Compagnony R, Lombardo B (2010) (Ultra)–high pressure metamorphism and orogenisis: an Alpine perspective. Gondwana Res 18:147–166

Bottinga Y (1968) Carbon isotope fractionation between graphite, diamond, and carbon dioxide. Earth Planet Sci Lett 5:301–307

Boyd FR, Gurney JJ, Richardson SH (1985) Evidence for a 150–200–km thick Archaean lithosphere from diamond inclusion thermobarometry. Nature 315:387–389

Broadley MB, Kagi H, Burgess R, Zedgenizov D, Mikhail S, Almayrac M, Ragozin A, Pomazansky B, Sumino H (2018) Plume–lithosphere interaction, and the formation of fibrous diamonds. Geochem Perspect Lett. 8:26–30

Bruguier O, Bosch D, Caby R, Vitale–Brovarone A, Fernandez L, Hammor D, Laouar R, Ouabadi A, Abdallah N, Mechati M (2017) Age of UHP metamorphism in the Western Mediterranean: Insight from rutile and minute zircon inclusions in a diamond-bearing garnet megacryst (Edough Massif, NE Algeria). Earth Planet Sci Lett 474:215–225

Brun J–P, Faccenna C (2008) Exhumation of high-pressure rocks driven by slab rollback. Earth Planet Sci Lett 272:1–7

Bundy FP (1980) The *P, T* phase and reaction diagram for elemental carbon. J Geophys Res Solid Earth 85:6930–6936

Bundy FP, Kasper JS (1967) Hexagonal diamond—A new form of carbon. J Chem Phys 46:3437–3446

Bureau H, Keppler H (1999) Complete miscibility between silicate melts and hydrous fluids in the upper mantle: experimental evidence and geochemical implications. Earth Planet Sci Lett 165:187–196

Busigny V, Cartigny P, Philippot P (2011) Nitrogen isotopes in ophiolitic metagabbros: a re–evaluation of modern nitrogen fluxes in subduction zones and implication for the early Earth atmosphere. Geochim Cosmochim Acta 75:7502–7521

Caby R, Bruguier O, Fernandez L, Hammor D, Boscha D, Mechati M, Laouar R, Ouabadi A, Abdallah N, Doucheta C (2014) Metamorphic diamonds in a garnet megacryst from the Edough Massif (northeastern Algeria). Recognition and geodynamic consequences. Tectonophysics 637:341–353

Cartigny P, de Corte K, Shatsky VS, Ader M, De Paepe P, Sobolev NV, Javoy M (2001) The origin and formation of metamorphic microdiamonds from the Kokchetav massif, Kazakhstan: a nitrogen and carbon isotopic study. Chem Geol 176:265–281

Cartigny P, Harris JW, Taylor A, Davies R, Javoy M (2003) On the possibility of a kinetic fractionation of nitrogen stable isotopes during natural diamond growth. Geochim Cosmochim Acta 67:1571–1576

Cartigny P (2005) Stable isotopes and the origin of diamond. Elements 1:79–84

Cartigny P, Palot M, Thomassot E, Harris JW (2014) Diamond formation: a stable isotope perspective. Annual Rev Earth Planet Sci 42:699–732

Chen Y, Yang JS, Xu Z, Tian Y, Lai S (2018) Diamonds and other unusual minerals from peridotites of the Myitkyina ophiolite, Myanmar. J Asian Earth Sci 164:179–193

Chopin C (1984) Coesite and pure pyrope in high-grade blueschists of the Western Alps: a first record and some consequences. Contrib Mineral Petrol 86:107–118

Chopin C (2003) Ultrahigh-pressure metamorphism: tracing continental crust into the mantle. Earth Planet Sci Lett 212:1–4

Chopin C, Sobolev NV (1995) Principal mineralogic indicators of UHP in crustal rocks. *In:* Ultrahigh-Pressure Metamorphism (Coleman RG, Wang X. eds) Cambridge University Press, p. 96–133

Claoué–Long JC, Sobolev NV, Shatsky VS, Sobolev AV (1991) Zircon response to diamond–pressure metamorphism in the Kokchetav massif, USSR. Geology 19:710–713

Clarke Jr RS, Appleman DE, Ross DR (1981) An Antarctic iron meteorite contains preterrestrial impact–produced diamond and lonsdaleite. Nature 291:396–398

Danilenko VV (2004) Shock-wave sintering of nanodiamonds. Phys Solid State 46:711–715

Das SA, Basu R, Mukherjee BK (2017) In situ peridotitic diamond in Indus ophiolite sourced from hydrocarbon fluids in the mantle transition zone. Geology 45:755–758

Daulton TL, Eisenhour DD, Bernatowicz TJ, Lewis RS, Buseck PR (1996) Genesis of presolar diamonds: Comparative high-resolution transmission electron microscopy study of meteoritic and terrestrial Nano-diamonds. Geochim Cosmochim Acta 60:4853–4872

Davidson LM (1979) Nagssugtoqidian granulite facies metamorphism in the Holsteinsborg region, West Greenland. Grønlands Geologiske Undersøgelse Rapport 89:97–108

Davies GR, Nixon PH, Pearson DG, Obata M (1993) Tectonic implications of graphitized diamonds from the Ronda, peridotite massif, southern Spain. Geology 21:471–474

Davies R, Harlow GE (2002) The high-pressure stability of K–cymrite and phases in the system Or–H_2O. Eos Trans AGU 83(47), Fall Meet Suppl Abstr, V72B–1308

de Corte K, Cartigny P, VShatsky VS, Sobolev NV, Javoy M (1998) First evidence of fluid inclusions in metamorphic microdiamonds from the Kokchetav massif, Northern Kazakhstan. Geochim Cosmochim Acta 62:3765–3777

de Corte K, Taylor WR, De Paepe P (2002) Inclusion contents of microdiamonds from UHP metamorphic rocks of the Kokchetav massif. *In:* The Diamond-bearing Kokchetav Massif. Parkinson CD, Katayma I, Liou JG, Maryama S (eds), Universal Academy Press Inc, Kazakhstan, p. 115–135

De Stefano A, Kopylova MG, Cartigny P, Afanasiev V (2009) Diamonds and eclogites of the Jericho kimberlite (Northern Canada). Contrib Mineral Petrol 158:295–315

Denisov VN, Mavrin BN, Serebryanaya NR, Dubitsky GA, Aksenenkov VV, Kirichenko AN, Kuzmin NV, Kulnitskiy BA, Perezhogin IA, Blank VD (2011) First–principles, UV Raman, X–ray diffraction and TEM study of the structure and lattice dynamics of the diamond–lonsdaleite system. Diam Relat Mater 20:951–953

Derjaguin BV, Fedoseev DV (1994) Physico–chemical synthesis of diamond in metastable range. Prog Surf Sci 45:71–80

Dien E, Gamal H, Arai S, Doucet L–S, Li ZX, Kil Y, Fougerouse D, Reddy SM, Saxey DW, Hamdy M (2019) Cr-spinel records metasomatism not petrogenesis of mantle rocks. Nat Commun 10:1–12

Dilek Y, Thy P, Hacker B, Grundvig S (1999) Structure and petrology of Tauride ophiolites and mafic dike intrusions (Turkey): Implications for the Neotethyan ocean. GSA Bull 111:1192–1216

Dilek Y, Furnes H (2011) Ophiolite genesis and global tectonics: geochemical and tectonic fingerprinting of ancient oceanic lithosphere. Geol Soc Am Bull 123:387–411

Dilek Y, Yang J (2018) Ophiolites, diamonds, and ultrahigh-pressure minerals: new discoveries and concepts on upper mantle petrogenesis. Lithosphere 10:3–13

Dobrzhinetskaya LF (2012) Microdiamonds—frontier of ultrahigh-pressure metamorphism: a review. Gondwana Res 21:207–223

Dobrzhinetskaya LF, Faryad SW (2011) Frontiers of ultrahigh-pressure metamorphism: view from field and laboratory. *In:* Ultrahigh-Pressure Metamorphism—25 Years After the Discovery of Coesite and Diamond. Dobrzhinetskaya LF, Faryad SW, Wallis S, Cuthbert S (eds), p 1–3

Dobrzhinetskaya LF, Green HW (2007a) Diamond synthesis from graphite in presence of water and SiO_2: implications for diamond formation in quartzites from Kazakhstan. Int Geol Rev 49:389–400
Dobrzhinetskaya LF, Green II HW (2007b) Experimental studies of mineralogical assemblages of metasedimentary rocks at Earth's mantle transition zone conditions. J Metamorph Geol 25:83–96
Dobrzhinetskaya LF, Eide EA, Larsen RB, Sturt BA, Trønnes RG, Smith DC, Taylor WR Posukhova TV (1995) Microdiamond in high-grade metamorphic rocks of the Western Gneiss region, Norway. Geology 23:597–600
Dobrzhinetskaya LF, Green II HW, Mitchell TE, Dickerson RM (2001) Metamorphic diamonds: mechanism of growth and inclusion of oxides. Geology 29:263–266
Dobrzhinetskaya LF, Green II HW, Weschler M, Darus M, Wang YC, Massonne HJ, Stöckhert B (2003) Focused ion beam technique and transmission electron microscope studies of microdiamonds from the Saxonian Erzgebirge, Germany Earth Planet Sci Lett 210:399–410
Dobrzhinetskaya LF, Renfro AP, Green II HW (2004) Synthesis of skeletal diamonds: Implications for microdiamond formation in orogenic belts. Geology 32:869–872
Dobrzhinetskaya LF, Wirth R, Green HW (2005) Direct observation and analysis of a trapped COH fluid growth medium in metamorphic diamond. Terra Nova 17:472–477
Dobrzhinetskaya LF, Wirth R, Green II HW (2006a) Nanometric inclusions of carbonates in Kokchetav diamonds from Kazakhstan: A new constraint for the depth of metamorphic diamond crystallization. Earth Planet Sci Lett 243:85–93
Dobrzhinetskaya LF, Liu Z, Cartigny P, Zhang J, Tchkhetia D, Hemley RJ, Green II HW (2006b) Synchrotron infrared and Raman spectroscopy of microdiamonds from Erzgebirge, Germany. Earth Planet Sci Lett 248:340–349
Dobrzhinetskaya LF, Wirth R, Yang J, Hatcheon ID, Weber P, Green HW (2009) Nitrides and oxides recording a highly reduced mantle environments form an ophiolite. PNAS 106:19233–19238
Dobrzhinetskaya LF, Green II HW, Takahata N, Sano Y, Shirai K (2010) Crustal signature of $\delta^{13}C$ and nitrogen content in microdiamonds from Erzgebirge, Germany: Ion microprobe studies. J Earth Sci 21:623–634
Dobrzhinetskaya LF, Wirth R, Green II HW, Schreiber A, O'Bannon III EF (2013) First find of polycrystalline diamond in ultrahigh-pressure metamorphic terrane of Erzgebirge, Germany. J Metamorph Geol 31:5–18
Dobrzhinetskaya LF, Wirth R, Green II HW (2014a) Diamonds in Earth's oldest zircons from Jack Hills conglomerate, Australia, are contamination. Earth Planet Sci Lett 387:212–218
Dobrzhinetskaya LF, Wirth R, Yang JS, Bai W, Green HW, Hutcheon ID, Weber PK, Grew E (2014b) Qingsongite, natural cubic boron nitride: The first boron mineral from the Earth's mantle. Am Mineral 99:764–772
Dubinchuk VT, Simakov SK, Pechnikov VA (2010) Lonsdaleite in diamond-bearing metamorphic rocks of the Kokchetav Massif. Dokl Earth Sci 430:40–42
Eggler DH, Baker DR (1982) Reduced volatiles in the system C–O–H: implications to mantle melting, fluid formation and diamond genesis. *In*: High Pressure Research in Geophysics. Akimoto S, Manghnani MH (eds), Center Academic Publisher, Tokyo, p. 237–250
Ekimova TE (1992) Diamond inclusions in rock–forming minerals of metamorphic rocks. Dokl Akad Nauk 322:366–368
El Atrassi F, Brunet F, Bouybaouene M, Chopin C, Chazot G (2011) Melting textures and microdiamonds preserved in graphite pseudomorphs from the Beni Bousera peridotite massif, Morocco. Eur J Mineral 23:157–168
Ernst WG, Liou JG (1999) Overview of UHP metamorphism and tectonics in well-studied collisional orogens. Int Geol Rev 41:477–493
Ernst WG, Liou JG (2008) High-and ultrahigh-pressure metamorphism: Past results and future prospects. Am Mineral 93:1771–86
Essenov CE, Efimov LA, Shiygin ED, Abduicabirova MA, Vedernicov NN, Nuriybaev AN (1968) To problem of the diamond deposits of the Northern Kazakhstan. Vestn Akad Nauk Kaz SSR 1:37–45
Fang Q, Bai WJ (1981) The discovery of Alpine-type diamond-bearing ultrabasic intrusions in Tibet. Geol Rev (Beijing) 27:455 –457
Farré-de-Pablo J, Proenza JA, González–Jiménez JM, Garcia–Casco A, Colás V, Roqué–Rossell J, Camprubí A, Sánchez–Navas A (2018) A shallow origin for diamonds in ophiolitic chromitites. Geology 47:75–78
Farré-de-Pablo J, Proenza JA, González–Jiménez JM, Garcia–Casco A, Colás V, Roqué–Rossell J, Camprubí A, Sánchez–Navas A (2019) A shallow origin for diamonds in ophiolitic chromitites: REPLY. Geology 47:e477–e478
Farré-de-Pablo J, Proenza JA, González–Jiménez JM, Aiglsperger T, Garcia–Casco A, Escuder–Viruete J, Colás V, Longo F (2020) Ophiolite hosted chromitite formed by supra–subduction zone peridotite –plume interaction. Geosci Front 11:2083–2102
Faryad SW, Cuthbert SJ (2020) High-temperature overprint in (U)HPM rocks exhumed from subduction zones; A product of isothermal decompression or a consequence of slab break–of (slab)? Earth Sci Rev 202:103108
Fasshauer DW, Chatterjee ND, Marler B (1997) Synthesis, structure, thermodynamic properties, and stability relations of K–cymrite, $K[AlSi_3O_8]\cdot H_2O$. Phys Chem Minerals 24:455–462
Faure M, Fabbri O, Monie P (1988) The Miocene bending of southwest Japan: new $^{39}Ar/^{40}Ar$ and microtectonic constraints from the Nagasaki schists (western Kyushu), an extension of the Sanbagawa high-pressure belt. Earth Planet Sci Lett 91:105–16
Fedoseev DV, Galimov EM, Varnin VP, Prokhorov VS, Deryagin BV (1971) Carbon isotopes fractionation at physical–chemical synthesis of diamond from gas. Doklady Akademii Nauk SSSR 201:1149–1150 (In Russian)

Ferrando S, Frezzotti ML, Dallai L, Compagnoni R (2005) Multiphase solid inclusions in UHP rocks (Su–Lu, China): Remnants of supercritical silicate-rich aqueous fluids released during continental subduction. Chem Geol 233:68–81

Ferrari AC, Robertson J (2000) Interpretation of Raman spectra of disordered and amorphous carbon. Phys Rev B 61:14095

Frezzotti ML (2019) Diamond growth from organic compounds in hydrous fluids deep within the Earth. Nat Comm 10:1–8

Frezzotti ML, Ferrando S, Dallai L, Compagnoni R (2007) Intermediate alkali–alumina–silicate aqueous solutions released by deeply subducted continental crust: fluid evolution in UHP OH-rich topaz–kyanite quartzites from Donghai (Sulu, China). J Petrol 48:1219–1241

Frezzotti ML, Selverstone J, Sharp ZD, Compagnoni R (2011) Carbonate dissolution during subduction revealed by diamond-bearing rocks from the Alps. Nat Geosci 4:703–706

Frezzotti ML, Huizenga JM, Compagnoni R, Selverstone J (2014) Diamond formation by carbon saturation in C–O–H fluids during cold subduction of oceanic lithosphere. Geochim Cosmochim Acta 143:68–86

Frondel C, Marvin UB (1967) Lonsdaleite, a hexagonal polymorph of diamond. Nature 214:587–589

Frost BR, Frost CD (2014) Essential of igneous and metamorphic petrology. Cambridge University Press, Cambridge UK

Galimov EM, Karpov GA, Sevast'yanov VS, Shilobreeva SN, Maksimov AP (2016) Diamonds in the products of the 2012–2013 Tolbachik eruption (Kamchatka) and mechanism of their formation. Geochem Int 54:829–833

Galimov EM, Kaminsky FV, Shilobreeva SN, Sevastyanov VS, Voropaev SA, Khachatryan GK, Wirth R, Schreiber A, Saraykin VV, Karpov GA, Anikin LP (2020a) Enigmatic diamonds from the Tolbachik volcano, Kamchatka Am Mineral 105:498–509

Galimov EM, Kaminsky FV, Karpov GA, Shilobreeva SN, Sevastyanova VS, Voropaev SA, Anikin LP, Wirth R, Khachatryan GK, Saraykin VV (2020b) The nature and compositional peculiarities of volcanogenic diamonds. Russ Geol Geophys 61:1065–1074

Galimov EM, Kaminsky FV (2021) Diamond in the oceanic lithosphere, volcanic diamonds and diamonds in ophiolites. Geochem Int 59:1–11

Gautheron C, Cartigny P, Moreira M, Harris JW, Allègre CJ (2005) Evidence for a mantle component shown by rare gases, C and N isotopes in polycrystalline diamonds from Orapa (Botswana). Earth Planet Sci Lett 240:559–572

Gerya TV (2010) Introduction to Numerical Geodynamic Modelling. Cambredge University Press, Cambridge UK

Glassley WE, Sørensen K (1980) Constant Ps–T amphibolite to granulite facies transition in Agto (West Greenland) metadolerites: implications and applications. J Petrol 21:69–105

Glassley WE, Korstgard J, Sorensen K, Platou SW (2014) A new UHP metamorphic complex in the ~1.8 Ga Nagssugtoqidian orogen of West Greenland. Am Mineral 99:1315–1334

Godard G, Smith DC, Thouvenin C (2003) Microdiamond within zircon in thin section in the Straumen coesite–kyanite–eclogite pod, Norway. *In*: The Alice Wain Memorial West Norway Eclogite Field Symposium, Abstr volume (Eide EA (ed). Norges Geologiske Undersøkelse, Rapport 2003.055

Godard G, Smith DC, Moreau M (2004) Raman mapping of microdiamonds and other carbon phases included in zircons in a Norwegian eclogite. 32nd Int Geol Cong, Florence 20–28 August 2004, Abstr 153–2

Gordeev EI, Karpov GA, Anikin LP, Krivovichev SV, Filatov SK, Ovsyannikov AA (2014) Diamonds in lavas of the Tolbachik fissure eruption in Kamchatka. Dokl Earth Sci 454:47–49

Goryainov SV, Likhacheva AY, Rashchenko SV, Shubin AS, Afanas'ev VP, Pokhilenko NP (2014) Raman identification of lonsdaleite in Popigai impactites. J Raman Spectrosc 45:305–13

Graham DW (2002) Noble gas isotope geochemistry of mid–ocean ridge and ocean island basalts: Characterization of mantle source reservoirs. Rev Mineral Geochem 47:247–317

Green HW (2005) Psychology of a changing paradigm: 40+ years of high-pressure metamorphism. Int Geol Rev 45:439–456

Green II HW, Dobrzhinetskaya LF, Bozhilov KN (2010) Alpe Arami story: triumph of the data over prejudice. J Earth Sci 21:731–743

Griffin WL, Afonso JC, Belousova EA, Gain SE, Gong XH, Gonzalez Jimenez JM, Howell D, Huang JX, McGowan N, Pearson NJ, Satsuawa T, Shi R, Williams P, Xiong Q, Yang JS, Zhang M, O'Reilly SY (2016) Mantle recycling: transition zone metamorphism of Tibetan ophiolitic peridotites and its tectonic implications. J Petrol 57:655–684

Griffin WL, Howell D, Gonzalez–Jimenez JM, Xiong Q, O'Reilly SY (2018) Comment on "Ultra-high pressure and ultra-reduced minerals in ophiolites may form by lightning strikes" Geochem Persp Let 7:1–2

Guillot S, Mahéo G, de Sigoyer J, Hattori KH, Pecher A (2008) Tethyan and Indian subduction viewed from the Himalayan high-to ultrahigh-pressure metamorphic rocks. Tectonophysics 451:225–241

Guo GL, Yang JS, Liu XD, Xu XZ, Zhang ZM, Tian YZ, Xiong FH, Wu Y (2015) Implications of unusual minerals in Zedang mantle peridotite. Tibet. Geol China 42:1483–1492

Hainschwang T, Fritsch E, Notari F, Rondeau B, Katrusha A (2013) The origin of color in natural C center bearing diamonds. Diam Rel Mater 39:27–40

Hanneman RE, Strong HM, Bundy FP (1967) Hexagonal diamonds in meteorites: Implications. Science 155:997–999

Harris JW, Hawthorne JB, Oosterveld MM, Wehmeyer E (1975) A classification scheme for diamonds and a comparative study of South African diamond characteristics. *In*: Physics and Chemistry of the Earth. Ahrens LH, Dawson JB, Duncan AR, Erlank AJ (eds) Pergamon Press p.765–783

Hattori H, Shibata K (1982) Radiometric dating of Pre–Neogene granitic and metamorphic rocks in northwestern Kyushu, Japan—with emphasis on geotectonics of the Nishisonogi zone. Bull Geol Surv Jpn 33:57–84
Herchen H, Cappelli MA (1991) First–order Raman spectrum of diamond at high temperatures. Phys Rev B 43:11740
Hermann J, Rubatto D, Korsakov A, Shatsky VS (2006) The age of metamorphism of diamondiferous rocks determined with SHRIMP dating of zircon. Rus Geol Geophys 47:513–520
Honda M, Reynolds JH, Roedder E, Epstein S (1987) Noble gases in diamonds: occurences of solarlike helium and neon. J Geophys Res 92:12521
Honda M, McDougall I, Patterson DB, Doulgeris A, Clague DA (1991) Possible solar noble–gas component in Hawaiian basalts. Nature 349:149–151
Honda M, Phillips D, Harris JW, Yatsevich I (2004) Unusual noble gas compositions in polycrystalline diamonds: preliminary results from the Jwaneng kimberlite, Botswana. Chem Geol 203:347–358
Hong SM, Akaishi M, Yamaoka S (1999) Nucleation of diamonds in the system of carbon and water under very high pressure and temperature. J Cryst Growth 200:326–329
Hopkins MD, Harrison TM, Manning CE (2008) Low heat flow inferred from > 4 Gyr zircons suggests Hadean plate boundary interactions. Nature 456:493–496
Hopkins MD, Harrison TM, Manning CE (2010) Constraints on Hadean geodynamics from mineral inclusions in > 4 Ga zircons. Earth Planet Sci Lett 298:367–376
Hopkins MD, Harrison TM, Manning CE (2012) Metamorphic replacement of mineral inclusions in detrital zircon from Jack Hills, Australia: Implications for the Hadean Earth: Comment. Geology 40:281–281
Howell D, Griffin WL, Yang J, Gain S, Stern RA, Huang JX, Jacob DE, Xu X, Stokes AJ, O'Reilly SY, Pearson, NJ (2015) Diamonds in ophiolites: Contamination or a new diamond growth environment? Earth Planet Sci Lett 430:284–295
Huang Z, Yang JS, Robinson PT, Wang Y, Xiong F, Zhang Z, Xu W (2015) The discovery of diamonds in chromitite of the Hegenshan ophiolite, Inner Mongolia. Acta Geol Sin–Eng 89:32–38
Hwang SL, Shen P, Chu HT, Yui TF (2000) Nanometer-size α-PbO_2-type TiO_2 in garnet: A thermobarometer for ultrahigh-pressure metamorphism. Science 288:321–324
Hwang SL, Shen P, Yui TF, Chu HT (2003) Metal–sulfur–COH–silicate fluid mediated diamond nucleation in Kokchetav ultrahigh-pressure gneiss. Eur J Mineral 15:503–511
Hwang SL, Shen P, Chu HT, Yui TF, Liou JG, Sobolev NV, Shatsky VS (2005) Crust-derived potassic fluid in terrestrial diamonds. Earth Planet Sci Lett 231:295–306
Hwang SL, Chu HT, Yui TF, Shen PY, Schertl H–P, Liou JG, Sobolev NV (2006) Nanometer–size P/K-rich silica glass (former melt) inclusions in microdiamond from gneisses of Kokchetav and Erzgebirge massifs: diversified characteristics of the formation media of metamorphic microdiamond in UHP rocks. Earth Planet Sci Lett 243:94–106
Imamura K, Ogasawara Y, Yurimoto H, Kusakabe M (2013) Carbon isotope heterogeneity in metamorphic diamond from the Kokchetav UHP dolomite marble, northern Kazakhstan. Int Geol Rev 55:453–467
Ishida H, Ogasawara Y, Ohsumi K, Saito A (2003) Two stage growth of microdiamond in UHP dolomite marble from Kokchetav Massif, Kazakhstan. J Metamorph Geol 21:515–522
Jackson MG, Carlson RW, Kurz MD, Kempton PD, Francis D, Blusztajn J (2010) Evidence for the survival of the oldest terrestrial mantle reservoir. Nature 466:853–856
Jacob DE, Dobrzhinetskaya LF, Wirth R (2014) New insight into polycrystalline diamond genesis from modern nanoanalytical techniques. Earth Sci Rev 136:21–35
Jacob DE, Wirth R, Enzmann F, Kronz A, Schreiber A (2011) Nano-inclusion suite and high resolution micro–computed–tomography of polycrystalline diamond (framesite) from Orapa, Botswana. Earth Planet Sci Lett 308:307–316
Jagoutz E, Shatsky VS, Sobolev NV (1990) Sr–Nd–Pb isotopic study of ultra-high *PT* rocks from Kokchetav massif. EOS 71:1707
Jagoutz E, Shatsky VS, Sobolev NV (1991) The origin and history of ultrahigh *PT* rocks from Kokchetav Massif. Terra Abstr 3:83
Janák M, Froitzheim N, Lupták B, Vrabec M, Ravna EJK (2004) First evidence for ultrahigh-pressure metamorphism of eclogites in Pohorje, Slovenia: Tracing deep continental subduction in the Eastern Alps. Tectonics 23:TC5014
Janák M, Froitzheim N, Vrabec M, Krogh Ravna EJ, De Hoog JCM (2006) Ultrahigh-pressure metamorphism and exhumation of garnet peridotite in Pohorje, Eastern Alps. J Metamorph Geol 24:19–31
Janák M, Krogh Ravna EJ, Kullerud K, Yoshida K, Milovský R, Hirajima T (2013) Discovery of diamond in the Tromsø Nappe, Scandinavian Caledonides (N. Norway). J Metamorph Geol 31:691–703
Janák M, Froitzheim N, Yoshida K, Sasinková V, Nosko M, Kobayashi T, Hirajima T, Vrabec M (2015) Diamond in metasedimentary crustal rocks from Pohorje, Eastern Alps: a window to deep continental subduction. J Metamorph Geol 33:495–512
Kaneoka I (1983) Noble gas constraints on the layered structure of the mantle. Nature 302:698–700
Karpov GA, Silaev VI, Anikin LP, Rakin VI, Vasil'ev EA, Filatov SK, Petrovskii VA, Flerov GB (2014) Diamonds and accessory minerals in products of the 2012–2013 Tolbachik fissure eruption. J Volcanol Seissmol 8:323–339
Kashkarov IF, Polkanov YA (1964) On discovery of diamonds in titanium–zirconium sands. Dokl Akad Nauk SSSR (Proc Acad Sci USSR) 157:1129 (in Russian)
Katayama I, Parkinson CD, Okamoto K, Nakajima Y, Maruyama S (2000) Supersilicic clinopyroxene and silica exsolution in UHPM eclogite and pelitic gneiss from the Kokchetav massif, Kazakhstan. Am Mineral 10:1368–1374

Katayama I, Maruyama S, Parkinson CD, Terada K, Sano Y (2001a) Ion micro–probe U–Pb zircon geochronology of peak and retrograde stages of ultrahigh-pressure metamorphic rocks from the Kokchetav massif, northern Kazakhstan. Earth Planet Sci Lett 188:185–198

Katayama I, Zayachkovsky AA, Maruyama S (2001b) Prograde pressure–temperature records from inclusions in zircons from ultrahigh-pressure–high-pressure rocks of the Kokchetav Massif, northern Kazakhstan. Island Arc 9:417–427

Katayama I, Ohta, M, Ogasawara Y (2002) Mineral inclusions in zircon from diamond-bearing marble in the Kokchetav massif, northern Kazakhstan. Eur J Mineral 14:1103–1108

Klonowska I, Janák M, Majka J, Petrik I, Froitzheim N, Gee DG, Sasinková V (2017) Microdiamond on Åreskutan confirms regional UHP metamorphism in the Seve Nappe Complex of the Scandinavian Caledonides. J Metamorph Geol 35:541–564

Koeberl C, Masaitis VL, Shafranovsky GI, Gilmour I, Langenhorst F, Schrauder M (1997) Diamonds from the Popigai impact structure, Russia. Geology 25:967–970

Kohn MJ (2010) Carbon isotope compositions of terrestrial C3 plants as indicators of (paleo) ecology and (paleo) climate. PNAS 107:19691–5

Konzett J, Frost DJ (2009) The high P–T stability of hydroxyl–apatite in natural and simplified MORB—an experimental study to 15 GPa with implications for transport and storage of phosphorus and halogens in subduction zones. J Petrol 50:2043–2062

Konzett J, Rhede D, Frost DJ (2012) The high *PT* stability of apatite and Cl partitioning between apatite and hydrous potassic phases in peridotite: an experimental study to 19 GPa with implications for the transport of P, Cl and K in the upper mantle. Contrib Mineral Petrol 163:277–296

Korsakov A, Herman J (2006) Silicate and carbonate melt inclusions associated with diamonds in deeply subducted carbonate rocks. Earth Planet Sci Lett 241:104–118

Korsakov A, Theunissen K, Smirnova LV (2004) Intergranular diamonds derived from partial melting of crustal rocks at ultrahigh-pressure metamorphic conditions. Terra Nova 16:146–151

Kotková J, O'Brien PJ, Ziemann MA (2011) Diamonds in the Bohemian Massif—evidence for ultrahigh-pressure metamorphism. Geologické výzkumy na Morave a ve Slezsku 18:35–38

Kröner A, Willner AP (1998) Time of formation and peak of Variscan HP–HT metamorphism of quartz–feldspar rocks in the central Erzgebirge, Saxony, Germany. Contrib Mineral Petrol 132:1–20

Krueger A (2008) Diamond nanoparticles: Jewels for chemistry and physics. Adv Mater 20:2445–2449

Kumar MS, Akaishi M, Yamaoka S (2001) Effect of fluid concentration on the formation of diamond in the CO_2–H_2O–graphite system under HP–HT conditions. J Cryst Growth 222:9–13

Kurz MD (1986) Cosmogenic helium in a terrestrial igneous rock. Nature 320:435–439

Kurz MD, Jenkins WJ, Hart SR (1982) Helium isotopic systematics of oceanic islands and mantle heterogeneity. Nature 297:43–47

Kurz MD, Gurney JJ, Jenkins WJ, Lott III DE (1987) Helium isotopic variability within single diamonds from the Orapa kimberlite pipe. Earth Planet Sci Lett 86:57–68

Kurz MD, Curtice J, Fornari D, Geist D, Moreira M (2009) Primitive neon from the center of the Galapagos hotspot. Earth Planet Sci Lett 286:23–34

Kvasnitsya V, Wirth R, Dobrzhinetskaya L, Matzel J, Jacobsen B, Hutcheon I, Tappero, R, Kovalyukh M (2013) New evidence of meteoritic origin of the Tunguska cosmic body. Planet Space Sci 84:131–140

Lal D (1989) An important source of ^{4}He (and ^{3}He) in diamonds. Earth Planet Sci Lett 96:1–7

Langenhorst F (2003) Nanostructures in ultrahigh-pressure metamorphic coesite and diamond: a genetic fingerprint. Mitt Österr Miner Ges 148:401–412

Lavrova LD (1991) New type of diamond deposits. Priroda (Nature) 12:62–68 (in Russian)

Lavrova LD, Petchnikov VA, Petrova MA, Ekimova TE, Nadezhdina ED (1995) New genetic type of diamond deposits–geological peculiarities and origin. *In*: International Kimberlite Conference: Extended Abstr 6:311–313

Lavrova LD, Pechnikov VA, Petrova MA, Ekimova TE, Karpenko SF, Lyalikov AV, Spiridonov VG, Bibikova EV, Fugzan MM, Shukolyukov YA (1997) Diamond formation in the age succession of geological events on the Kokchetav massif: evidence from isotopic geochronology. Geokhimiya (Geochemistry) 675–682 (in Russian)

Letnikov FA (1983) Diamond origin in deep–seated tectonic zones. Dokl Akad Nauk SSSR (Proc Acad Sci USSR) 271:433–435

Leung I, Winston R (2002) Microstructures and superelasticity in natural diamond. EOS Trans Am Geophys Union 83:MR61A–1028

Lian D, Yang J (2019) Ophiolite-hosted diamond: A new window for probing arbon cycling in the deep mantle. Engineering 5:406–420

Lian D, Yang J, Dilek Y, Wu W, Zhang Z, Xiong F, Liu F, Zhou W (2017) Deep mantle origin and ultra-reducing conditions in podiform chromitite: Diamond, moissanite, and other unusual minerals in podiform chromitites from the Pozanti–Karsanti ophiolite, southern Turkey. Am Mineral 102:1101–1113

Lian D, Yang JS, Wiedenbeck M, Dilek Y, Rocholl A, Wu W (2018a) Carbon and nitrogen isotope, and mineral inclusion studies on the diamonds from the Pozanti–Karsanti chromitite, Turkey. Contrib Mineral Petrol 173:72

Lian D, Yang JS, DilekY, Rocholl A (2018b) Mineralogy and geochemistry of peridotites and chromitites in the Aladag Ophiolite (southern Turkey): melt evolution of the Cretaceous Neotethyan mantle J Geol Soc 176:958–974

Liati A, Gebauer D, Fanning CM (2011) Geochronology of the Alpine UHP Rhodope zone: a review of isotopic ages and constraints on the geodynamic evolution. *In*: Ultrahigh-Pressure Metamorphism: 25 Years After The Discovery of Coesite and Diamond. Dobrzhinetskaya LF, Faryad SW, Wallis S, Cuthbert S (eds), Elsevier, London, p. 295–316

Liou JG, Tsujimori T, Zhang RY, Katayama I, Maruyama S (2004) Global UHP metamorphism and continent subduction/collision. The Himalayan Model. Int Geol Rev 46:1–27

Liou JG, Ernst WG, Zhang RY, Tsujimori T, Jahn BM (2009) Ultrahigh-pressure minerals and metamorphic terranes–the view from China. J Asian Earth Sci 35:199–231

Liou JG, Tsujimori T, Yang J, Zhang RY, Ernst WG (2014) Recycling of crustal materials through study of ultrahigh-pressure minerals in collisional orogens, ophiolites, and mantle xenoliths: A review. J Asian Earth Sci 96:386–420

Lipp MJ, Baonza VG, Evans WJ, Lorenzana HE (1997) Nanocrystalline diamond: Effect of confinement, pressure, and heating on phonon modes. Phys Rev B 56:5978

Litasov KD, Kagi H, Bekker TB, Hirata T, Makino Y (2019a) Cuboctahedral type Ib diamonds in ophiolitic chromitites and peridotites: the evidence for anthropogenic contamination. High Pres Res 39:480–488

Litasov KD, Kagi H, Voropaev SA, Hirata T, Ohfuji H, Ishibashi H, Makino Y, Bekker TB, Sevastyanov VS, Afanasiev VP, Pokhilenko NP (2019b) Comparison of enigmatic diamonds from the Tolbachik arc volcano (Kamchatka) and Tibetan ophiolites: Assessing the role of contamination by synthetic materials. Gondwana Res 75:16–27

Litasov KD, Bekker TB, Kagi H, Ohfuji H (2020) Reply to the comment on "Comparison of enigmatic diamonds from the Tolbachik arc volcano (Kamchatka) and Tibetan ophiolites: Assessing the role of contamination by synthetic materials" by Litasov et al. (2019) (Gondwana Research, 75, 16–27) by Yang et al. Gondwana Res 79:304–307

Litasov KD, Kagi H, Bekker TB, Makino Y, Hirata T, Brazhkin VV (2021) Why Tolbachik diamonds cannot be natural. Am Mineral 106:44–53

Liu L, Zhang J, Green, HW, Jin Z, Bozhilov KN (2007) Evidence of former stishovite in metamorphosed sediments, implying subduction to >350 km. Earth Planet Sci Lett 263:180–191

Liu L, Zhang J, Cao Y, Green, HW, Yang W, Xu H, Liao H, Kang L (2018) Evidence of former stishovite in UHP eclogite from the South Altyn Tagh, western China. Earth Planet Sci Lett 484:353–362

McGowan NM, Griffin WL, González–Jiménez JM, Belousova E, Afonso JC, Shi R, McCammon CA, Pearson NJ, O'Reilly SY (2015) Tibetan chromitites: Excavating the slab graveyard. Geology 43:179–182

Majka J, Rosén Å, Janák M, Froitzheim N, Klonowska I, Manecki M, Sasinková V, Yoshida K (2014) Microdiamond discovered in the Seve Nappe (Scandinavian Caledonides) and its exhumation by the "vacuum–cleaner" mechanism. Geology 42:1107–1110

Manning CE (2004) The chemistry of subduction–zone fluids. Earth Planet Sci Lett 223:1–16

Martini JEJ (1991) The nature, distribution and genesis of the coesite and stishovite associated with the pseudotachylite of the Vredefort Dome, South Africa. Earth Planet Sci Lett 101:285–300

Masaitis VL, Futergendler SI, Gnevushev MA (1972) Diamonds in impactites of the Popigai meteorite crater. All-Union Mineral Soc Proc 1:108–112

Masaitis VL, Shafranovsky GL, Grieve RA, Langenhorst F, Peredery W, Balmasov EL, Fedorova IG, Therriault A (1997) Discovery of diamonds at the Sudbury Structure. Lunar Planet Inst Contrib 922:33

Masaitis VL, Shafranovsky GI, Fedorova IG, Koivisto M, Korhonen JV (1998) Lappajarvi Astrobleme: The first find of impact diamonds on the Fennoscandian Shield. Lunar Planet Instit Contrib 1171

Massonne H–J (1999) A new occurrence of microdiamonds in quartzofeldspathic rocks of the Saxonian Erzgebirge, Germany, and their metamorphic evolution. Proc. 7th Int Kimberlite Confer, Cape Town 1998, P.H. Nixon Vol, p. 533–539

Massonne H–J (2003) A comparison of the evolution of diamondiferous quartz-rich rocks from the Saxonian Erzgebirge and the Kokchetav Massif: are so–called diamondiferous gneisses magmatic rocks? Earth Planet Sci Lett 216:347–364

Massonne H–J, O'Brien PJ (2003) The Bohemian massif and the NW Himalaya. *In*: Ultrahigh Pressure Metamorphism. Carswell DA, Compagnoni R, Rolfo F (eds) p 145–187

Massonne H–J, Kennedy A, Nasdala L, Theye T (2007a) Dating of zircon and monazite from diamondiferous quartzofeldspathic rocks of the Saxonian Erzgebirge—hints at burial and exhumation velocities. Mineral Mag 71:371–389

Massonne H–J, Tu W (2007b) $\delta^{13}C$ signature of early graphite and subsequently formed microdiamond from the Saxonian Erzgebirge, Germany. Terra Nova 19:476–480

Massonne H–J, Fockenberg T (2012) Melting of metasedimentary rocks at ultrahigh pressure—Insights from experiments and thermodynamic calculations. Lithosphere 4:269–285

Massonne H–J (2019) A shallow origin for diamonds in ophiolitic chromitites: COMMENT. Geology 47: e476

Mathez EA, Fogel RA, Hutcheon ID, Marshintsev VK (1995) Carbon isotopic composition and origin of SiC from kimberlites of Yakutia, Russia. Geochim Cosmochim Acta 59:781–791

McGowan NM, Griffin WL, González–Jiménez JM, Belousova E, Afonso JC, Shi R, McCammon CA, Pearson NJ, O'Reilly SY (2015) Tibetan chromitites: Excavating the slab graveyard. Geology 43:179–182

Mengel FC (1983) Chemistry of coexisting mafic minerals in granulite facies amphibolites from West Greenland: clues to conditions of metamorphism. Neues Jahrbuch für Mineralogie Abhandlungen 147:315–340

Menneken M, Nemchin AA, Geisler T, Pidgeon RT, Wilde SA (2007) Hadean diamonds in zircon from Jack Hills, Western Australia. Nature 448:917–920
Menneken M, Geisler T, Nemchin AA, Pollok K, Whitehouse M, Pidgeon RT, Wilde SA (2014) Is there really carbon in the detrital zircons from Jack Hills, Western Australia? Geophysical Research Abstr, EGU General Assembly 2014 16:EGU2014–13489
Menneken M, Geisler T, Nemchin AA, Whitehouse M, Wilde SA, Gasharova B, Pidgeon RT (2017) CO_2 fuid inclusions in Jack Hills zircons. Contrib Mineral Petrol 172:66–78
Meyers PA (2014) Why are the $\delta^{13}C_{org}$ values in Phanerozoic black shales more negative than in modern marine organic matter? Geochem Geophys 15:3085–106
Milledge HJ 1961 Coesite as an inclusion in G.E.C. synthetic diamonds. Nature 190:1181
Moe KS, Yang JS, Johnson P, Xu X, Wang W (2018) Spectroscopic analysis of microdiamonds in ophiolitic chromitite and peridotite. Lithosphere 10:133–141
Mposkos ED, Kostopoulos DK (2001) Diamond, former coesite and supersilicic garnet in metasedimentary rocks from the Greek Rhodope: a new ultrahigh-pressure metamorphic province established. Earth Planet Sci Lett 192:497–506
Mukhopadhyay S (2012) Early differentiation and volatile accretion recorded in deep–mantle neon and xenon. Nature 486:101–104
Murri M, Smith RL, McColl K, Hart M, Alvaro M, Jones AP, Németh P, Salzmann CG, Corà F, Domeneghetti MC, Nestola F. (2019) Quantifying hexagonal stacking in diamond. Sci Reports 9:1–8
Naemura K, Ikuta D, Kagi H, Odake S, Ueda T, Ohi S, Kobayashi T, Svojtka M, Hirajima T (2011) Diamond and other possible ultradeep evidence discovered in the orogenic spinel–garnet peridotite from the Moldanubian Zone of the Bohemian Massif, Czech Republic. *In:* Ultrahigh-Pressure Metamorphism. Elsevier, p. 77–111
Nakamuta Y, Toh S (2013) Transformation of graphite to lonsdaleite and diamond in the Goalpara ureilite directly observed by TEM. Am Mineral 98:574–581
Nasdala L, Massonne H–J (2000) Microdiamonds from the Saxonian Erzgebirge, Germany: in situ micro–Raman characterisation. Eur J Mineral 12:495–498
Nasdala L, Grambole D, Wildner M, Gigler AM, Hainschwang T, Zaitsev AM, Harris JW, Milledge J, Schulze DJ, Hofmeister W, Balmer WA (2013) Radio-colouration of diamond: a spectroscopic study. Contrib Mineral Petrol 165:843–61
Nasdala L, Steger S, Reissner C (2016) Raman study of diamond-based abrasives, and possible artefacts in detecting UHP microdiamond. Lithos 265:317–327
Nemchin AA, Whitehouse MJ, Menneken M, Geisler T, Pidgeon RT, Wilde SA (2008) A light carbon reservoir recorded in zircon-hosted diamond from the Jack Hills. Nature 454:92–95
Németh P, Garvie LA, Aoki T, Dubrovinskaia N, Dubrovinsky L, Buseck PR (2014) Lonsdaleite is faulted and twinned cubic diamond and does not exist as a discrete material. Nat Comm 5:1–5
Nestola F, Goodrich CA, Morana M, Barbaro A, Jakubek RS, Christ O (2020) Impact shock origin of diamonds in ureilite meteorites. PNAS 117:25310–25318
Nishiyama T, Ohfuji H, Fukuba K, Terauchi M, Nishi U, Harada K, Unoki K, Moribe Y, Yoshiasa A, Ishimaru S, Mori Y (2020) Microdiamond in a low–grade metapelite from a Cretaceous subduction complex, western Kyushu, Japan. Sci Rep 10:1–1
O'Bannon EF, Xia G, Wirth R, Shi F, King A, Dobrzhinetskaya L (2020) The transformation of diamond to graphite: Experiments reveal the presence of an intermediate linear carbon phase. Diam Relat Mater 108:107876
Ogasawara Y (2005) Microdiamonds in ultrahigh-pressure metamorphic rocks. Elements 1:91–96
Ogasawara Y, Ohta M, Fukusava K, Katayama I, Maruyama S (2000) Diamond bearing and diamond–free metacarbonate rocks from Kumdy–Kol from the Kokchetav massif, northern Kasakhstan. The Island Arc 9:400–416
Ogasawara Y, Fukasawa K, Maruyama S (2002) Coesite exsolution from supersilicic titanite in UHP marble from the Kokchetav Massif, northern Kazakhstan. Am Mineral 87:454–461
Ohfuji H, Irifune T, Litasov KD, Yamachita T, Isobe F, Afanasiev V, Pokhilenko NP (2015) Natural occurrence of pure Nano-polycrystalline diamond from impact crater. Sci Rep 5:14702
Ohta M, Mock T, Ogasawara Y, Rumble D (2003) Oxygen, carbon, and strontium isotope geochemistry of diamond-bearing carbonate rocks from Kumdy–Kol, Kokchetav Massif, Kazakhstan. Lithos 70:77–90
Okay A, Xu ST, Sengor AMC (1988) Coesite from the Dabie Shan ecologite, Central China. Eur J Mineral 1:595–598
Orwa JO, Nugent KW, Jamieson DN, Prawer S (2000) Raman investigation of damage caused by deep ion implantation in diamond. Phys Rev B 62:5461
Ozima M, Podosek FA (2002) Noble Gas Geochemistry. Cambridge Univ. Press, Cambridge
Ozima M, Zashu S (1988) Solar-type Ne in Zaire cubic diamonds. Geochim Cosmochim Acta 52:19–25
Ozima M, Zashu S (1991) Noble gas state of the ancient mantle as deduced from noble gases in coated diamonds. Earth Planet Sci Lett 105:13–27
Pal'yanov Y, Sokol A, Borzdov Y, Khokhryakov A, Sobolev NV (1999) Diamond formation from mantle carbonate fluids. Nature 400:417–418
Pal'yanov YuN, Sokol AG, Khokhryakov, AF, Pal'yanova GA, Borzdov YuM, Sobolev NV (2000) Diamond and graphite crystallization in COH fluid at PT parameters of the natural diamond formation. Doklady Nauk o Zemle (Proc Earth Sci) 375:1395–1399 (in Russian)

Pal'yanov N, Sokol AG, Borzdov M, Khokhryakov AF (2002) Fluid-bearing alkaline carbonate melts as the medium for the formation of diamonds in the Earth's mantle: an experimental study. Lithos 60:145–159
Pal'yanov YN, Bataleva YV, Sokol AG, Borzdov YM, Kupriyanov IN, Reutsky VN, Sobolev NV (2013) Mantle–slab interaction and redox mechanism of diamond formation. PNAS 110:20408–20413
Palot M, Pearson DG, Stern RA, Stachel T, Harris JW (2013) Multiple growth events, processes and fluid sources involved in diamond genesis: a micro–analytical study of sulphide-bearing diamonds from Finsch mine, RSA. Geochim. Cosmochim. Acta 106:51–70
Parman SW (2007) Helium isotopic evidence for episodic mantle melting and crustal growth. Nature 446:900–903
Pearson DG, Davies GR, Nixon PH, Milledge HJ (1989) Graphitized diamonds from a peridotite massif in Morocco and implications for anomalous diamond occurrences. Nature 338:60–62
Pearson DG, Davies GR, Nixon PH, Mattey DP (1991) A carbon isotope study of diamond facies pyroxenites from Beni Bousera, N. Morocco. Spec Ed J Petrol: Orogenic Lherzolites and Mantle Processes, 175–189
Pechnikov VA, Kaminsky FV (2008) Diamond potential of metamorphic rocks in the Kokchetav Massif, northern Kazakhstan. Eur J Mineral 20:395–413
Pechnikov VA, Kaminsky FV (2011) Structural and microstructural regularities of the distribution of diamond in metamorphic rocks of the Kumdy–Kol and Barchi–Kol deposits, Kokchetav Massif, Northern Kazakhstan. Can Mineral 49:673–690
Pedroza-Montero M, Chernov V, Castañeda B, Meléndrez R, Gonçalves JA, Sandonato GM, Bernal R, Cruz–Vázquez C, Brown F, Cruz–Zaragoza E, Barboza–Flores M (2005) TL, OSL, Raman spectroscopy and SEM characterization of boron doped diamond films. Phys Status Solidi B 202:2154–59
Perraki M, Proyer A, Mposkos E, Kaindl R, Hoinkes G (2006) Raman micro–spectroscopy on diamond, graphite and other carbon polymorphs from the ultrahigh-pressure metamorphic Kimi Complex of the Rhodope Metamorphic Province, NE Greece. Earth Planet Sci Lett 241:672–685
Perraki M, Korsakov AV, Smith DC, Mposkos E (2009) Raman spectroscopic and microscopic criteria for the distinction of microdiamonds in ultrahigh-pressure metamorphic rocks from diamonds in sample preparation materials. Am Mineral 94:546–56
Perraki M, Faryad SW (2014) First finding of microdiamond, coesite and other UHP phases in felsic granulites in the Moldanubian Zone: Implications for deep subduction and a revised geodynamic model for Variscan Orogeny in the Bohemian Massif. Lithos 202:157–166
Platt JP, Behr WM, Johanesen K, Williams JR (2013) The Betic–Rif arc and its orogenic hinterland: a review. Annu Rev Earth Planet Sci 41:313–357
Pleshakov AM, Shukolyukov YA (1994) Isotopic variations of helium in the diamonds of the Kokchetav massif's metamorphic rocks, Kazakhstan. in: Matsuda, J. (Ed.), Noble Gas Geochemistry and Cosmochemistry, Terra Scientific Publishing Company (TERRAPUB), Tokyo, p. 229–243
Pokhilenko NP, Shumilova TG, Afanas'ev VP, Litasov KD (2019) Diamonds in the Kamchatka peninsula (Tolbachik and Avacha volcanoes): Natural origin or contamination? Russian Geol Geoph 60:463–472
Porcelli D, Ballentine CJ (2002) Models for distribution of terrestrial noble gases and evolution of the atmosphere. Rev Mineral Geochem 47:411–48
Porcelli D, Elliott T (2008) The evolution of He isotopes in the convecting mantle and the preservation of high $^{3}He/^{4}He$ ratios. Earth Planet Sci Lett 269:175–185
Prawer S, Rosenblum I, Orwa JO, Adler J (2004) Identification of the point defects in diamond as measured by Raman spectroscopy: comparison between experiment and computation. Chem Phys Lett 390:458–461
Pujol–Sola N, Garcia–Casco A, Proenza JA, Gonzalez–Jimenez JM, del Campo A, Colas V, Canals À, Sánchez–Navas A, Roque–Rosell J (2020) Diamond forms during low pressure serpentinisation of oceanic lithosphere. Geochem Perspect Lett 15:19–24
Rasmussen B, Fletcher IR, Muhling JR, Wilde SA (2010) In situ U–Th–Pb geochronology of monazite and xenotime from the Jack Hills belt: Implications for the age of deposition and metamorphism of Hadean zircons. Precambrian Res 180:26–46
Rasmussen B, Fletcher IR, Muhling JR, Gregory CJ, Wilde SA (2011) Metamorphic replacement of mineral inclusions in detrital zircon from Jack Hills, Australia: Implications for the Hadean Earth. Geology 39:1143–1146
Rasmussen B, Fletcher IR, Muhling JR, Gregory CJ, Wilde SA (2012) Metamorphic replacement of mineral inclusions in detrital zircon from Jack Hills, Australia: Implications for the Hadean Earth: REPLY. Geology 40:282–283
Reinecke T (1991) Very–high-pressure metamorphism and uplift of coesite-bearing metasediments from the Zermatt–Saas zone, Western Alps. Eur J Mineral 3:7–17
Robinson PT, Bai WJ, Malpas J, Yang JS, Zhou MF, Fang QS, Hu XF, Cameron S, Staudigel H (2004) Ultra-high pressure minerals in the Luobusa Ophiolite, Tibet, and their tectonic implications. Geol Soc London Spec Publ 226:247–271
Robinson PT, Trumbull RB, Schmitt A, Yang JS, Li JW, Zhou MF, Erzinger J, Dare S, Xiong F (2015) The origin and significance of crustal minerals in ophiolitic chromitites and peridotites. Gondwana Res 27:486–506
Rollinson H (2016) Surprises from the top of the mantle transition zone. Geol Today 32:58–64
Rosing MT (1999) ^{13}C-depleted carbon microparticles in >3700–Ma sea–floor sedimentary rocks from West Greenland. Science 283:674–676

Rost R, Dolgov YA, Vishnevsky SA (1978) Gases in inclusions of impact glass in the Ries Crater, West Germany, and finds of high-pressure carbon polymorphs. Dokl Akad Nauk SSSR 241:695–698
Rozen OM (1972) A find of the diamonds linked with eclogites of the Precambrian Kokchetav massif. Dokl Akad Nauk SSSR 203:674–676
Rozen OM, Zayachkovsky AA, Kljuev YuA, Smirnov VL (1979) Peculiarities of trace–minerals composition and conditions of the formation of the North Kazakhstan eclogites. *In:* A.V. Sidorenko (Editor), Problems of Sedimentary Geology of Precambrian. Nauka Press, Moscow p. 170–186 (in Russian with English Abstract)
Reutsky V, Borzdov Y, Palyanov Y, Sokol A, Izokh O (2015) Carbon isotope fractionation during experimental crystallisation of diamond from carbonate fluid at mantle conditions. Cont Mineral Petrol 170:41
Ruiz-Cruz MD, de Galdeano CS (2012) Diamond and coesite in ultrahigh-pressure–ultrahigh-temperature granulites from Ceuta, Northern Rif, northwest Africa. Mineral Mag 76:683–705
Ruiz-Cruz MD, de Galdeano CS (2013) Coesite and diamond inclusions, exsolution microstructures and chemical patterns in ultrahigh pressure garnet from Ceuta (Northern Rif, Spain). Lithos 177:184–206
Ruiz-Cruz MD, de Galdeano CS (2014) Garnet variety and zircon ages in UHP meta-sedimentary rocks from the Jubrique zone (Alpujárride Complex, Betic Cordillera, Spain): evidence for a pre-Alpine emplacement of the Ronda peridotite. Int Geol Rev 56:845–868
Salzmann CG, Murray BJ, Shephard JJ (2015) Extent of stacking disorder in diamond. Diam Relat Mater 59:69–72
Sarda P, Staudacher T, Allègre CJ (1988) Neon isotopes in submarine basalts. Earth Planet Sci Lett 91:73–88
Schertl HP, O'Brien (2013) Continental crust at mantle depths: key minerals and microstructures. Elements 9:261–266
Schertl HP, Sobolev NV (2013) The Kokchetav massif, Kazakhstan: "Type locality" of diamond-bearing UHP metamorphic rocks. J Asian Earth Sci 63:5–38
Schönig J, von Eynatten H, Meinhold G, Lünsdorf NK (2019) Diamond and coesite inclusions in detrital garnet of the Saxonian Erzgebirge, Germany. Geology 47:715–718
Seno T, Rehman HU (2011) When and why the continental crust is subducted: Examples of Hindu Kush and Burma. Gondwana Res 19:327–333
Shatsky VS, Sobolev NV (1993) Some aspects of origin of diamonds in metamorphic rocks. Doklady Akademii Nauk (Proc Acad Sci) 331:1217–1219 (in Russian)
Shatsky VS, Sobolev NV, Vavilov MA (1995) Diamond–beraing metamorphic rocks of the Kokchetav massif (northern Kazakhstan). *In*: Ultrahigh Pressure Metamorphism, Coleman RG, Wang X (eds) Cambridge Univ Press, Cambridge, p 427–455
Shimizu R, Ogasawara Y (2014) Radiation damage to Kokchetav UHPM diamonds in zircon: varations in Raman, photoluminescence and cathodoluminiscence spestra. Lithos 206:201–213
Shirey S, Cartigny P, Frost D, Keshav S, Nestola F, Pearson G, Sobolev N, Walter MJ (2013) Diamonds and the geology of mantle carbon. Rev Mineral Geochem 75:355–421
Shukolyukov YuA, Pleshakov AM, Lavrova LD (1993) The unprecedentedly high $^{3}He/^{4}He$ ratio in diamonds from a metamorphic rock of the Kokchetav massif, Kazakhstan. Petrologia (Petrology) 1:110–119 (in Russian)
Shumilova TG, Mayer E, Isaenko SI (2011) Natural monocrystalline lonsdaleite. Dokl Earth Sci 441:1552–1554
Simakov SK (2010) Metastable nanosized diamond formation from a CHO fluid system. J Mat Res 25:2336–2340
Simakov SK (2015) Different sizes of diamond formation in natural processes. Dokl Earth Sci 461:419–421
Simakov SK (2018) Nano-and micron–sized diamond genesis in nature: an overview. Geosci Front 9:1849–1858
Simakov SK, Dubinchuk VT, Novikov MP, Drozdova IA (2008) Formation of diamond and diamond-type phases from the carbon-bearing fluid at *PT* parameters corresponding to processes in the Earth's crust. Dokl Earth Sci 421:835
Sitnikova ES, Shatsky VS (2009) New FTIR spectroscopy data on the composition of the medium of diamond crystallization in metamorphic rocks of the Kokchetav Massif. Russ Geol Geophys 50:842–849
Smart KA, Chacko T, Stachel T, Muehlenbachs K, Stern RA, Heaman LM (2011) Diamond growth from oxidized carbon sources beneath the Northern Slave Craton, Canada: a $\delta^{13}C$–N study of eclogite-hosted diamonds from the Jericho kimberlite. Geochim Cosmochim Acta 75:6027–47
Smit KV, Shirey SB, Wang W (2016) P Type Ib diamond formation and preservation in the West African lithospheric mantle: Re–Os age constraints from sulphide inclusions in Zimmi diamonds. Precambrian Res 286:152–156
Smith CB, Walter MJ, Bulanova GP, Mikhail S, Burhama AD, Gobbo L, Kohn SC (2016) Diamonds from Dachine, French Guiana: A unique record of early Proterozoic subduction. Lithos 265:82–95
Stähle V, Altherr R, Koch M, Nasdala L (2008) Shock–induced growth and metastability of stishovite and coesite in lithic clasts from suevite of the Ries impact crater (Germany). Contribut Mineral Petrol 155:457–472
Stachel T, Cartigny P, Chacko T, Pearson DG (2022) Carbon and nitrogen in mantle-derived diamonds. Rev Mineral Geochem 88:809–876
Stan CV, O'Bannon EF, Mukhin P, Tamura N, Dobrzhinetskaya LF (2020) X–ray Laue microdiffraction and Raman spectroscopic investigation of natural silicon and moissanite. Minerals 10:204–220
Steger S, Nasdala L, Wagner A (2013) Raman spectra of diamond abrasives and possible artefacts in detecting UHP microdiamond. CORALS Conf Raman Lumin Spectrosc Earth Sci, Vienna, Austria, p. 95–96
Stöckhert B, Duyster J, Trepmann C, Massonne H–J (2001) Microdiamond daughter crystals precipitated from supercritical COH + silicate fluids included in garnet, Erzgebirge, Germany. Geology 29:391–394

Stöckhert B, Trepmann CA, Massonne H–J (2009) Decrepitated UHP fluid inclusions: about diverse phase assemblages and extreme decompression rates (Erzgebirge, Germany). J Metamorph Geol 27:673–684

Stuart FM, Lass–Evans S, Fitton JG, Ellam RM (2003) High $^{3}He/^{4}He$ ratios in picritic basalts from Baffin Island and the role of a mixed reservoir in mantle plumes. Nature 424:57–59

Sumino H, Dobrzhinetskaya LF, Burgess R, Kagi H (2011) Deep-mantle-derived noble gases in metamorphic diamonds from the Kokchetav massif, Kazakhstan. Earth Planet Sci Lett 307:439–449

Sverjensky DA, Stagno V, Huang F (2014) Important role for organic carbon in subduction–zone fluids in the deep carbon cycle. Nat Geosci 7:909–913

Taylor WR (1990) A reappraisal of the nature of fluids included by diamond — a windowto deep–seated mantle fluids and redox conditions. *In*: Herbert HK, Ho SE (eds.) Stable Isotopes and Fluid Processes in Mineralization. University of Western Australia, Perth 23:333–349

Taylor WR, Milledge HJ, Griffin BJ, Nixon PH, Kamperman M, Mattey DP (1995) Caracteristics of microdiamonds from ultramafic massifs in Tibet: authentic ophiolitic diamonds or contamination? Int Kimberlite Conf: Extended Abstr 6:623–624

Taylor WR, Canil D, Milledge HJ (1996) Kinetics of Ib to IaA nitrogen aggregation in diamond. Geochim Cosmochim Acta 60:4725–4733

Tian Y, Yang JS, Zhang Z, Xiong F, Li Y, Liu Z, Liu F, Niu XL (2015) Discovery and implication of unusual mineral group from Sarthay high-Al chromitites, Xinjiang. Acta Petrol Sinica 31:3650–3662

Timmerman S, Chinn IL, Fisher D, Davies GR (2018) Formation of unusual yellow Orapa diamonds. Mineral Petrol 112:209–218

Timmerman S, Honda M, Phillips D, Jaques AL, Harris JW (2018) Noble gas geochemistry of fluid inclusions in South African diamonds: implication for the origin of diamond–forming fluids. Mineral Petrol 112:181–195

Tirel C, Brun J–P, Burov E, Wortel MJR, Lebedev S (2013) A plate tectonics oddity: Caterpillar–walk exhumation of subducted continental crust. Geology 41:555–558

Tretiakova LI, Lyukhin AM (2016) Impact–cosmic–metasomatic origin of microdiamonds from Kumdy–Kol deposit, northern Kazakhstan. National Geology (Otechestvennaya Geologiya) 2:69–77 (in Russian)

Tretiakova LI, Lyukhin AM (2017) Impact–cosmic–metasomatic origin of microdiamonds from Kumdy–Kol Deposit, Kokchetav Massiv, N. Kazakhstan. 11th Int Kimberlite Conf Extended Abstr 11IKC:4506

Trieloff M, Kunz J, Clague DA, Harrison D, Allègre CJ (2000) The nature of pristine noble gases in mantle plumes. Science 288:1036–1038

Uman MA (1986) All About Lightning. Dover Publications Inc New York 167

van Roermund HL, Carswell DA, Drury MR, Heijboer TC (2002) Microdiamonds in a megacrystic garnet websterite pod from Bardane on the island of Fjørtoft, western Norway: Evidence for diamond formation in mantle rocks during deep continental subduction. Geology 30:959–962

Verchovsky AB, Ott U, Begemann F (1993) Implanted radiogenic and other noble gases in crustal diamonds from Northern Kazakhstan. Earth Planet Sci Lett 120:87–102

Vogel DE (1966) Nature and chemistry of the formation of clinopyroxene–plagioclase symplectite from omphacite. Neues Jahrb Mineral Monatsh 6:185–189

Vrijmoed JC, Van Roermund HL, Davies GR (2006) Evidence for diamond–grade ultra-high pressure metamorphism and fluid interaction in the Svartberget Fe–Ti garnet peridotite–websterite body, Western Gneiss Region, Norway. Mineral Petrol 88:381–405

Vrijmoed JC, Smith DC, Van Roermund HLM (2008) Raman confirmation of microdiamond in the Svartberget Fe–Ti type garnet peridotite, Western Gneiss Region, Western Norway. Terra Nova 20:295–301

Wada N, Matsuda J (1998) A noble gas study of cubic diamonds from Zaire: constraints on their mantle source. Geochim Cosmochim Acta 62:2335–2345

Wang H, Wu Y–B, Gao S, Zheng J–P, Liu Q, Liu X–C, Qin Z–W, Yang S–H, Gong H–J (2014) Deep subduction of continental crust in accretionary orogen: Evidence from U–Pb dating on diamond-bearing zircons from the Qinling orogen, central China. Lithos 190:420–429

Warren JM (2016) Global variations in abyssal peridotite compositions. Lithos 248:193–219

Wu BR, Xu JA (1998) Total energy calculations of the lattice properties of cubic and hexagonal diamond. Phys Rev B 57:13355

Wu W, Yang J, Ma C, Milushi I, Lian D, Tian Y (2017) Discovery and significance of diamonds and moissanites in chromitite within the Skenderbeu massif of the Mirdita Zone Ophiolite, West Albania. Acta Geol Sin Eng 91:882–897

Wu W, Yang J, Wirth R, Zheng J, Lian D, Qiu T, Milushi I (2019) Carbon and nitrogen isotopes and mineral inclusions in diamonds from chromitites of the Mirdita ophiolite (Albania) demonstrate recycling of oceanic crust into the mantle. Am Mineral 104:485–500

Wu W, Yang J, Zheng J, Lian D, Qiu T, Rui H (2020) Origin of the Diamonds within Chromitite from the Mirdita Ophiolite (Albania) and its Geological Significance. Acta Geol Sin–Eng 94:64–64

Xiong F, Yang J, Robinson PT, Dilek Y, Milushi I, Xu X, Chen Y, Zhou W, Zhang Z, Lai S, Tian Y, Huang Z (2015) Petrology and geochemistry of high Cr-podiform chromitites of Bulqiza, Eastern Mirdita Ophiolite (EMO), Albania. Ore Geol Rev 70:188–207

Xiong F, Yang J, Robinson PT, Dilek Y, Milushi I, Xu X, Zhou W, Zhang Z, Rong H (2017) Diamonds discovered from high-Cr podiform chromitites of Bulqiza, eastern Mirdita ophiolite, Albania. Acta Geol Sin–Eng 9:455–468

Xiong F, Yang J, Robinson PT, Dilek Y, Xu X , Zhang Z (2018) Origin and significance of diamonds and other exotic minerals in the Dingqing ophiolite peridotites, eastern Bangong–Nujiang suture zone, Tibet. Lithosphere 10:142–155

Xu S, Okay AI, Ji S, Sengor AMC, Su W, Liu Y, Jiang L (1992) Diamond from the Dabie Shan metamorphic rocks and its implication for tectonic setting. Science 256:80–82

Xu S, Liu Y, Chen G, Compagnoni R, Rolfo F, He M, Liu H (2003) New finding of micro–diamonds in eclogites from Dabie–Sulu region in central–eastern China. Chinese Sci Bull 48:988–994

Xu X, Chen S, Yang J (2009) Unusual mantle mineral group from chromitite orebody Cr–11 in Luobusa ophiolite of Yarlung–Zangbo suture zone, Tibet. J Earth Sci 20:284–302

Xu XZ, Yang, JS, Ba DZ, Zhang ZM, Xiong FH, LiY (2015) Diamond discovered from the Dongbo mantle peridotite in the Yarlung Zangbo suture zone, Tibet. Geol China 42:1471–1482

Xu X, Cartigny P, Yang JS, Dilek Y, Xiong F, Guo G (2018) Fourier transform infrared spectroscopy data and carbon isotope characteristics of the ophiolite-hosted diamonds from the Luobusa ophiolite, Tibet, and Ray-Iz ophiolite, Polar Urals. Lithosphere 10:156–169

Yamaoka S, Kumar MS, Akaishi M, Kanda H (2000) Reaction between carbon and water under diamond–stable high pressure and high temperature conditions. Dia Relat Mater 9:1480–1486

Yang JS, Xu Z, Dobrzhinetskaya LF, Green II, HW, Pei X, Shi R, Wu C, Wooden JL, Zhang J, Wan Y, Li H (2003) Discovery of metamorphic diamonds in Central China: an indication of a >4000 km–long–zone of deep subduction resulting from multiple continental collisions. Terra Nova 15:370–379

Yang JS, Dobrzhinetskaya LF, Bai WJ, Fang QS, Robinson PT, Zhang JF, Green II HW (2007a) Diamond– and coesite-bearing chromitites from the Luobusa ophiolite, Tibet. Geology 35:875–878

Yang JS, Bai WJ, Fang Q S, Meng FC, Chen SY, Zhang ZM, Rong H (2007b) Discovery of diamond and an unusual mineral group from the podiform chromite, Polar Ural. Geol China 34:950–952

Yang JS, Xu XZ, Li Y, Li JY, Ba DZ, Rong H, Zhang ZM (2011) Diamonds recovered from peridotite of the Purang ophiolite in the Yarlung–Zangbo suture of Tibet: A proposal for a new type of diamond occurrence. Acta Petrol Sinica 27:3171–3178

Yang JS, Xu XZ, Zhang ZM, Rong H, LiY, Xiong FH, Liang FH, Liu Z, Liu F, Li JY, Li ZL, Chen SY, Guo GL, Robinson P (2013) Ophiolite-type diamonds and deep genesis of chromitite. Acta Geosci Sin 34:643–653 (in Chinese with English Abstract)

Yang JS, Robinson PT, Dilek Y (2014) Diamonds in ophiolites. Elements 10:127–130

Yang JS, Meng F, Xu X, Robinson PT, Dilek Y, Makeyev AB, Wirth R, Wiedenbeck M, Griffin WL, Cliff J (2015a) Diamonds, native elements and metal alloys from chromites of the Ray-Iz ophiolite of the Polar Urals. Gondwana Res 27:459–485

Yang JS, Robinson PT, Dilek Y (2015b) Diamond-bearing ophiolites and their geological occurrence. Episodes 38:344–364

Yang JS, Trumbull R, Robinson PT, Xiong FH, Lian DY (2018) Comment 2 on "Ultra-high pressure and ultra-reduced minerals in ophiolites may form by lightning strikes". Geochem Perspect Lett 8:6–7

Yang J, Robinson PT, Xu X, Xiong F, Lian D (2019a) Diamond in oceanic peridotites and chromitites: evidence for deep recycled mantle in the global ophiolite record. Acta Geol Sin–Eng 892:341–350

Yang J, Lian D, Robinson PT, Qiu T, Xiong F, Wu W (2019b) A shallow origin for diamonds in ophiolitic chromitites: COMMENT. Geology 47:e475

Yang J, Simakov SK, Moe K, Scribano V, Lian D, Wu W (2020) Comment on "Comparison of enigmatic diamonds from the Tolbachik arc volcano (Kamchatka) and Tibetan ophiolites: assessing the role of contamination by synthetic materials" by Litasov et al. 2019. Gondwana Res 79:301–303

Yang J, Lian D, Wu W, Rui H (2021) Peridotites, chromitites and diamonds in ophiolites. Nat Rev Earth Environ 2:198–212

Ye K, Cong BL, Ye DN (2000) The possible subduction of continental material to depths greater than 200 km. Nature 407:734–736

Zhang KJ, Cai JX, Zhang YX, Zhao TP (2006) Eclogites from central Qiangtang, northern Tibet (China) and tectonic implication. Earth Planet Sci Lett 245:722–729

Zhang RY, Liou JG, Iizuka Y, Yang JS (2009) First record of K–cymrite in North Qaidam UHP eclogite, Western China. Am Mineral 94:222–228

Zhang J, Prakapenka V, Kubo A, Kavner A, Green HW II, Dobrzhinetskaya LF (2011) Diamond formation from amorphous carbon and graphite in presence of COH fluids: an in situ high-pressure and–temperature laser–heated diamond anvil cell experiments. *In:* Ultrahigh Pressure Metamorphism: 25 Years After the Discovery of Coesite and Diamond, Dobrzhinetskaya LF, Faryad SW, Wallis S, Cuthbert S (eds) Elsevier, London, p.113–124

Zhang RY, Liou JG, Lo CH (2017) Raman spectra of polycrystalline microdiamond inclusions in zircons, and ultrahigh-pressure metamorphism of a quartzofeldspathic rock from the Erzgebirge terrane, Germany. Int Geol Rev 59:779–792

Zhou MF, Robinson PT, Su BX, Gao JF, Li JW, Yang JS, Malpasa J (2014) Compositions of chromite, associated minerals, and parental magmas of podiform chromite deposits: The role of slab contamination of asthenospheric melts in suprasubduction zone environments. Gondwana Res 26:262–283